A STUDY OF THE SATURATION CHARACTERISTICS OF IONIZATION CHAMBERS

by

PATRICIA BARRIE SCOTT

Thesis presented for the Degree of Doctor of Philosophy of the University of Edinburgh in the Faculty of Medicine, October, 1962.

ACKNOWLEDGEMENTS.

I wish to thank Dr. J.R. Greening, Director of the Department of Medical Physics at the University of Edinburgh, for his constant guidance and unfailing encouragement throughout the course of the present work. I must also record my gratitude for all the help and advice given by the Staff of the Department.

This research programme has been supported by a grant from the Medical Research Council.

C O N T E N T S

SYMBOLS USED THROUGHOUT TEXT.

a = beam diameter (cm.)

α = recombination coefficient ($cm.^3/sec.$)

d = plate separation (cm.)

D = diffusion coefficient ($cm.^2/sec.$)

e = electronic charge (e.s.u.)

E = field strength (V/cm.)

j = observed current per $cm.^2$ of plate.

j_s = saturation current per $cm.^2$ of plate.

k_1 = positive ion mobility ($cm.^2/sec.V$).

k_2 = negative ion mobility ($cm.^2/sec.V$).

L = doserate (r/min.)

q = ionization intensity e.s.u./$cm.^3$ sec.

V = collecting voltage (V).

CHAPTER 1.

INTRODUCTION

Fig. 1

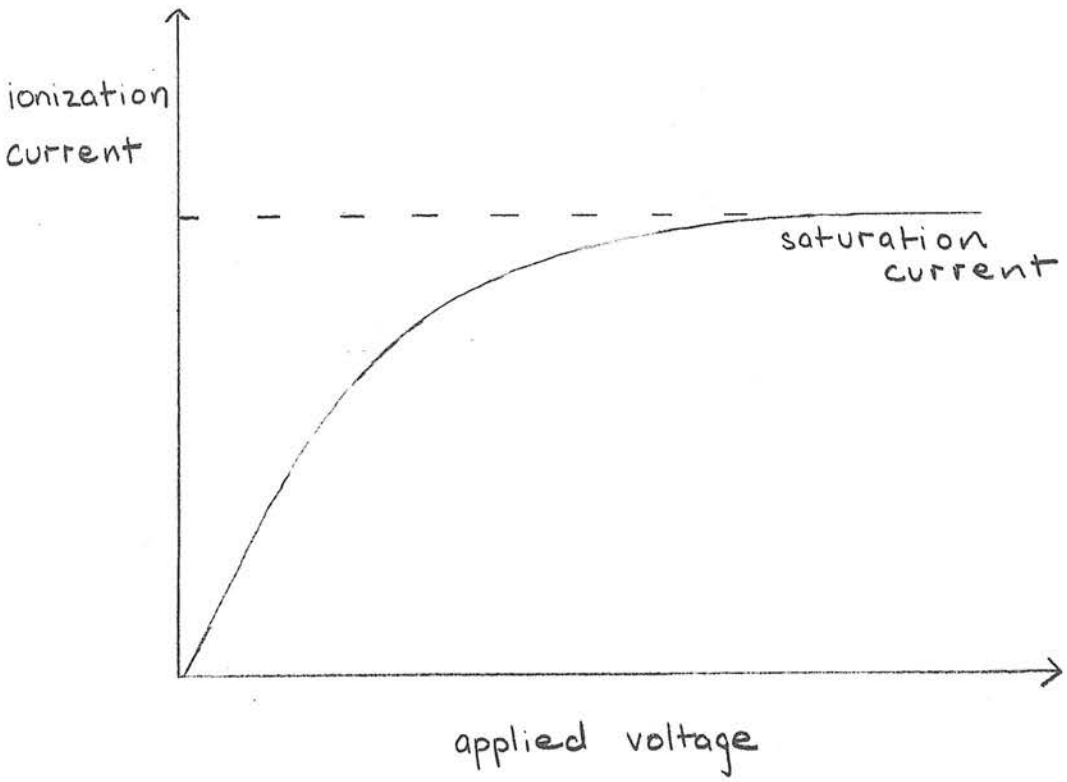

Relationship between ionization current and applied voltage

1.1 Causes of Saturation Losses in Ionization Chambers.

The fundamental components of an ionization chamber are two electrodes maintained at different potentials and a gas occupying the space between the electrodes. When the gas is uniformly irradiated by X or γ rays, the resulting positive and negative ions move towards their respective electrodes, constituting a flow of current. The relationship between this ionization current and the applied voltage is shown in Fig.1.

If the intensity of the irradiation is kept constant and the applied voltage is increased from zero, the collected current rises, at first almost linearly with voltage, then more slowly until at large voltages it becomes constant. This constant value is the saturation current for the given radiation intensity and is attained when the applied voltage is sufficient to collect all the ions which are being formed. At lower voltages ions are lost by diffusion and recombination. (Loeb 1955).

1.1 (1) Diffusion.

Ions in a gas are in constant contact with the gas molecules and so take part in their random thermal movements. As a result of this thermal motion any accumulation of ions in a gas will move in such a way as to decrease the initial concentration. This process is known as diffusion and is always present, despite any more directed motion, e g.that caused by an electric field.

In a thoroughly ionized gas at N.T.P. the separation of the ions is $\sim$ 10^{-4} cm. and their average kinetic energy is twenty times the potential energy between the ions. This means that the inter-ionic forces can be neglected and ionic diffusion is dependent on the Brownian motion of the surrounding molecules or on the agitation energies of the ions if an electric field is present.

Diffusion causes ion losses in an ionization chamber in two ways. Lateral diffusion results in ions escaping through the boundaries of the collecting region into non-ionized portions of the gas. Losses are also due to ions diffusing to and being collected by the "wrong" electrode, despite the opposing effect of the electric field.

1.1 (2) Recombination.

Recombination is the process by which ions of opposite sign recombine with each other and may occur in several ways depending on the type of ionizing radiation and the gas pressure. There are two types of recombination associated with ionization due to fast electrons and X-rays at atmospheric pressure. Under these conditions the positive and negative ions are initially distributed in clusters of ion pairs along the electron tracks. Initial recombination takes place when the recombining ions were formed in the same cluster while Volume Recombination sets in when the ions have diffused apart to random and isotropic distributions.

Recombination losses in an ionization chamber under α, β or γ irradiation at atmospheric pressure are due to a mixture of initial and volume recombination. The relative magnitudes of these two processes will be determined by the type and energy of the radiation, the field strength and the doserate. The amount of initial recombination taking place is dependent only on the density of ionization along the electron track, and is not influenced by the doserate. Volume recombination is, however, dependent on the doserate which determines the number of tracks in a given volume. At high doserates, volume recombination is thus the dominant process since the secondary electron tracks soon overlap through diffusion even in the absence of an electric field which increases the rate of separation of the ions. When doserates and field strengths are low, initial recombination becomes more important since the ions take longer to assume isotropic distributions.

1.1 (3) Space Charge.

The relationship between the ionization current and the applied voltage may also be modified by the presence of space charges. The movement of the ions towards their respective electrodes alters the uniform distribution of the field, particularly in the vicinity of the electrodes. Near the anode the positive ions created in the neighbouring volume are removed by the current which brings in negative ions. Near the cathode the situation is reversed.

Fig. 2

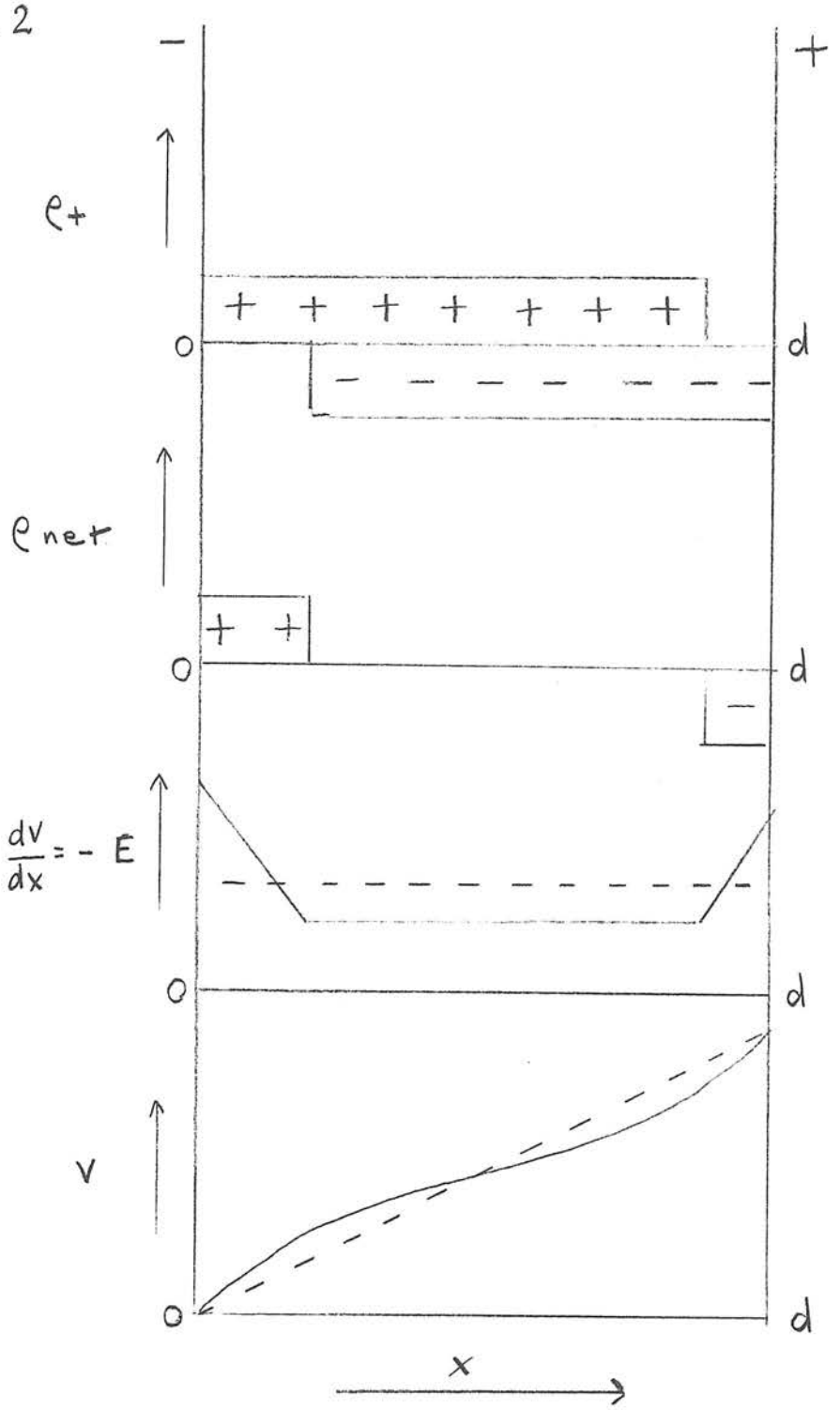

Effect of a space charge density ρ on the voltage V and field strength E in a parallel plate chamber under uniform ionization

---- represent V(x) and E(x) for ρ = 0

If the ions have different mobilities then the space charge effects at the two electrodes will differ. Von Engel (1955) summarises in graphical form (Fig.2) the effect of a space charge density ρ on the voltage V and the field strength E in a parallel plate chamber under uniform ionization. For appreciable space charge the potential distribution between the plates is no longer a straight line but a curve, and the field strength, while constant in the middle of the gap, changes rapidly in the vicinity of the electrodes.

1.1.

The saturation characteristics of any ionization chamber are thus dependent on three parameters - ionic diffusion, recombination and space charge.

1.2 Existing Theories and Experimental Data.

The theory of electric conduction through an ionized gas was first developed by J.J. Thomson (1903, 1928) at the beginning of this century. He considered the case of two infinite parallel plates maintained at different potentials and immersed in an ionized gas, and set up the basic differential equation governing the transport of ions across the gap. His treatment took into account the effects of diffusion, recombination, space charge and drift under the electric field.

Mie (1904) and Seeliger (1910) attempted to solve this equation by approximate methods in order to determine the relationship between the ionization current and the applied voltage in an ionization chamber. They ignored ion diffusion and considered recombination and the influence of space charge on the electric field. Seaman (1912) verified Mie's numerical solution by carrying out a series of experiments to determine saturation curves for plate separations d ranging from 1 to 5 cm. and ionization intensities q from 0.3 to 1.6 r/min. Mie's equation, however, was not in a useful form since it involved a parameter R - the apparent resistance of the ionized gas at very low collecting voltage - which was difficult to measure accurately.

Later, Von Engel and Steenbeck (1932) derived a more convenient formula governing recombination in a parallel gap. They simplified theory by assuming that the densities of the positive and negative ions remained constant between the plates, whereas in

fact the positive ion density is zero at the positive plate and reaches a maximum value at the negative plate and the negative ion density varies in a similar fashion in the opposite direction. They defined a correction factor K_s by which an observed ionization current must be multiplied to correct for recombination, and derived an expression for K_s in terms of the plate separation, the field strengtn and the doserate. Their equation was verified experimentally by Seeliger (1934) who found good agreement with theory when ion losses due to diffusion were taken into account.

Further investigation into the saturation characteristics of ionization chambers was stimulated by their use in the determination of dosages in radiation therapy. The high doserates obtainable meant that it became difficult to attain saturation conditions in an ion chamber without increasing the field to such an extent that ionization by collision ensued. It was thus of importance both in the operation and design of ion chambers to be able to calculate the degree of saturation obtainable under given experimental conditions.

Boag and Wilson (1952) tackled the problem of estimating the saturation curve in a parallel plate chamber at high ionization intensities. By making a dimensional analysis of all the experimental variables which influence saturation losses, they showed that the collection efficiency f, i.e. the ratio of the observed current density to the saturation current density, could be expressed as a function of $\left(\frac{d^2 \sqrt{q}}{V} \right)$. They verified this concept of a generalised saturation curve by a series of experiments for plate

separations ranged from 0.0625 to 0.253 cm. and ionization intensities from 1000 to 118,000 r/sec. Boag and Wilson also derived a theoretical expression for f in terms of d, q and V, using an approximate solution to Thomson's equation. They assumed that the ion densities varied linearly across the plates and ignored ion diffusion and space charge effects. Good agreement between theory and experiment was obtained when the value of the parameter * $M = \sqrt{\frac{\alpha}{e\ k_1\ k_2}}$ was taken as 19.4 in their calculations. They pointed out, however, that this empirical value for m is considerably less than that obtained if the generally accepted values for these constants are substituted. This discrepancy was thought to arise because at the small plate separations and high field strengths used in their experiments a considerable proportion of electrons crossed the gap without attachment to neutral gas molecules to form negative ions. This would increase the effective value of k_2.

Shevyrev (1960) carried out experimental studies on the saturation characteristics of parallel plate chambers using plate separations in the range 0.3 to 3.0 cm. and ionization intensities from 1 to 10^5 r/hr. He converted the equations of Mie and others to the form $f = \psi \frac{d^2\sqrt{q}}{V}$ and compared these graphically with his experimental results. Most of his experimental points grouped

* α = recombination coefficient ($cm.^3/sec.$)
e = electronic charge (e.s.u.).
k_1 = positive ion mobility ($cm.^2/sec.V.$)
k_2 = negative ion mobility ($cm.^2/sec.V.$)

round the curve calculated from Mie's equation except at low ionization intensities and small plate separations where losses due to ion diffusion can no longer be neglected. Under near saturation conditions, allowance for ion diffusion was made from a formula due to Rossi and Staub (1949) and again good agreement was obtained with Mie's theory. For recombination losses of more than 20 per cent Shevyrev showed that Mie's equation could still be used to predict experimental points provided the parameter M was increased to correct for diffusion. He compiled graphs illustrating the necessary change in M for different d and q.

Shevyrev's experimental results at high ionization intensities agreed with the equation of Boag and Wilson calculated for M = 39. He suggested that their low experimental value for M might have been caused by additional ionization created by scattered electrons outside the assumed active volume and diffusion of ions into non-irradiated regions of the chamber. He did find some evidence of decrease in electron attachment at the highest intensities but concluded that for doserates of up to 10^5 r/hr. the effect of free electrons on the ionization current could be neglected.

In supporting Mie's theory Shevyrev also emphasised the importance of considering the influence of space charge on the electric field in the estimation of saturation losses.

The recombination theories mentioned so far have dealt solely with general recombination where the distribution of ions is isotropic.

The first theory concerning initial recombination was developed by Jaffé (1913) who studied α particle ionization. In this case the ions are initially distributed among a number of densely ionized columns. Jaffé's columnar theory assumed that the ion distribution was cylindrically symmetrical about the track of an α particle and that the ion density fell off with increasing radius. He considered the effects on this distribution of diffusion, recombination and drift under an electric field and set up a differential equation governing the fraction of ions escaping recombination. Good agreement between theory and experiment was obtained, but unsuccessful attempts to apply Jaffe's theory to X and γ -ray ionization were made until Lea (1934) postulated the cluster theory.

In X and γ -ray ionization, the ions are localised in clusters along the tracks of the secondary electrons. Lea assumed the clusters had spherical symmetry and used Jaffé's method to calculate ion losses. Cluster recombination proceeds until neighbouring clusters overlap when columnar theory becomes applicable. Lea's theory was verified by experiments with extremely low intensity γ -rays at high pressures and was further developed by Kara-Michailova and Lea (1940). Their work is discussed in some detail in Chapter 5.

Fig 3

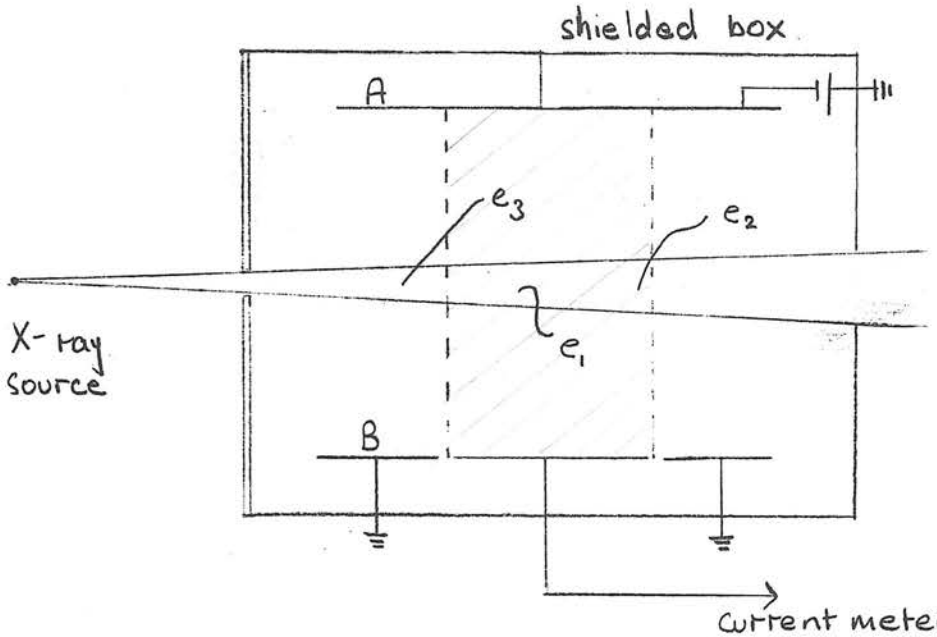

Schematic view of typical free-air chamber

1.3 Description of Free-Air and Extrapolation Ionization Chambers.

The work described in this thesis concerned two adaptations of the parallel plate ionization chamber - the free-air chamber and the extrapolation chamber.

1.3 (1) Free-Air Chamber.

The free-air chamber was developed to measure X-ray dosage in accordance with the definition of the roentgen (I.C.R.U. 1956). As its name implies, the X-ray beam and its associated secondary electrons pass through it without striking any material other than air. A typical free-air chamber is shown schematically in Fig.3. A narrow beam of X-rays diverging from a point source enters the chamber through a hole in the diaphragm and passes between the parallel plates A and B. An electric field of about 100V/cm. is applied across the plates and the guard plates in electrode B define the collecting region and ensure the parallelism of the lines of electric force. The plate separation must be sufficient to allow all the secondary electrons, e_1 , e_2 , e_3 etc. to expend their energies in air and conditions of electronic equilibrium must hold. Electrons such as e_1 will complete their tracks within the ion collecting region. Others like e_2 originate in the collecting space but cause ionization outside it. This ionization loss is compensated for, however, by electrons like e_3 which enter the

sensitive volume from the other side. Electronic equilibrium means that the collected ions are effectively those caused by X-ray absorption in the volume shown shaded in Fig.3. The X-ray intensity at the defining diaphragm of area S can be calculated as if the total current I collected by a plate of length D came from secondary electrons originating in the air volume SD. There have been many papers on the design criteria for free-air chambers and these have been summarised by Wyckoff and Attix (1957).

Since free-air chambers are capable of making absolute measurements of radiation, they are maintained in the standardising laboratories of various countries. They are essentially laboratory instruments and are usually unsuited to making quantity measurements under clinical conditions. Instead they are used as primary standards for calibrating thimble chambers which, being light and compact, are more suitable for routine dosage measurements.

1.3 (2) Extrapolation Chamber.

The extrapolation chamber was first devised by Failla (1937). Its construction will be discussed in detail in Chapter 7, but it consists basically of a parallel plate ionization chamber with variable plate separation. The volume from which the ionization is collected is a small coin-shaped region at the centre of the plates, surrounded by a wide guard ring. If the ionization per c.c. is determined for different plate separations and a curve plotted from the data, the ionization per c.c. for a vanishingly small volume can be found by extrapolation.

The extrapolation chamber has proved a good means for measuring surface and depth dose rates from β ray sources. It can also be used to calibrate thimble chambers for the estimation of the dosage due to radioactive isotopes uniformly distributed in tissue.

1.4 Aims of Thesis

The aim of this thesis was to make a combined theoretical and experimental investigation into the saturation characteristics of two types of parallel plate ionization chambers - the free-air chamber and the extrapolation chamber.

Despite the great importance of free-air chambers in standardising laboratories, little theoretical consideration seems to have been given to their saturation losses. The theories surveyed in 1.2 deal with uniform ionization in a parallel gap and are not directly applicable to a free-air chamber where the X-ray beam often occupies a small proportion of the collecting volume. Hübner (1958) appears to be the first to calculate the recombination occurring in a free-air chamber. He modified the equation of Von Engel and Steenbeck to take into account the fact that the ionization did not fill the space between the electrodes. He claimed that correction factors calculated from his formula agreed within 0.3 per cent with factors determined experimentally at the National Bureau of Standards. We found that these experimental results covered only a limited range of conditions and as they concerned corrections usually less than 1 per cent, hardly constituted an accurate check of the theory.

We felt that Hübner's treatment could be improved upon by a different choice of recombination formula. Although Shevyrev's work pointed to Mie's equation, we decided to use the derivation due to Boag and Wilson which was in a more convenient form for the further modifications we intended to carry out. By

considering the effects of space charge and ion diffusion on the basic recombination equation, we sought to derive an expression for the saturation losses in a free-air chamber. We then planned to check our theory by experiments using a free-air chamber (Greening, 1960) over a wide range of operating conditions.

It was foreseen that it would be a formidable task to set up a theory governing saturation losses in an extrapolation chamber. Loevinger (1953) quoted an empirical relation for f as a function of $\left(\frac{1}{\sqrt{Vd}}\right)$ obtained from experiments with β-ray sources for plate spacings in the range 0.01 to 0.2 cm. and ionization intensities up to 25 e.s.u./cm.^{3} sec. This function for f is at variance with all previously described theories. We would expect the situation in an extrapolation chamber to be an extremely complex one since the use of very small air gaps and low β-intensities is likely to result in losses from diffusion and initial recombination superimposed on volume recombination losses. Loevinger's result does, however, seem surprising since all theories describing these types of losses contain V to the power 1 if not higher.

It seemed worth-while, therefore, to design and construct a simple extrapolation chamber and make an intensive study of the variation of ionization current with the various parameters involved. We planned to discuss the theoretical significance of these experimental results, making quantitative evaluations where possible.

CHAPTER 2.

DEVELOPMENT OF THEORY FOR SATURATION LOSSES IN A FREE-AIR CHAMBER

2.1 Hübner's Treatment.

Hübner (1958) provides the only theoretical treatment of recombination in free-air chambers of which we are aware. He adopts the formula derived by Von Engel and Steenbeck (1932) who considered uniform ionization between two infinitely long parallel plates: -

Suppose the ion density is N ion pairs/cm.^{3} and the rate of formation of ions is $\frac{dN}{dt}$ ion pairs/cm.^{3} sec.

Ions recombine in the gap at the rate $\left(\frac{dN}{dt}\right)_{rec.}$

and are removed by the electrodes at $\left(\frac{dN}{dt}\right)_j$

In equilibrium

$$\left(\frac{dN}{dt}\right) + \left(\frac{dN}{dt}\right)_{rec} + \left(\frac{dN}{dt}\right)_j = 0$$

Now

$$\left(\frac{dN}{dt}\right)_{rec} = - \alpha N^2$$

and the current density $j = - ed \left(\frac{dN}{dt}\right)_j$

but $j = eN (k_1 + k_2)E$ ---------- (1)

$$\therefore \left(\frac{dN}{dt}\right)_j = - \frac{E}{d} (k_1 + k_2) N$$

$\therefore$ Rate of formation of ions $\frac{dN}{dt} = \alpha N^2 + \frac{E}{d} (k_1 + k_2)E$

$$\therefore N^2 + \frac{E}{\alpha d} (k_1 + k_2) N - \frac{1}{\alpha} \left(\frac{dN}{dt}\right) = 0$$

$$\text{i.e. } N = \frac{E}{2\alpha d} (k_1 + k_2) \left[\sqrt{1 + \frac{4d^2 \alpha}{(k_1 + k_2)^2 E^2} \left(\frac{dN}{dt}\right)} - 1 \right]$$

Fig. 4

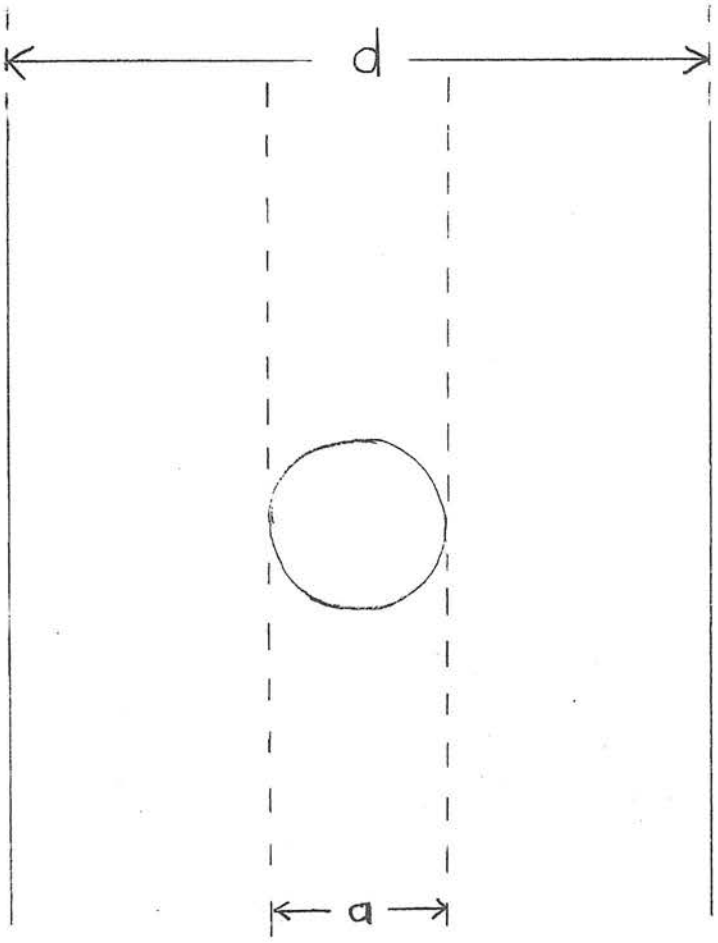

Virtual electrodes at beam edge.

Substituting this value for N in equation (1) we get: -

$$j = e\,(k_1 + k_2)^2\,E^2\left[\sqrt{1 + \frac{4\,\mathcal{L}\,d^2}{(k_1 + k_2)^2\,E^2}\left(\frac{dN}{dt}\right)} - 1\right]$$

The saturation current density $j_s = ed\left(\frac{dN}{dt}\right)$

Correction factor $K_s = j_s / j$

$$\therefore \quad K_s = \frac{\frac{2\,\mathcal{L}}{(k_1 + k_2)^2}\left(\frac{d}{E}\right)^2 \frac{dN}{dt}}{\sqrt{1 + 2\,\frac{2\,\mathcal{L}}{(k_1 + k_2)^2}\left(\frac{d}{E}\right)^2 \frac{dN}{dt}} - 1} \qquad \text{---------(2)}$$

Equation (2) is the formula of Von Engel and Steenbeck. Hübner applied this to a free-air chamber by assuming that all the ionization is confined within the geometrical shape of the X-ray beam and that virtual collecting electrodes exist at the beam edge (Fig.4).

Using a to represent the beam diameter and expressing $\frac{dN}{dt}$ in terms of the doserate L equation (2) becomes: -

$$K_s = \frac{n\left(\frac{a}{E}\right)^2 L}{\sqrt{1 + 2n\left(\frac{a}{E}\right)^2 L} - 1} \qquad \text{----------(3)}$$

where $n = \frac{69.4\,\mathcal{L} \times 10^6}{(k_1 + k_2)^2}$

(1 r/min. = $\frac{2.1 \times 10^9}{60}$ ion prs./cm.^{3} per min.

$\therefore \quad \frac{dN}{dt} = 3.5 \times 10^7\,L$)

Fig. 5

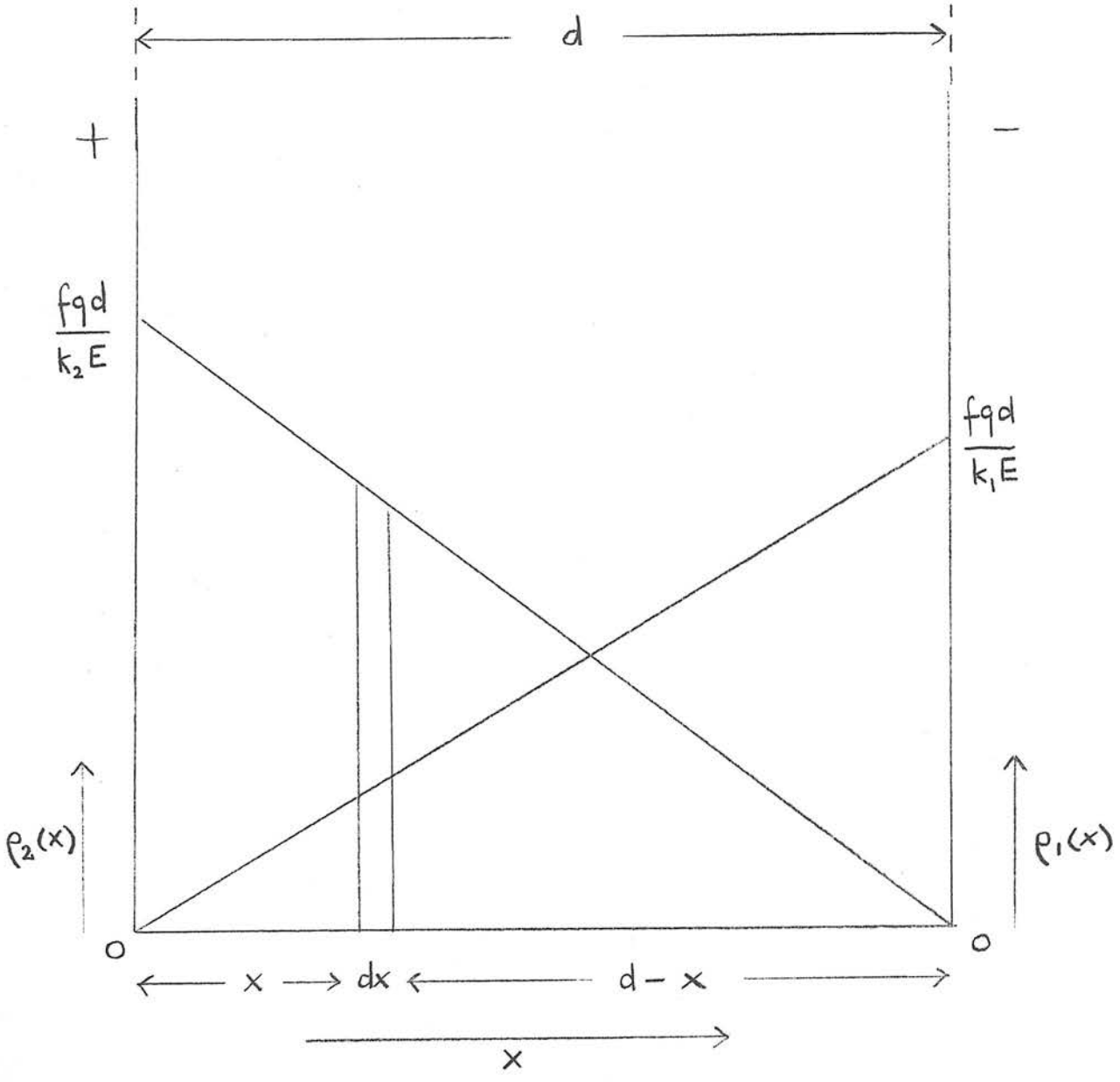

Distribution of charge density between the electrodes under near saturation conditions.

2.2 Improved Basic Recombination Formula.

Boag and Wilson's treatment (1952) of recombination in parallel plate chambers is an improvement on that of Von Engel and Steenbeck since they take into account the varying distributions of the positive and negative charges across the gap between the plates (Fig.5).

Suppose the ionization intensity is q e.s.u./cm.^{3} sec. at all points in the gas between the plates. Then for negligible space charge and negligible recombination, the positive charge density $\rho_1(x)$ will rise linearly from zero at the positive plate to a maximum of qd/k_1E at the negative plate, while the negative charge density $\rho_2(x)$ will have a similar distribution in the opposite direction. For a collection efficiency $f = j/j_s$ less than unity, the current reaching each plate is only fqd e.s.u./cm.^{2} sec., but Boag and Wilson assume the charge distributions continue to vary linearly between the plates for recombination up to 10 per cent.

The rate of recombination of charge per unit volume at the plane x is then: -

$$\frac{\alpha}{e}\ \rho_1(x)\ \rho_2(x) = \frac{\alpha}{e}\left(\frac{x}{d}\ \frac{fqd}{k_1E}\right)\left(1 - \frac{x}{d}\right)\ \frac{fqd}{k_2E}$$

thus total recombination throughout the space per unit area of plate per second is

$$R = \int_0^d \frac{\alpha}{e}\ \rho_1(x)\ \rho_2(x)\ dx$$

$$= \frac{\alpha}{e} \cdot \frac{f^2 q^2 d^2}{E^2} \cdot \frac{d}{6\, k_1\, k_2}$$

Now $f = 1 - R/qd$

$$\therefore \quad f = \frac{2}{1 + \sqrt{1 + z^2}}$$

where $$z = \sqrt{\frac{2}{3} \cdot \frac{\mathcal{L}}{e} \cdot \frac{1}{k_1 k_2}} \left(\frac{d^2 \sqrt{q}}{V} \right)$$

$$\therefore \quad \frac{1}{f} = \frac{1 + \sqrt{1 + m \left(\frac{d}{E}\right)^2 L}}{2} \qquad \text{where } m = \frac{1}{90} \quad \frac{\mathcal{L}}{e} \quad \frac{1}{k_1 k_2}$$

Hübner's method of applying this result to a free-air chamber necessitates replacing d by a. Theoretically Hubner's $K_s = j_s/j$ should equal 1/f. Rationalising the denominator of equation (3) we find

$$K_s = \frac{1 + \sqrt{1 + 2n \left(\frac{a}{E}\right)^2 L}}{2}$$

where $$n = \frac{69.4 \, \mathcal{L} \times 10^6}{(k_1 + k_2)^2}$$

The difference between the constants n and m arises because Boag takes into account the distribution of charge. Adopting Boag's constant m, Hübner's formula becomes

$$K_s = 1/2 + 1/2 \sqrt{1 + m \left(\frac{a}{E}\right)^2 L} \qquad \text{---------- (4)}$$

N.B. Equation (4) gives rise to smaller values of K_s than does equation (3) because of the difference in constants. In his paper Hubner refers to Boag and Wilson's treatment and says that they obtain larger values for K_s . This mistake occurred because in the example Hubner adopted (private communication) he did not correctly replace the d in Boag's formula by a.

Fig. 6

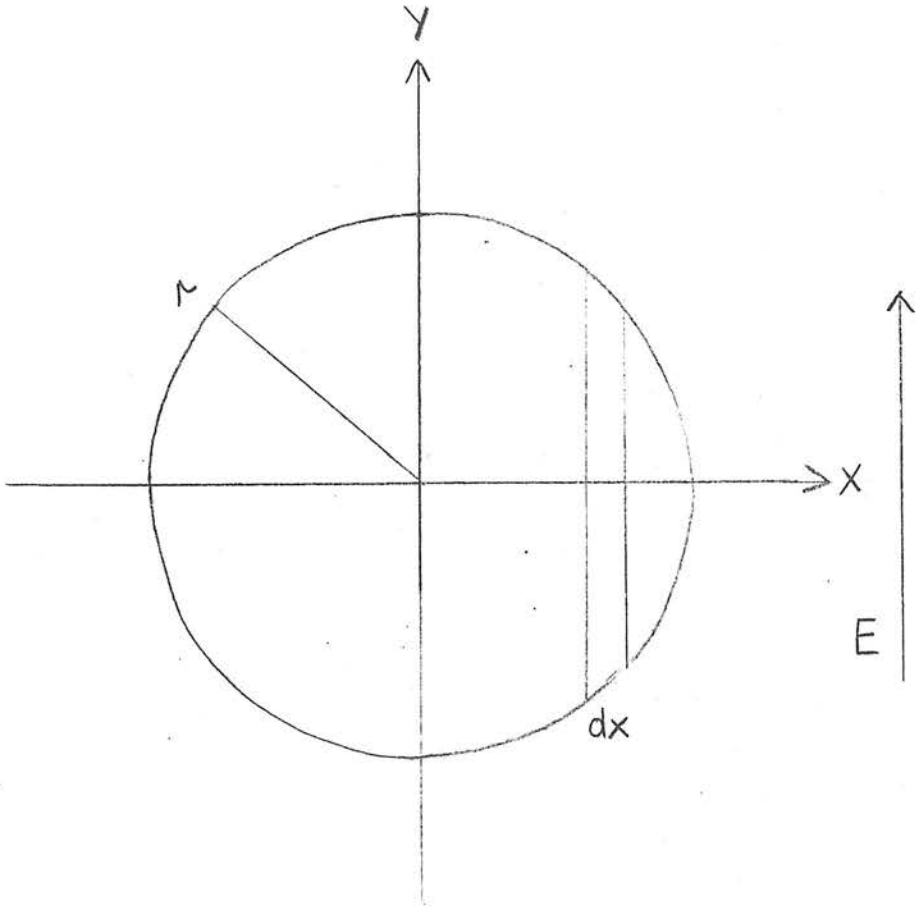

Effective cross-section of circular X-ray beam.

2.3. Allowance for Circular Cross Section of X-ray Beam.

The theory used by Hubner considers an infinite plane sheet of ionization of thickness a. In practice it is normal to use X-ray beams of circular cross section. The theory must be modified to allow for this.

Consider a strip of ionized gas parallel to the electric field and of width dx (Fig.6). Ionization in the strip is proportioned to the area, i.e. 2y. dx. For small values of recombination, equation (4) can be written

$$K_S = 1/2 + 1/2 + \frac{m}{4}\left(\frac{a^2}{E}\right) . L$$

i.e. given E and L $(K_S - 1) \propto a^2$

Therefore the fractional recombination in the strip is proportional to $(2y)^2$

$\therefore$ Total recombination in the strip $\propto 8y^3\, dx$.

Total recombination in the beam $\propto \int_{-r}^{+r} 8y^3\, dx = 3\pi r^4$

Total ionization in the beam $\propto \int_{-r}^{+r} 2y\, dx = \pi r^2$

$\therefore$ Fractional recombination in whole beam $\propto 3\pi r^4 / \pi r^2$

$\propto 3 r^2$, $\propto \frac{3}{4}(2r)^2$

Hubner's theory indicates that fractional recombination is proportional to a^2 where $a = 2r$. Therefore the effective diameter of a circular beam of diameter a is $\sqrt{\frac{3a^2}{4}} = a\sqrt{\frac{3}{2}}$

Fig. 7

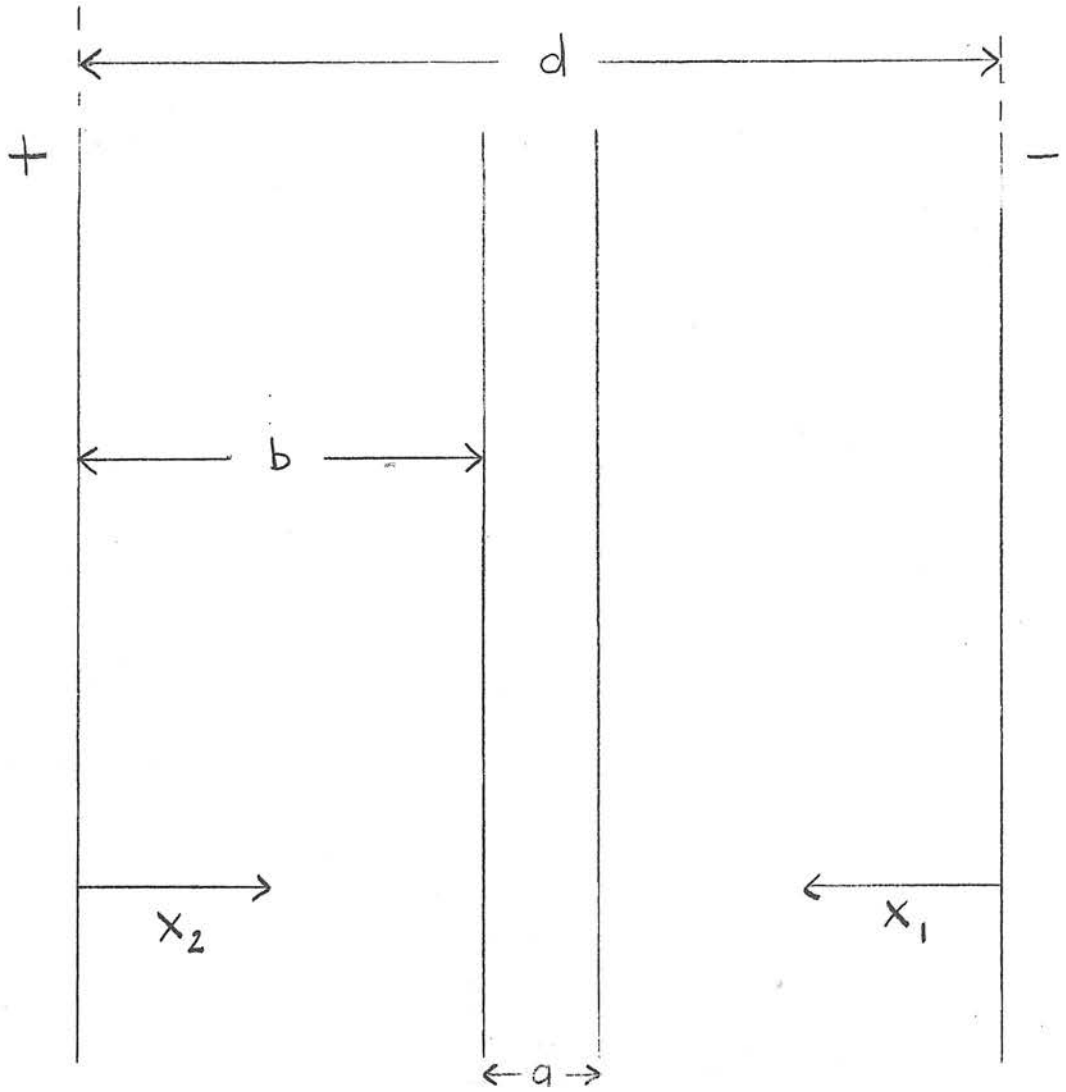

Free-air ionization chamber

2.4 Space Charge Effects.

Hübner did not consider space charge effects. Boag (1950) gave a very useful treatment of space charge effects in ionization chambers exposed to pulsed radiation beams. He came to the conclusion that in a chamber of plane geometry, the screening effect of the space charge is negligible. This is not true, however, in the case of a free-air chamber where the beam does not completely fill the space between the plates and there is continuous exposure to radiation.

Boag's treatment can be modified to suit these conditions. (Fig.7). Let E_{x_1} be the field at a distance x_1 from the negative plate

n_1 = number of positive ions/c.c.

n_2 = number of negative ions/c.c.

then $$\frac{dE_{x_1}}{dx_1} = -4\pi n_1 e$$

$$\therefore E_{x_1} = E_b + 4\pi n_1 e (b - x_1)$$

Similarly

$$E_{x_2} = E_b + 4\pi n_2 e (b - x_2)$$

Assuming a constant voltage gradient E_b in the irradiated volume of width a

$$V = E_b a + \int_o^b E_{x_1} dx_1 + \int_o^b E_{x_2} dx_2$$

$$= E_b a + 2\pi b^2 e (n_1 + n_2)$$

Now if N is the number of ion pairs formed per c.c. per second then

$n = \int N\,dt$ between the limits $t = 0$ and $t = \frac{a}{k\ V/d}$

($\frac{a}{k\ V/d}$ is the time taken for an ion of mobility k to traverse the irradiated volume under the influence of the average field across the plates, i.e. V/d or E).

Substituting $n = \frac{Na}{k\ V/d}$.

we find $$E_b = \frac{V}{d} - \frac{2\pi Ne\ a}{V}\left(\frac{d-a}{2}\right)^2\left[\frac{1}{k_1} + \frac{1}{k_2}\right]$$

This can be expressed in a more useful form in terms of the parameter (E/a)

i.e. $$\frac{E_b}{a} = \frac{E}{a} - \frac{7.75\ L}{V}(d-a)^2\left[\frac{1}{k_1} + \frac{1}{k_2}\right]$$

$$= \frac{E}{a} - 7.75\ L\left(\frac{a}{E}\right)\frac{(d-a)^2}{da}\left[\frac{1}{k_1} + \frac{1}{k_2}\right] \text{---------(5)}$$

A more rigorous treatment of this topic is given in the appendix.

2.5. Diffusion and Ion Spread.

Hübner's theory considered uniform ionization between two virtual plates. In reality, however, the ranges of the secondary electrons are such that the region of ionization is not restricted to the geometrical shape of the beam. This means that the ionization intensity is at a maximum along the beam axis and falls off to zero at a radius equal to beam radius plus the maximum range of the secondary electrons. The distribution of ion density is also influenced by diffusion of the ions outwards from the beam axis towards regions of lower concentration.

Saturation losses arising from this spread of ions beyond the beam diameter will depend on the dimensions of the chamber and the energy of the incident radiation. A free-air chamber ought to be designed so that both the plate separation and the plate length are sufficiently large as to allow the secondary electrons to reach their full range without striking the plates or the sides of the chamber. Attix and de la Vergne (1954) list data on losses for X-rays in the 60-250 KV range caused by plate separation inadequacy assuming the plate length to be sufficient. The plate length is usually greater than the separation since its effective length may be reduced by field distortion if the field is not properly guarded from the effects of the chamber casing (Kemp and Hall 1954). Provided the chamber geometry is

adequate, therefore, there will be no direct ion losses due to the spread of ions outside the beam.

Ion diffusion is also unlikely to cause losses in a free-air chamber. Since the plate separations are large there is little chance of an ion diffusing to the wrong electrode against the electric field. Similarly because of the long collecting plates, lateral diffusion will not result in ion losses.

The relationship between the ionization current and the applied voltage may, however, be affected by this spread of ions beyond the beam volume. As mentioned before (Chapter 2.3), equation (4) indicates that for small losses $(K_s - 1)$ is proportional to $(a/E)^2 L$. This implies that Hübner's formula remains unchanged by an increase in the beam diameter if the corresponding reduction in doserate is uniform since $L \propto 1/a^2$. This may not necessarily be true when one considers a central region of ionization surrounded by a fringe of low density ionization.

In order to investigate any change in the amount of recombination taking place due to this, let us consider a square beam of high density ionization surrounded by a larger square of lower density. Two square beams are chosen for mathematical simplicity since circular cross sections would involve more complicated integrations over width and ion density. (Fig.8).

Fig 8

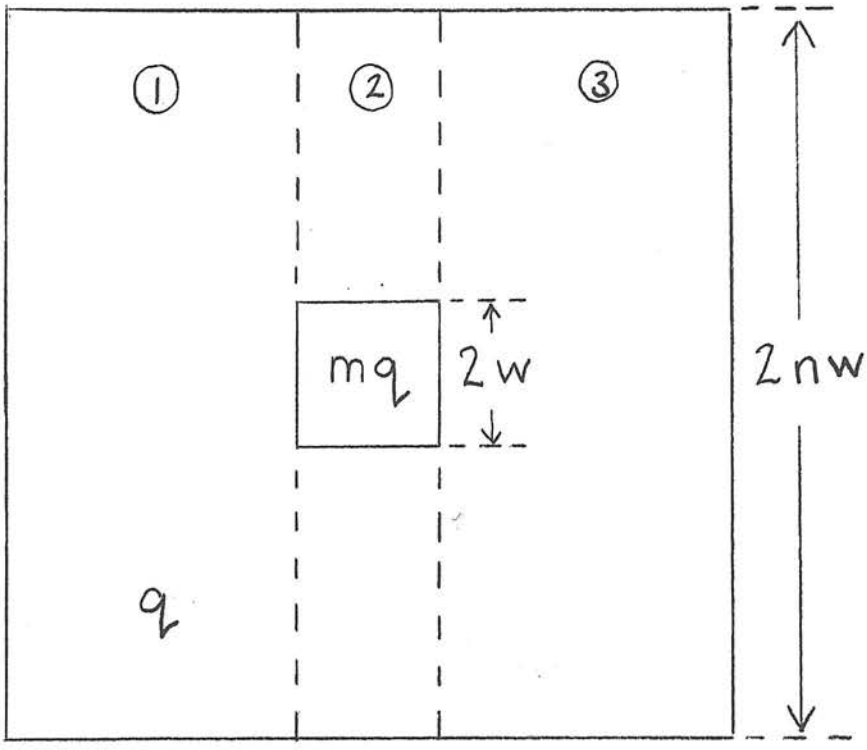

Non-uniform distribution of ionization in a square X-ray beam.

Fig. 9

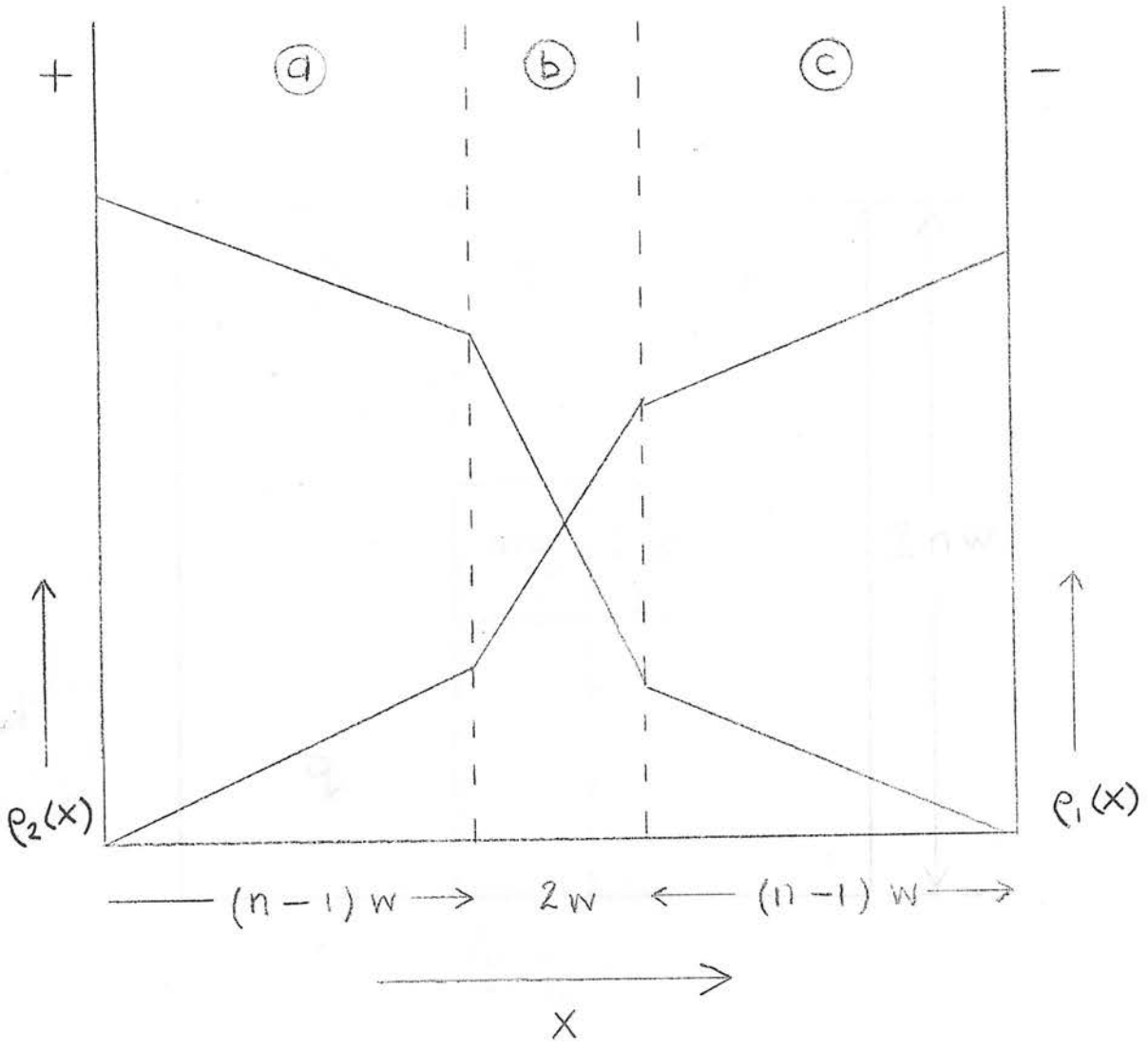

Distribution of charge density between the electrodes for region ② of Fig. 8

The diagram shows the cross-section of a beam comprised of a central square of side $2w$ where the ion production is mq. e.s.u./cm.^{3} sec. surrounded by a larger square of side $2nw$ where the ion production is q e.s.u./cm.^{3} sec.

Let $$\frac{f\ q\ w}{k_1\ k_2\ E} = C$$

Boag's theory gives $$R_1 = R_3 = \frac{\alpha}{e} C^2 (2n)^2 \frac{2\ n\ w}{6}$$

where R_1 represents the total recombination throughout region (1) per unit area of plate.

$$\therefore R_1 = R_3 = \frac{\alpha}{e} C^2 \frac{4\ n^3\ w}{3}$$

Fig. 9. shows the charge density distributions across the plates for region (2), which can be divided into three parts (a), (b) and (c). In part (a) the positive ion density ρ_1 (x) rises from zero at the positive plate to a value of C (n - 1) at x = (n - 1)w. In part (b) ρ_1 (x) increases more rapidly to a value of C (n - 1 + 2 m) at x = (n + 1) w. Finally in (c) ρ_1 (x) reaches C (2 n + 2 m - 2) at the negative plate with the same slope as in (a). The same argument can be applied to the negative ion density which rises in the opposite direction.

(a) Rate of recombination $= \frac{\alpha}{e} \rho_1 (x)\ \rho_2 (x)$

$$= \frac{\alpha}{e} \left[\frac{x}{(n-1)\ w} \cdot C (n-1) \right] \left[C (n-1) + 2 mC + \left(1 - \frac{x}{w(n-1)}\right) \cdot C (n-1) \right]$$

$$R_a = \int_0^{(n-1)w} \frac{\alpha}{e} \rho_1(x)\, \rho_2(x)\, dx = \frac{\alpha}{e} C^2 (n-1)^2 w \left[m + \frac{2n}{3} - \frac{2}{3} \right]$$

(c) Similarly $R_c = R_a$

(b)

$$R_b = \int_{(n-1)w}^{(n+1)w} \frac{\alpha}{e} \left[(n-1)C + \frac{[x-(n-1)w]mC}{w}\right]\left[(n-1)C + \frac{(1-[x-(n-1)w])2mC}{2w}\right] . dx$$

$$= \frac{\alpha}{e} C^2 2w \left[(n-1)^2 + 2m\left(\frac{m}{3} + n - 1\right)\right]$$

Total recombination per unit area of plate for region (2)

$$R_2 = R_a + R_b + R_c$$

$$\therefore \quad R_2 = \frac{\alpha}{e} \quad C^2 \quad 2w \left[(n-1)^2 \quad (m + \frac{2}{3} n + \frac{1}{3}) + 2 m \left(\frac{m}{3} + n - 1\right)\right]$$

Since R represents recombination throughout each region per unit area of plate, total recombination taking place between the plates is

$$r = R_1 \quad (n - 1) \; w \; + \; R_2 \; 2w \; + R_3 \; (n - 1) \; w$$

$$= \frac{\alpha}{e} \quad C^2 \quad \frac{4 \; w^2}{3} \left[(n-1)^2 \; (3 \; m + 2 \; n + 1) + 2 \; m \; (m + 3 \; n - 3) + 2n^3 \; (n-1)\right]$$

Now the total number of ions formed between the plates per second

$$= mq \; 4 \; w^2 + q \quad (4 \; n^2 \; w^2 \quad - 4 \; w^2)$$

$$= 4 \; w^2 \; q \quad (m + n^2 - 1)$$

This figure would also be obtained from a uniform intensity of ionization q.e.s.u./cm^3. sec. over a square of side $2 \; w \sqrt{m + n^2 - 1}$

In this case $R = \frac{\alpha}{e} \quad C^2 \; 4 \; (m + n^2 - 1) \quad \frac{2 \; w}{6} \sqrt{m + n^2 - 1}$

and $r = \frac{\alpha}{e} \quad C^2 \quad (m + n^2 - 1) \quad \frac{8 \; w^2}{6}$

$$\therefore \quad \frac{r \text{ unif}}{r \text{ non unif}} = \frac{2\,(m + n^2 - 1)^2}{\left[(n-1)^2\,(3m + 2n + 1) + 2m\,(m + 3n - 3) + 2n^3(n-1)\right]}$$

$$= y \quad \text{(say)}$$

Keeping m constant and differentiating y with respect to n, the condition for a stationary value for y is $\frac{dy}{dn} = 0$

$$\frac{dy}{dn} = n^4\,(1 - m) - 2\,n^2\,(1 - m) + (1 - m + m^2 + m^3) = 0$$

$$\therefore \quad n^2 = 1 \pm m$$

i.e. $n = \sqrt{1 + m}$ is the condition for a maximum value of y.

$$\therefore \quad y \text{ max} = \frac{8\,m^2}{m + 7\,m^2} = \frac{8\,m}{1 + 7\,m}.$$

$$\text{as } m \longrightarrow \infty \quad y \text{ max} \longrightarrow 8/7 = 1.143$$

Similarly by keeping n constant and differentiating y with respect to m we find the condition for $\frac{dy}{dm} = 0$ is $m = 1 \pm n^2$

Substituting $m = 1 + n^2$

$$y \text{ max} = \frac{8\,n^4}{n^2 + 7\,n^4} = \frac{8\,n^2}{1 + 7\,n^2}$$

$$\therefore \quad \text{as } n \longrightarrow \infty \quad y \text{ max} \longrightarrow 8/7.$$

This means that the maximum possible effect of non-uniformity of ionization on the amount of recombination is about 14 per cent. We have considered here a purely hypothetical situation in which there

Fig. 10

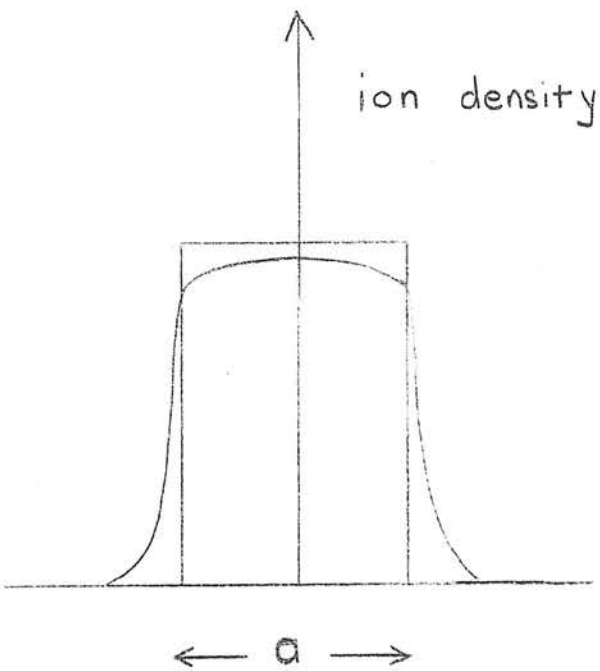

Schematic plot of ion density against distance from beam axis.

is a sharp boundary between the areas of high and low intensity ionization. In practice the distribution is not known accurately but will be approximately as in Fig. 10 and it seems reasonable to assume that y max. will be somewhat smaller in this case. It was decided, therefore, to ignore ion spread as far as the original Hübner formula was concerned.

On considering the space charge correction, however, we see that a reduction in ion density, whether uniform or not, will automatically reduce the screening effect of the space charge since it will be spread out over a larger volume. To take into account the ion spread we must replace the parameter $a\sqrt{\frac{3}{2}}$ in the space charge correction formula by $(a + c)\sqrt{\frac{3}{2}}$, where c represents the increase in diameter of the beam, and also reduce the dose-rate correspondingly. As an approximation c can be taken to be twice the average range of the secondary electrons.

Now at low tube voltages e.g. 10 - 50 KV, over 90 per cent of the secondary electrons are photo-electrons and these cause almost all the ionization, whereas at higher voltages e.g. 250 KV, most of the ionization is caused by the Compton recoil electrons. This means that for low voltages the average range of the photo-electrons should be chosen while at high voltages it is the average range of the Compton electrons which is required. At intermediate voltages, however, when neither the photo nor the recoil electron contribution can be neglected, it is extremely difficult to determine the appropriate range of the secondary electrons to be used in the theoretical formula.

2.6 Final Form of Theory.

The final form of the theory is thus obtained by substituting $(a + c)\frac{\sqrt{3}}{2}$ for a and $L\frac{a^2}{(a + c)^2}$ for L in the space charge equation for E_b (2.4) and then substituting for E_b in equation (4)

$$\text{i.e. } E_b = \frac{V}{d} - \frac{7.75\ L\ a}{V}(d - a)^2\left[\frac{1}{k_1} + \frac{1}{k_2}\right]$$

becomes

$$E_b = \frac{V}{d} - \frac{7.75\ L\ a^2\ (a+c)\frac{\sqrt{3}}{2}\left[(d-(a+c)\frac{\sqrt{3}}{2})\right]^2}{V\ (a + c)^2}\left[\frac{1}{k_1} + \frac{1}{k_2}\right]$$

$$\therefore \quad \frac{E_b}{a\frac{\sqrt{3}}{2}} = \frac{E}{a\frac{\sqrt{3}}{2}} - \frac{7.75\ L\ a}{V\ (a + c)}\left[d - (a + c)\frac{\sqrt{3}}{2}\right]^2\left[\frac{1}{k_1} + \frac{1}{k_2}\right]$$

$$\therefore \quad K_s = \tfrac{1}{2} + \tfrac{1}{2}\left\{1 + \frac{\frac{1}{90}\frac{\alpha}{e}\frac{1}{k_1 k_2}L}{\left[\frac{E}{a\frac{\sqrt{3}}{2}} - 7.75L\left(\frac{a\frac{\sqrt{3}}{2}}{E}\right)\frac{\left[d-(a+c)\frac{\sqrt{3}}{2}\right]^2}{d(a+c)\frac{\sqrt{3}}{2}}\left(\frac{1}{k_1}+\frac{1}{k_2}\right)\right]^2}\right\}^{1/2} \qquad \text{----------(6)}$$

While this equation provides a more accurate representation of the physical situation than does Hübner's formula, it must be remembered the suggested modifications are only approximate solutions to the problems involved.

CHAPTER 3.

OPERATION OF FREE-AIR CHAMBER AND EXPERIMENTAL RESULTS.

Fig 11.

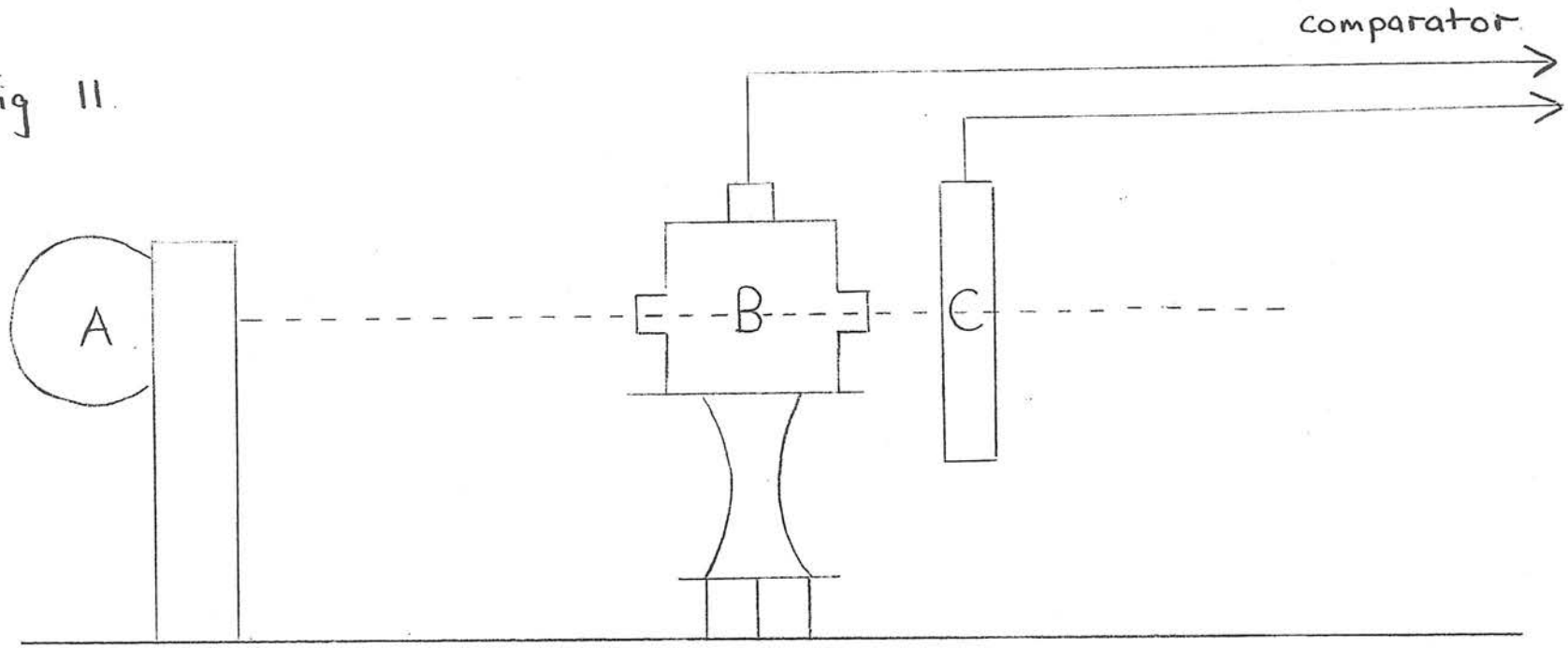

Experimental arrangement

A = X-ray tube head ; B = free-air chamber ; C = monitor chamber

Fig 12

Free-air Ionization Chamber

In order to verify Equation (6) a series of experiments was undertaken to determine the dependence of the ionization current on the various parameters involved, e.g. field strength, doserate, beam quality and aperture size and shape.

3.1 Apparatus.

The experimental arrangement is shown in Fig.11. The source of X-rays was a Müller superficial therapy set and the tube head was clamped to a stand at the end of the bench. The free-air chamber (Fig.12) was designed by Greening (1960) for use in the 10 - 50 KV. region. It is a simple compact chamber with a diameter of 6 cm. and a collecting electrode 1 cm. wide in the direction of the X-ray beam. The plate separation is 4 cm. and this value enables diaphragms of up to 1 cm. to be used without incurring ionization losses greater than 1 per cent. At low KV, absorption in the air between the diaphragm and the collecting electrode can be considerable, therefore it is desirable to make this distance as short as possible. The air absorption path in this chamber is 3.7 cm. which minimises the amount of absorption but is sufficient to ensure electronic equilibrium and prevent any electrons ejected from the diaphragm reaching the collecting volume. This small value

Fig 13

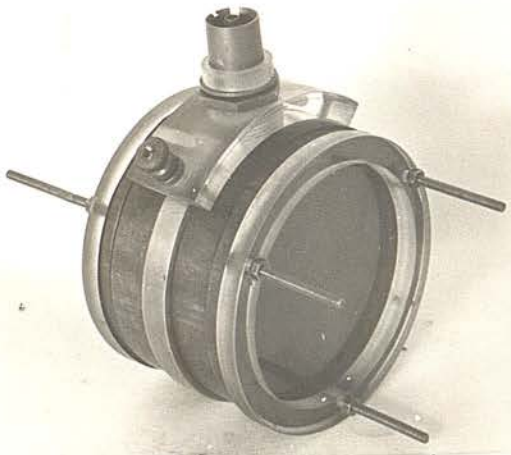

Monitor Chamber

for the air absorption path was made possible because Greening employed a new method of field guarding, i.e. the guard strip system, first proposed by Kemp (1956) and elaborated by Kemp and Barber (1957, 1958). These strips give very efficient electrical shielding and lead to the generally compact design of the chamber.

The monitor (Fig.13) was a coin-shaped chamber with a central collecting plate of graphited Tufnol mounted on the centre pin of a Telcon socket. The chamber volume was determined by an aluminium ring to which was clamped two high tension electrodes of graphited film base. The spacing between the collector and the H.T. plates could be increased by the addition of two similar brass rings. A set of rings of various widths was constructed so that the chamber volume could be altered as required.

The lead screen between the X-ray source and the free-air chamber had a central aperture thus allowing the beam to pass unimpeded through the chamber diaphragm, while preventing any scattered radiation from the tube and housing reaching the chambers. It also served as a holder for various filters.

The two chambers were fed with voltages of opposite polarity from a bank of dry batteries via coaxial screened cables. The ionization currents were compared by a modified version (Greening 1953) of the Kemp comparator (Kemp 1945, 1946).

In principle, the Kemp comparator consists of two Townsend balance circuits, one of which has a variable condenser (Fig.14). The ratio of the ionization currents is measured by adjusting the

Fig. 14.

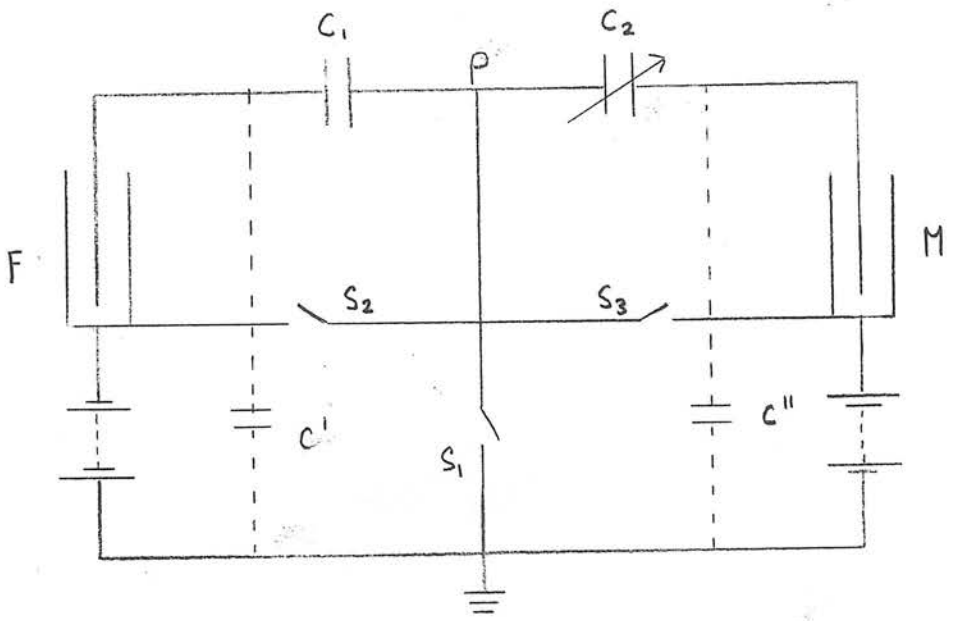

Circuit of Kemp Comparator

F - free-air chamber

M - monitor chamber

variable condenser C_2 so that the point P remains at earth potential when the shorting switches S_1, S_2 and S_3 are opened. It can be shown that if Q_1 and Q_2 are the charges which accumulate in the chambers F and M respectively in any given time, then P will stay at earth potential provided

$$\frac{Q_1}{Q_2} = \frac{C_1 + C^1}{C_2 + C''} \cdot \frac{C_2}{C_1}$$

where C' and C'' are the capacities to earth of systems F and M respectively.

This means that the setting on the capacity divider scale required to keep P at earth potential gives a measure of the ratio $\frac{Q_1}{Q_2}$

The modification suggested by Greening was the introduction of a variable condenser C_3 connected in parallel with C'' and ganged to C_2 in antiphase such that $C_2 + C_3$ is constant.

Then $$\frac{Q_1}{Q_2} = \frac{C' + C_1}{C'' + (C_2 + C_3)} \cdot \frac{C_2}{C_1}$$

and the charge ratio is thus independent of C' and C'' except for a constant factor. This means that the instrument can be calibrated to be direct reading and is independent of the cables and chambers used.

The point P of the comparator circuit is connected to a sensitive potential detecting device which indicates by a null deflection that C_1 and C_2 are correctly balanced. The null indicator in our instrument was the needle of a Lindemann electrometer. A Lindemann

has the advantages over an electrometer triode of requiring no warming-up period and having no possibility of inherent needle drift. The main disadvantage of a Lindemann is that observations are not so easily made as with the valve system (microscope eyepiece scale readings as against galvanometer readings).

In our experiments the comparator was operated with the fixed condenser C_1 shorted out as proposed by Worthley, Thompson and Tooze (1957) to ensure that the collector and guard plate were maintained at the same potential during the charge comparison. This is a necessary condition if the volume from which the ions are collected is to remain constant throughout the period of measurement.

3.2. Experimental Procedure.

Alinement of the free-air chamber along the beam axis was checked by taking radiographs of the beam emerging from the exit aperture. The monitor chamber supply was kept constant at 300 volts throughout the experimental series. Its plate separation and hence its ionization current was varied so that balance points were obtained in the most accurate region of the comparator dial. Measurements of up to 15 per cent ion loss were made by reducing the voltage across the free-air chamber. The maximum voltage usually applied to the chamber was about 1300 V (i.e. a field strength of 325 V/cm.). The ionization current was then assumed to be saturated provided it remained unchanged on the reduction of several hundred volts.

For most of the experiments the tube voltage was 45 KV and the filter was 0.021 in.Al. giving a doserate of 100 r/min. at a distance of 30 cm. from the focal spot. The doserates at the diaphragm of the free-air chamber were measured by an E.I.L. Model 37A portable electrometer. Values from 10 to 1000 r/min. were obtained by altering the distance of the chamber from the X-ray source. Three circular apertures - 1/16, 1/8 and 5/16 in. - were used over as wide a range of doserate as possible. Different aperture sizes were necessary since small apertures could not be used at low doserates because of lack of sensitivity while large apertures presented saturation problems at high doserates.

Fig 15.

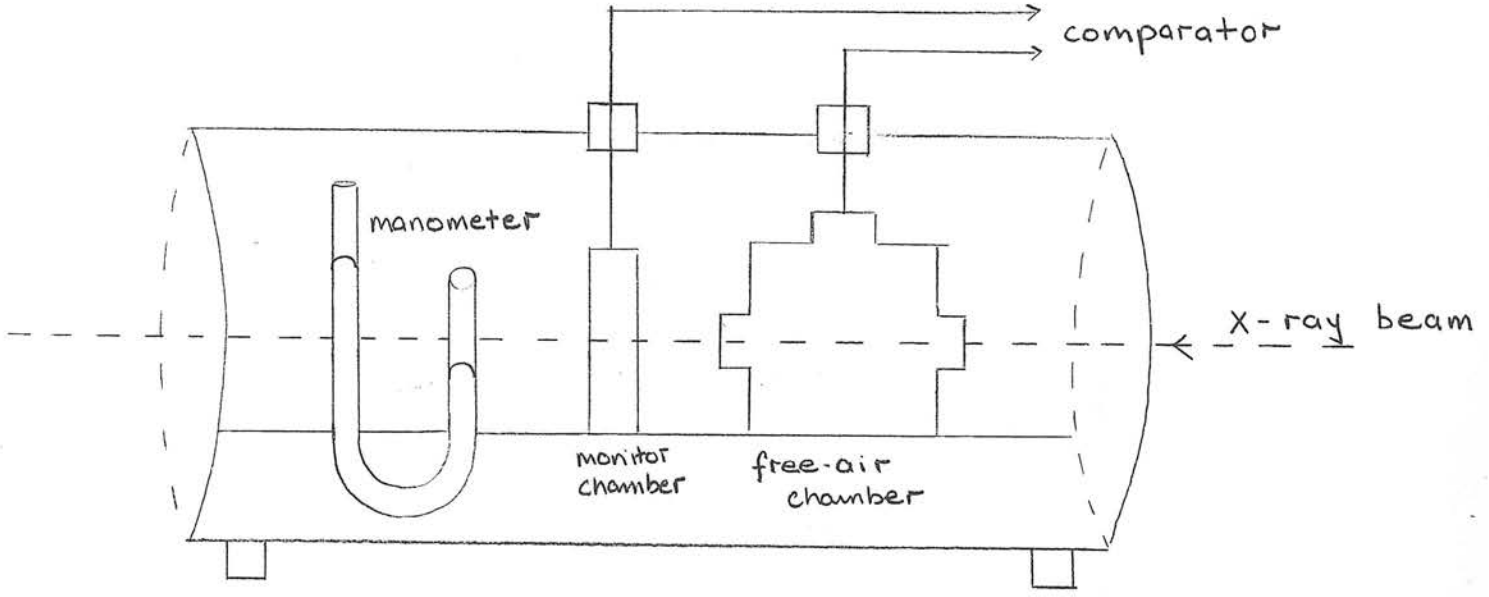

Experimental arrangement for performing saturation runs at various pressures.

In order to investigate the effect of aperture shape, several square and rectangular apertures were tried at different orientations. Some experiments were also carried out at 20 and 85 KV to observe the influence of beam quality. The half value layer (H.V.L.) of an X-ray beam is the filter thickness which reduces its doserate to one-half of its former value. The H.V.L. in aluminium for our various radiations were found graphically from measurements on the reduction in doserate with increasing filtration.

Room temperatures and pressures were recorded during each experimental run. The theoretical variation of K_s with temperature and pressure is discussed in Chapter 3.3. Since the temperature varied only slightly throughout the experimental series, no experimental confirmation was attempted. The effect of pressure was, however, investigated. This was done by enclosing the chambers in an airtight tin (Fig.15) and making experimental runs at various pressures.

The coaxial cables were connected to the chambers via rubber stoppers fitted tightly into the roof of the tin. Leakage of air along the screen braidings was minimised by coating the cable ends with Bostic and binding them with rubber tape. This remedy did not reduce the flexibility of the cables nor impair their insulation. Pressure measurements at the beginning and end of each run were made on a Mercury manometer connected to the side of the tin.

3.3. Correction of Results for Temperature and Pressure.

The experimental results for K_s require to be corrected to standard temperature and pressure conditions, i.e. 22°C and 760 mm. Hg. Boag (1952) defined a quantity

$$\eta = \frac{\alpha}{3e\ k_1\ k_2} \cdot j \cdot \frac{d^3}{V^2}$$

and proves that $f = 1/(1 + \eta)$

i.e. $K_s - 1 = \eta = \frac{\alpha}{3e\ k_1\ k_2} \cdot j \cdot \frac{d^3}{V^2}$

Thus for given V and D, $K_s - 1 \propto \frac{\alpha}{e} \cdot \frac{1}{k_1\ k_2} \cdot j$

Now for a given L, j is proportional to density, i.e. P/T

$\therefore$ for given V, d and L, $K_s - 1 \propto \frac{\alpha}{k_1\ k_2} \cdot \frac{P}{T}$

Von Engel (1955) discussed the variation of mobilities and recombination coefficient with temperature and pressure. He gives $k \propto$ 1/density i.e. $k \propto T/P$. and for air at pressures below 1,000 mm.Hg. $\alpha \propto P.T.^{-5/2}$

Thus $K_s - 1 \propto P.T.^{-5/2} \cdot \frac{P^2}{T^2} \cdot \frac{P}{T}$

$$\propto P^4 \cdot T^{-11/2}$$

The pressure dependence of K_s was verified experimentally by comparing the ratios of K_s values for the same L and E/a at different pressures with the theoretical ratios. The following results are for two pressures P_1 = 670 mm.Hg. and P_2 = 846 mm.Hg.

The respective temperatures are $T_1 = 21.5^{\circ}C$ and $T_2 = 23^{\circ}C$.

$$\left(\frac{P_1}{P_2}\right)^4 = 2.53 \qquad \left(\frac{T_2}{T_1}\right)^{11/2} = 1.03$$

$\therefore$ Theoretically $\dfrac{(K_s - 1)_1}{(K_s - 1)_2} = \left(\dfrac{P_1}{P_2}\right)^4 \times \left(\dfrac{T_2}{T_1}\right)^{11/2} = 2.61$

Experimental Results.

E/a	$(K_s - 1)_1$	$(K_s - 1)_2$	$\dfrac{(K_s - 1)}{(K_s - 1)_2}$
70	0.097	0.037	2.62
80	0.07	0.027	2.60
90	0.055	0.021	2.62
100	0.045	0.017	2.64
110	0.038	0.0145	2.62
120	0.032	0.012	2.66
			2.63 Mean.

Agreement between theory and experiment is within 1 per cent.

Fig. 16

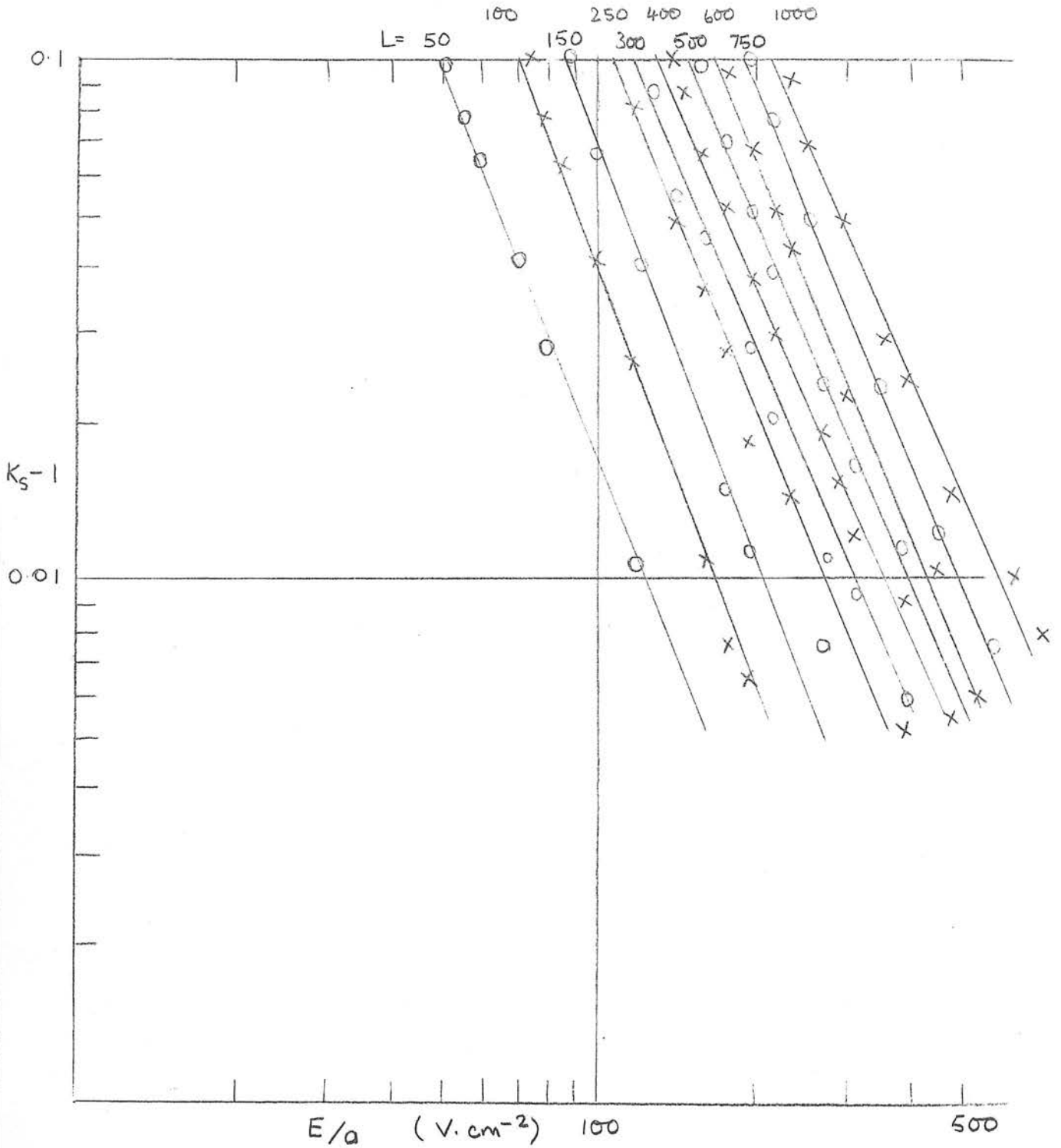

Plot of $(K_s - 1)$ against E/a for various doserates for 1/16 in. diaphragm.
(Dose rates and beam diameter are measured at diaphragm)

Fig 17

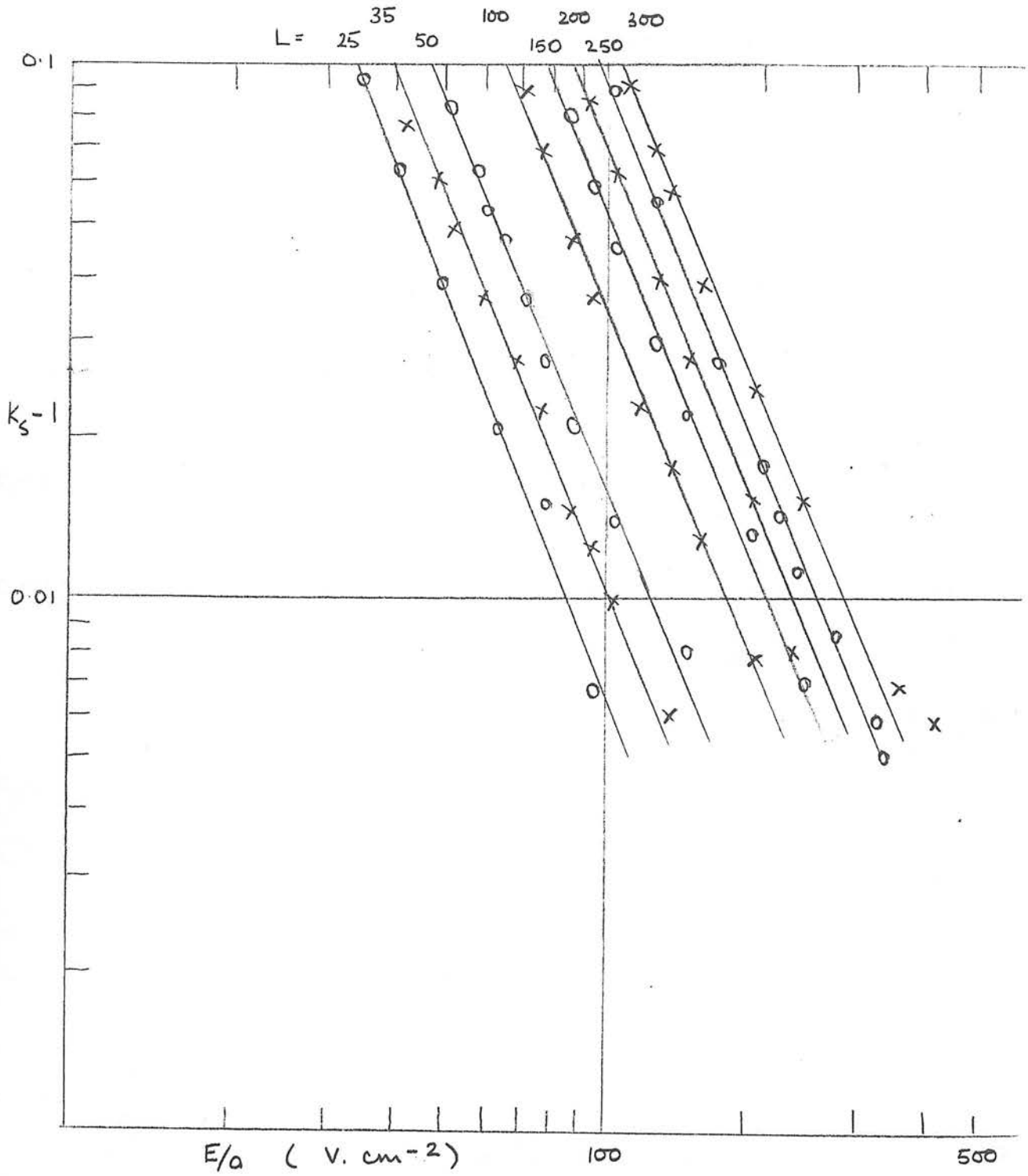

Plot of $(K_s - 1)$ against E/a for various doserates for $\frac{1}{8}$ in. diaphragm

Fig 18

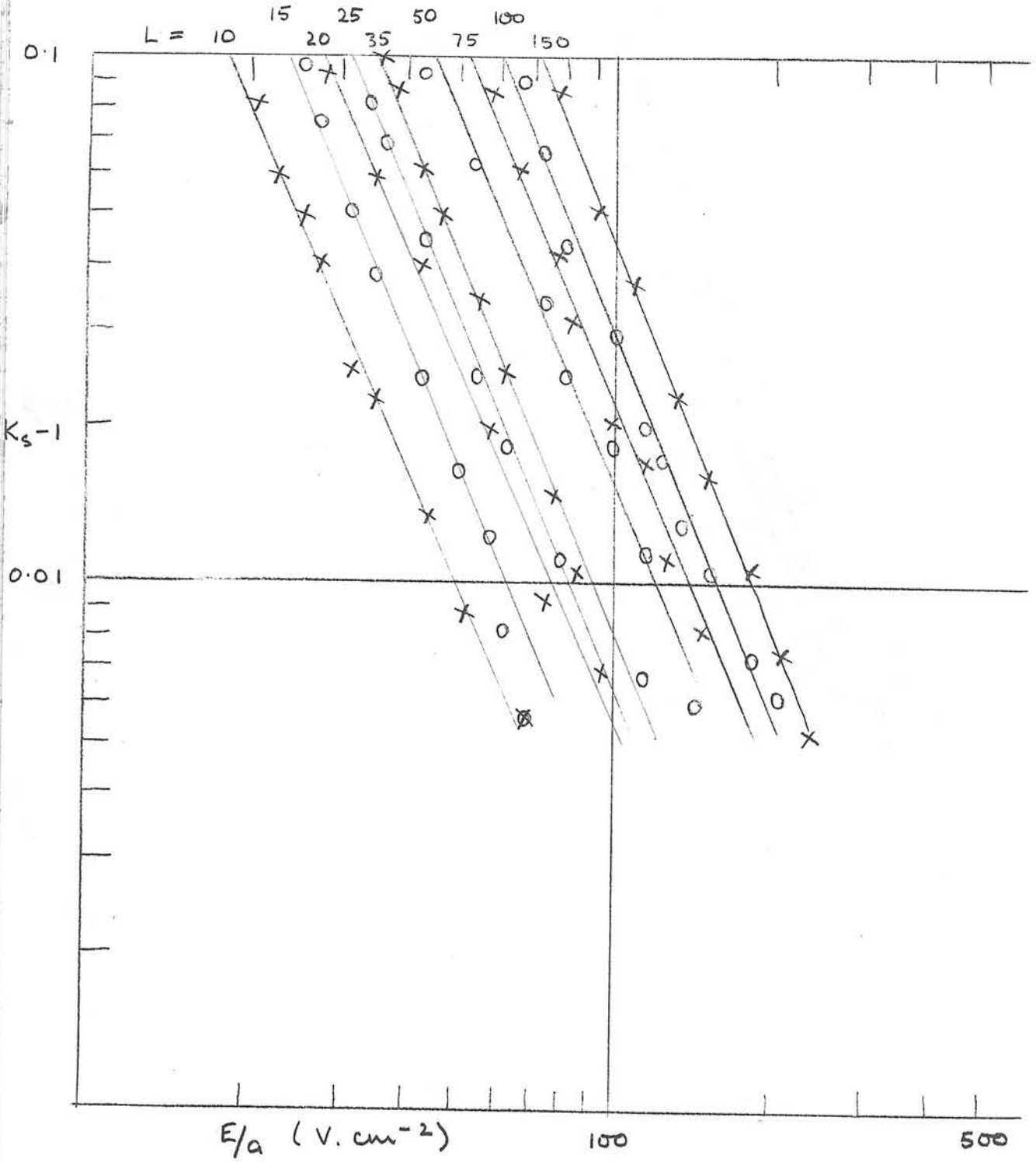

Plot of $(K_s - 1)$ against E/a for various dose rates for 5/16 in diaphragm

Fig 19

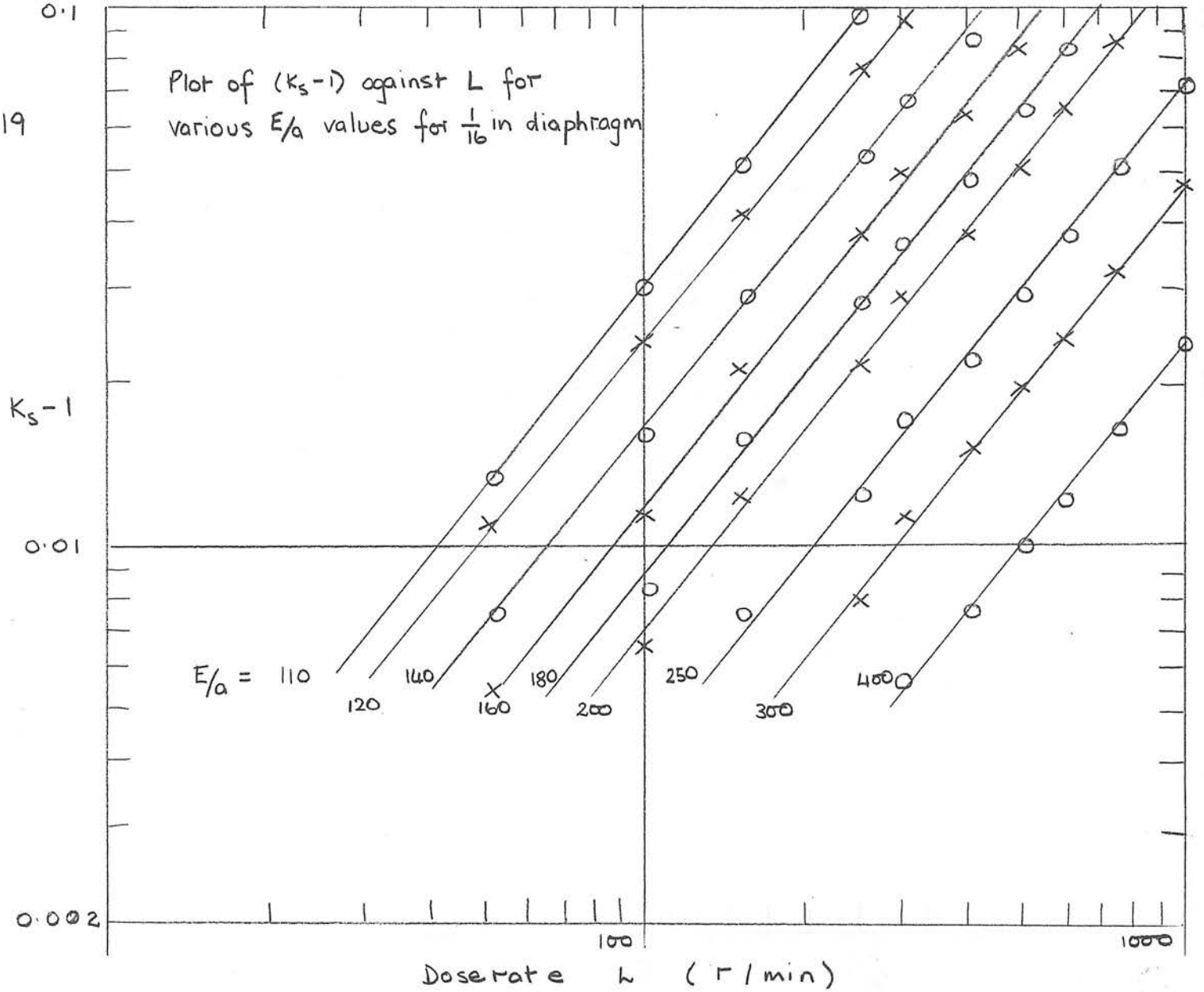
Plot of $(K_s - 1)$ against L for various E/a values for $\frac{1}{16}$ in diaphragm
0·1
0·01
0·002
$K_s - 1$
E/a = 110
120
140
160
180
200
250
300
400
100
1000
Dose rate L (r/min)

Fig 20

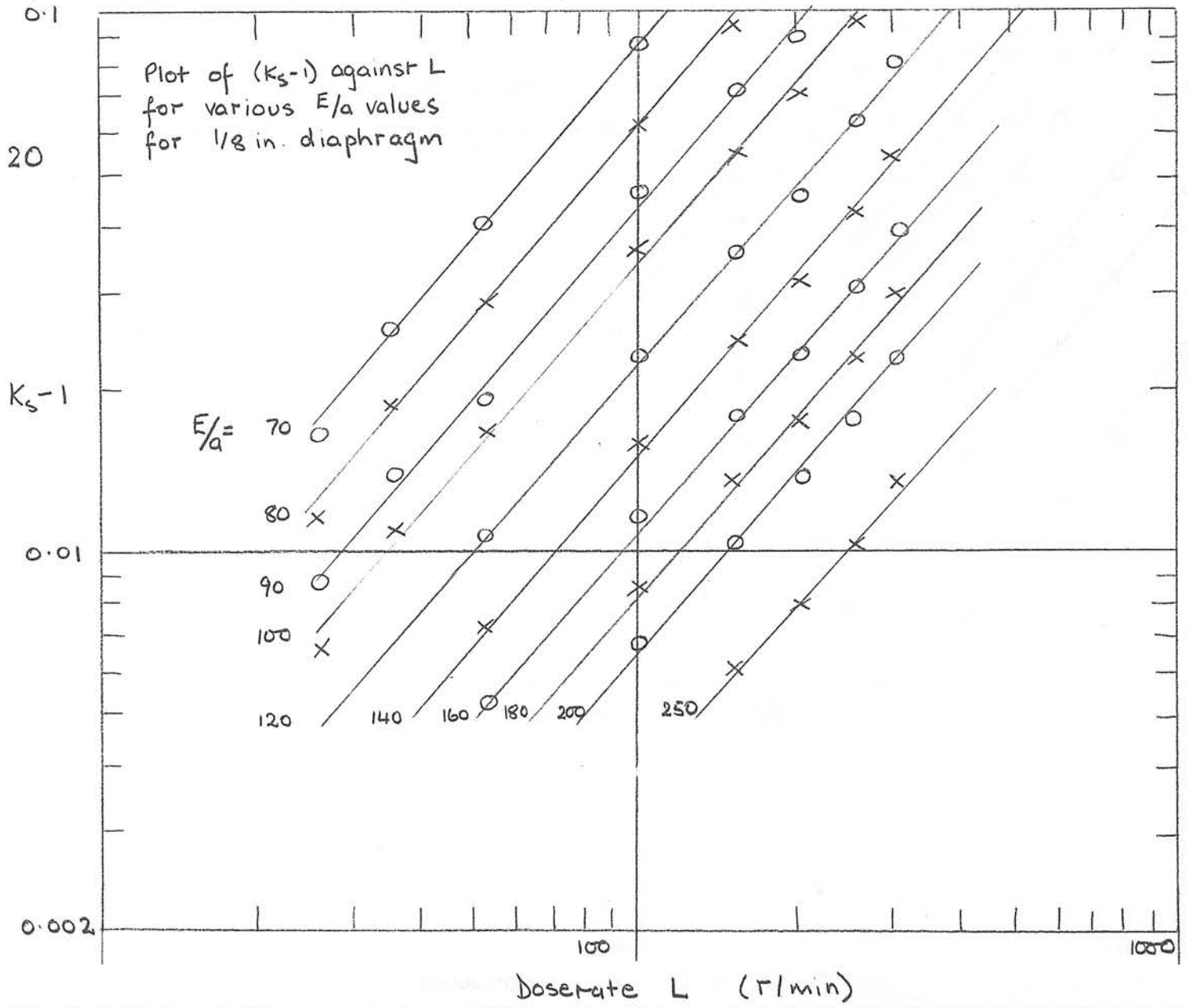
Plot of (K_s-1) against L for various E/a values for 1/8 in. diaphragm
K_s-1
0·1
0·01
0·002
E/a= 70
80
90
100
120
140
160
180
200
250
100
1000
Doserate L (r/min)

Fig 21

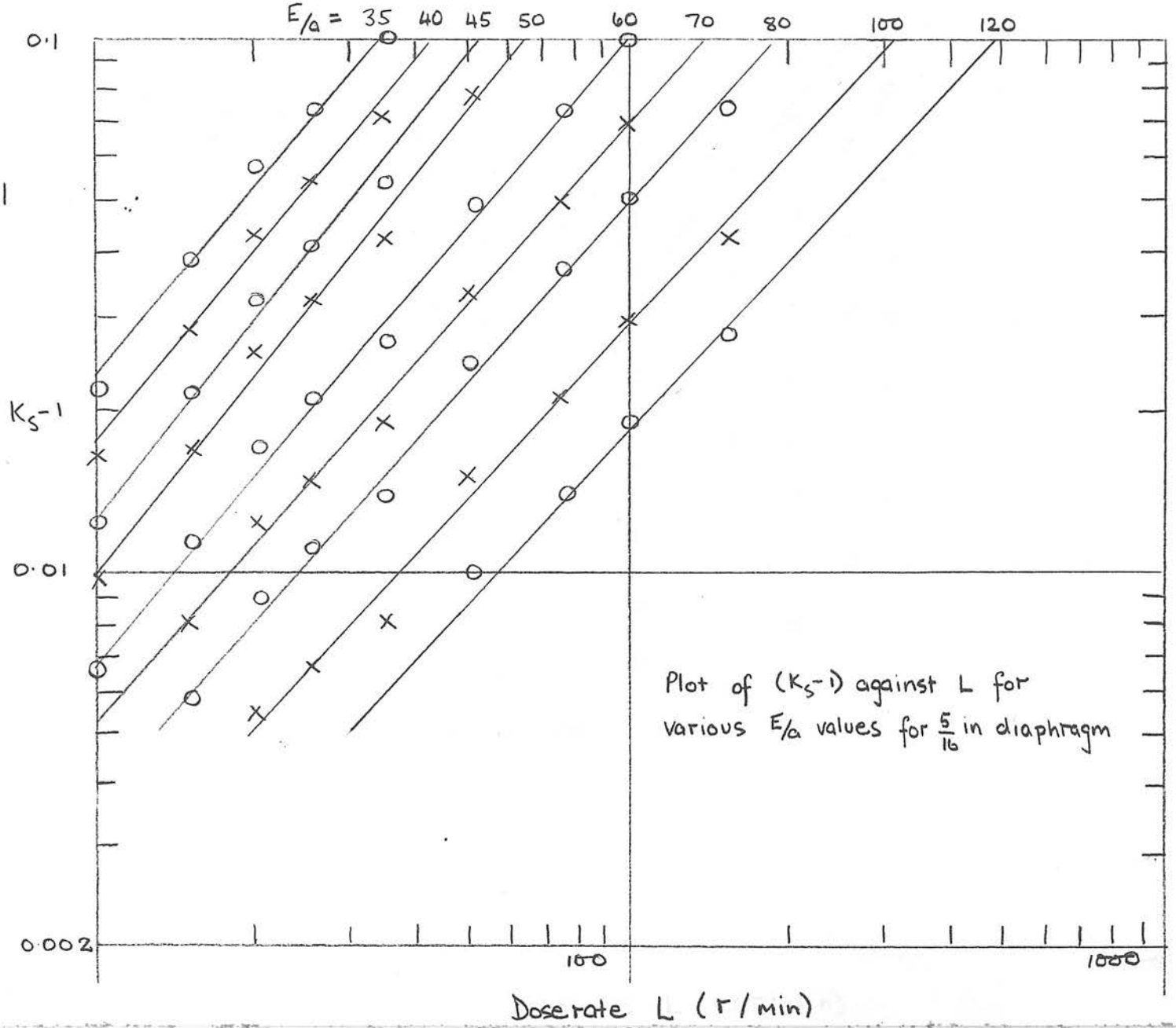
E/a = 35 40 45 50 60 70 80 100 120
0·1
$K_S - 1$
0·01
0·002
100
1000
Dose rate L (r/min)
Plot of $(K_S - 1)$ against L for various E/a values for $\frac{5}{16}$ in diaphragm

3.4 Experimental Results.

The simplest way to present the experimental results is graphically. $(K_s - 1)$ can either be plotted on a double log scale against E/a with L as parameter, or against L with E/a as parameter.

Examples of the graphs obtained are shown in Figures 16-21. When $(K_s - 1)$ is plotted against E/a for various doserates, a family of approximately straight parallel lines is obtained with an average slope of about - 2.6. Curves for the 1/16 in. aperture (Fig.16) and the 1/8 in. aperture (Fig.17) are almost coincident, while those for the 5/16 in. aperture (Fig.18) are displaced slightly in the direction of decreasing doserate. Taking E/a as parameter and plotting $(K_s - 1)$ against L results in another series of approximately straight parallel lines with an average slope of about 1.3 (Figs. 19 - 21).

These slopes are some 20 per cent greater than those predicted by Hubner's formula. For small values of K_s equation (4) may be written

$$K_s = 1/2 + 1/2 + \frac{m}{4}\left(\frac{a}{E}\right)^2 \cdot L$$

$$\therefore K_s - 1 = \frac{m}{4}\left(\frac{a}{E}\right)^2 L$$

$$\therefore \log (K_s - 1) = \log \frac{m}{4} - 2 \log\left(\frac{E}{a}\right) + \log L.$$

i.e. a plot of $\log (K_s - 1)$ against $\log \frac{E}{a}$ for constant L has a slope of -2.0 while that against log L for constant $\frac{E}{a}$ has a slope of 1.0.

3.5 Experimental Errors.

One source of experimental error lay in reading balance points on the comparator. Since care was taken always to use the most accurate region of the dial, the observational accuracy was 0.1 per cent throughout. Measurements of large ionization currents could be reproduced within this accuracy while for the lowest ionization currents, reproducibility was about 0.2 per cent.

The other main source of error arose in the determination of the saturation current. Since $K_s = j_{s/j}$ any ion losses due to inadequate chamber geometry will not affect K_s values but if the maximum applied voltage is not sufficient to attain saturation conditions, there will be an error in the value of j_s and hence K_s. Methods of estimating the degree of saturation at maximum voltage are considered in Chapter 5.2.

CHAPTER 4.

COMPARISON OF THEORY AND EXPERIMENT FOR A FREE-AIR CHAMBER.

Some thought had to be given to the choice of k_1, k_2 and $\mathcal{L}$ before theoretical values of K_s could be calculated. The values for these constants reported in the literature proved somewhat conflicting. Our two main sources of reference were Thomson and Thomson (1928) and Loeb (1955).

4.1. Mobilities.

Thomson and Thomson survey the data up to 1927. They point out that there is considerable divergence between the values for mobilities obtained by different observers suggesting that the results were affected by several per cent by the experimental conditions.

They give as the probable mean value

$k_1 = 1.36$ cm.^{2}/sec. V) Room temperature
$k_1 = 2.1$ cm.^{2}/sec. V) and pressure.

Loeb, however, says that mobilities measured under the older standard conditions only have significance when applied to the particular experimental arrangement used, due to the ageing of ions, impurities, method of ionization etc. He therefore dismisses the earlier published tables as of no value except for indicating the order of magnitude. He recommends the work of Bradbury (1932) who used an X-ray ionization method of high

resolving power in an all-glass, baked out chamber.

He found

$k_1 = 1.59$)
) filtered air at room temperature
$k_2 = 2.21$) and pressure

Loeb points out that data acquired early in the century before the development of short time resolution and employment of clean gases in outgassed chambers are subject to errors of at least 20 per cent compared to Bradbury's experimental errors of 2 per cent. We therefore decided to adopt Bradbury's results although no attempt had been made to filter the air in our free-air chamber.

4.2. Recombination coefficient.

Again Thomson and Thomson list values obtained by different observers. They recommend the work of Thirkell who used X-ray ionization and Langevin's method of measurement, resulting in

$$\alpha = 1.6 \times 10^{-6} \text{ cm.}^3 / \text{sec.}$$

Loeb has an excellent chapter on the recombination of ions. As before he criticises older methods of measurement which were carried out with outdated equipment and techniques, usually with impure gases and ions of indefinite and time-varying character. Owing to this, and to the lack of correction for losses and errors due to diffusion, the results of earlier studies are again of little value. Loeb recommends the work of Sayers (1938) using a commutator method with X-ray ionization and measurement of ion losses due to recombination. Before choosing a value for α, however, one must decide what type of recombination is taking place in the free-air chamber. In X-ray ionization at atmospheric pressure both initial and volume recombination may be present (Chapter 1.1). Since the ion density is greatest for the initial non-random distribution, the recombination coefficient will decrease from its initial value as the ions begin diffusing apart until a constant value is reached for the completely random distribution.

In our experiments even the lowest ionization intensity - 10 r./min. i.e. 3.5×10^8 ion pairs/cm.^{3} sec. - seemed sufficient to create a reasonably isotropic distribution of ions. The presence of a strong electric field also helped to minimise the amount of initial recombination which we therefore decided to ignore. Further justification of this assumption is given in Chapter 5.

Sayer's value for the volume recombination coefficient in air adopted by us is $\alpha = 2.3 \times 10^{-6}$ cm.^{3}/sec.

Perhaps a comment on Sayer's paper could be made at this point. He found that the value of α changed with X-ray intensity to a remarkable extent. For example, by trebling the exposure time of the X-Rays, i.e. by increasing the ion density by a factor of three, he obtained a decrease in the value for α of about 14 per cent. Also by replacing the glass wall of his ionization chamber with a piece of cardboard, he found α to decrease by approximately 60 per cent. He explained the lowering of α with exposure time by postulating the formation of complex molecules which decrease the ionic mobility. These findings cast some doubt on Sayer's work, especially since in our own experiments the single value chosen for α seems to satisfy all dose-rates which differ by as much as a factor of 100.

It seems surprising that some sixty years after ionic recombination was first investigated, more satisfactory information on α is not available.

Figs 22 - 23

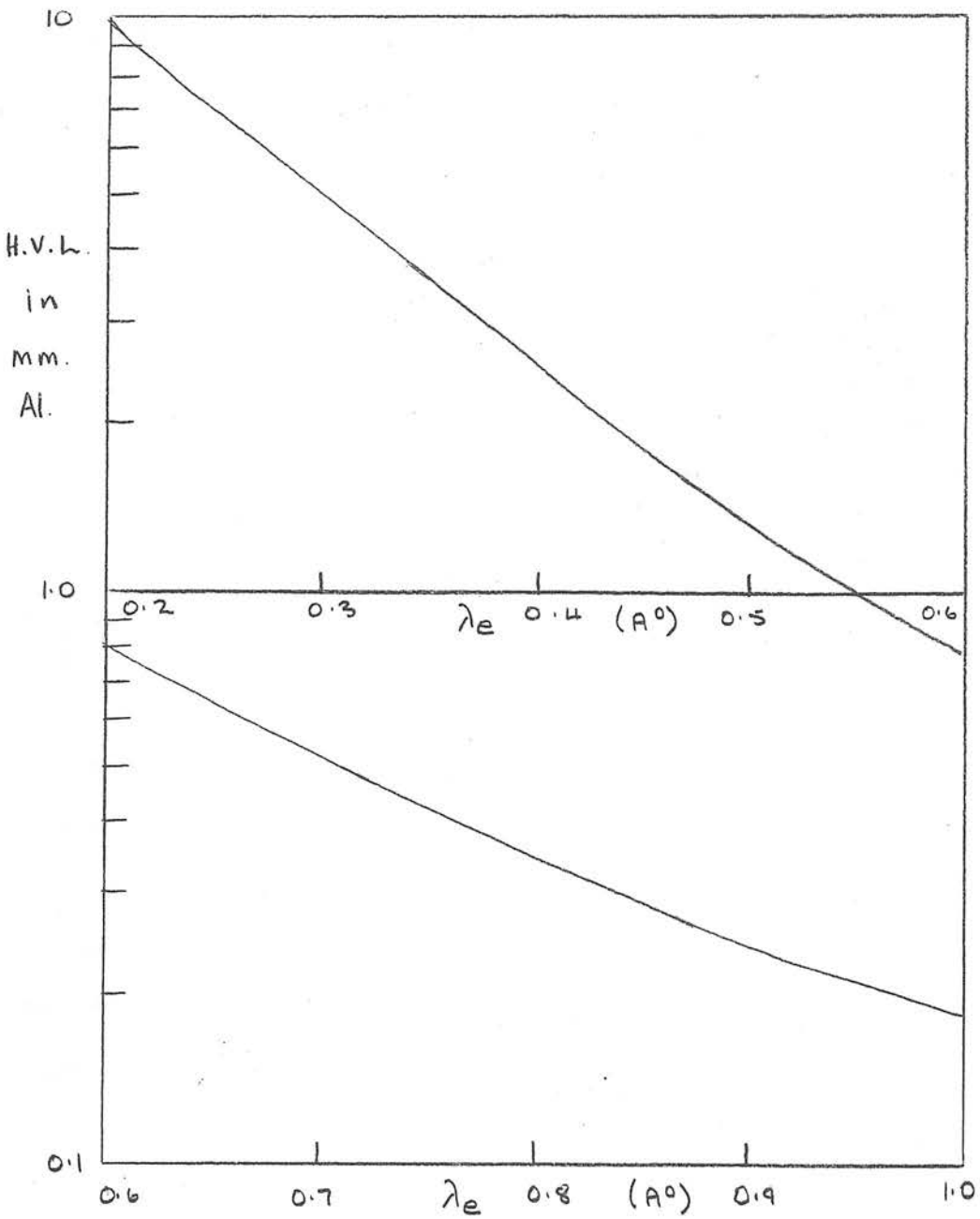

Relationship between effective wavelength λe in A° and H.V.L. in mm. Al.

4.3 Evaluation of c.

c was defined in Chapter 2.5 as twice the average range of the secondary electrons. One effective wavelength λ_e of an X-ray beam is the wavelength of the monochromatic radiation which has the same H.V.L. Figures 22-23 illustrate the relationship between the effective wavelength and the H.V.L. in aluminium. These curves were derived from the formula $\mu(\lambda_e) = \frac{\cdot 6931}{\text{H.V.L.}} (\lambda_e)$ using values for the absorption coefficient μ compiled by Greening (1947). The effective energy of the secondary electrons in KeV is connected to the effective wavelength in A^o by the relation KeV $= 12.4/\lambda_e$

Thus a measurement of the H.V.L. of an X-ray beam provides an estimate of the electron energy. The average range of electrons (photo or recoil depending on the tube voltage) for this energy was found from data given by Lea (1946).

Table 1 shows the photo-electron ranges in air for the various H.V.L. values used in our experiments. These ranges are, of course, approximate values since there is a spread of electron energies present and the electron tracks are not always straight, due to scattering by atoms.

Table 1.

Tube KV	H.V.L. in mm.Al.	Effective Secondary electron KeV	Proportion of energy appearing as photo electrons	Approx. range in mm. air.
20	0.19	13	0.999	3.5
20	0.36	16	0.996	4.5
45	0.45	17	0.990	5.0
85	0.75	20	0.986	7.0
85	4.46	41	0.833	22.0

Fig 24

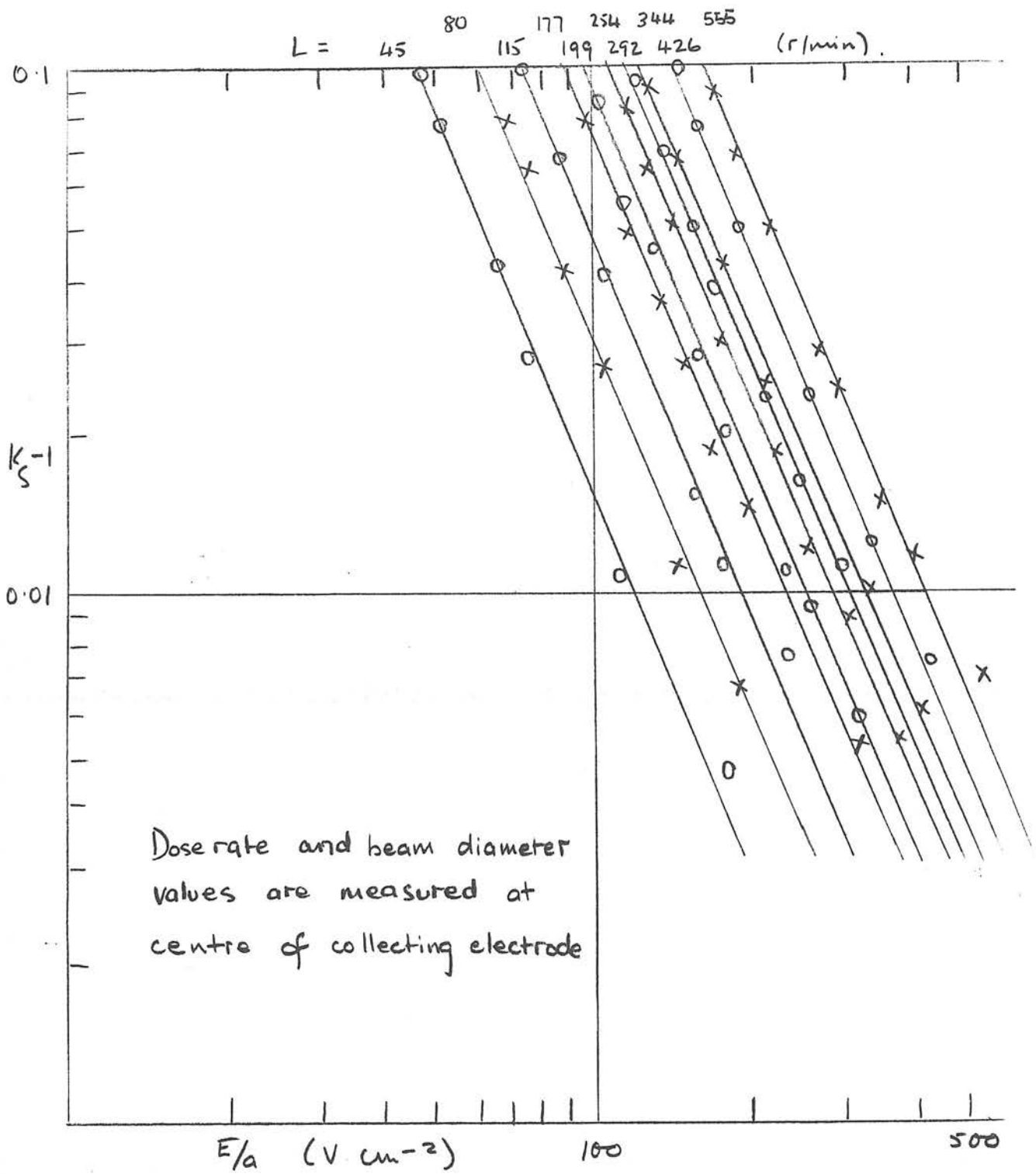

Comparison for 1/16 in. diagram of theoretical ($K_S - 1$) values drawn as continuous curves with experimental results represented as points

Fig 25

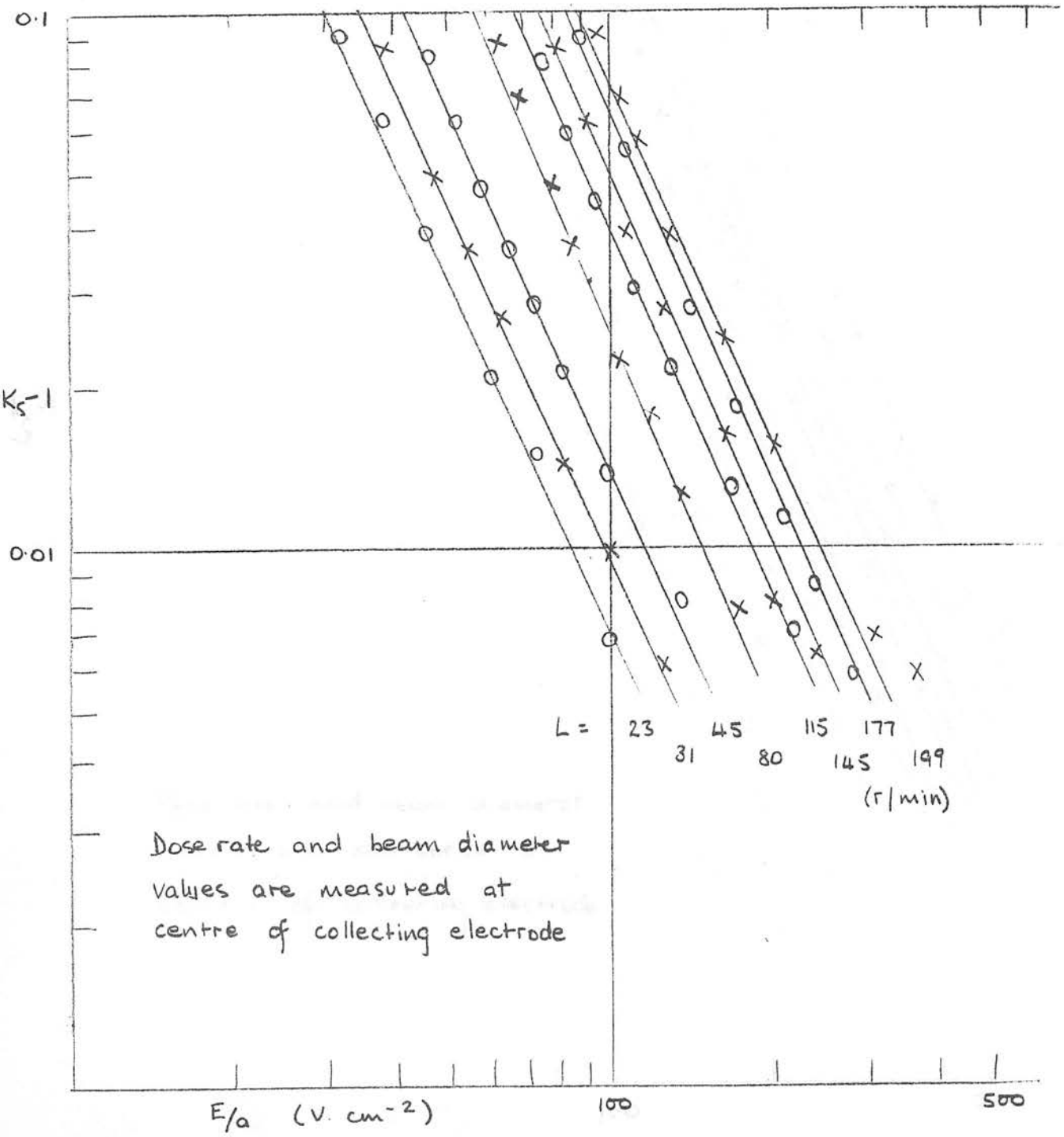

Comparison for 1/8 in diaphragm of theoretical values of $(K_s - 1)$ drawn as continuous curves with experimental results represented as points

Fig 26

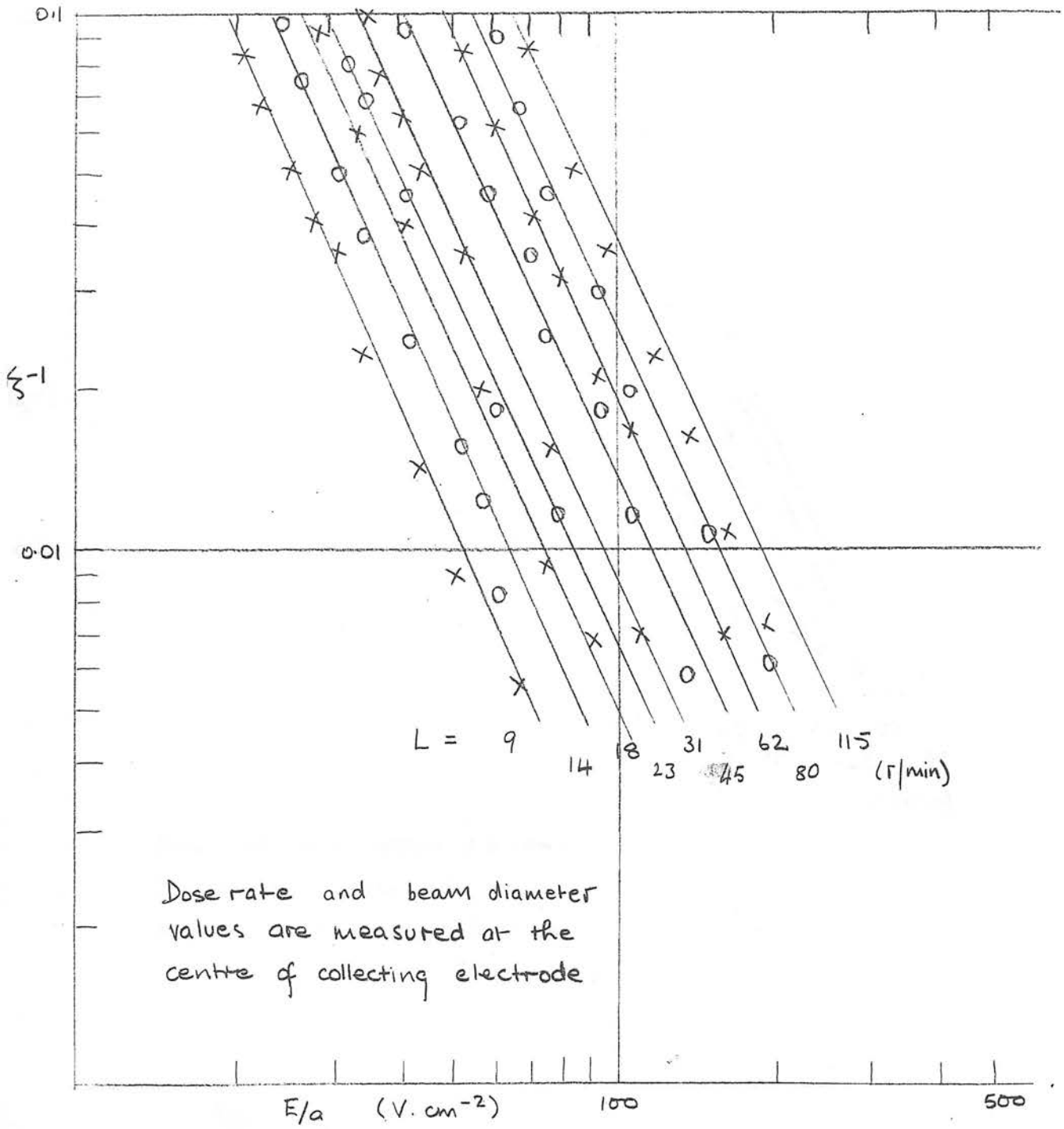

Comparison for 5/16 in. diaphragm of theoretical values of (K_s^{-1}) drawn as continuous curves with experimental results represented as points

Fig 27

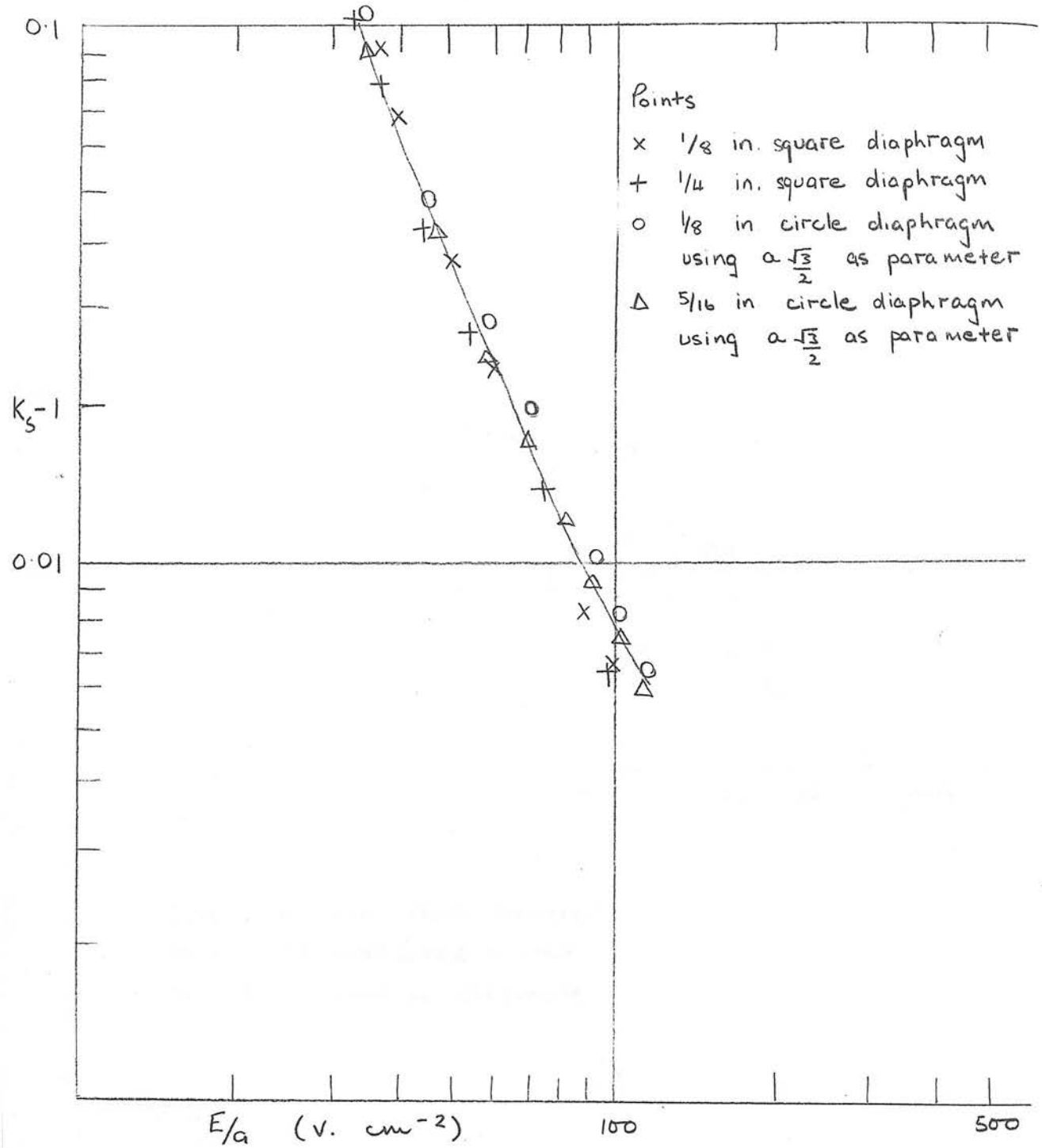

Plot of $(K_s - 1)$ against E/a for various diaphragms
Doserate approximately 20 r/min. at the diaphragm

Fig 28

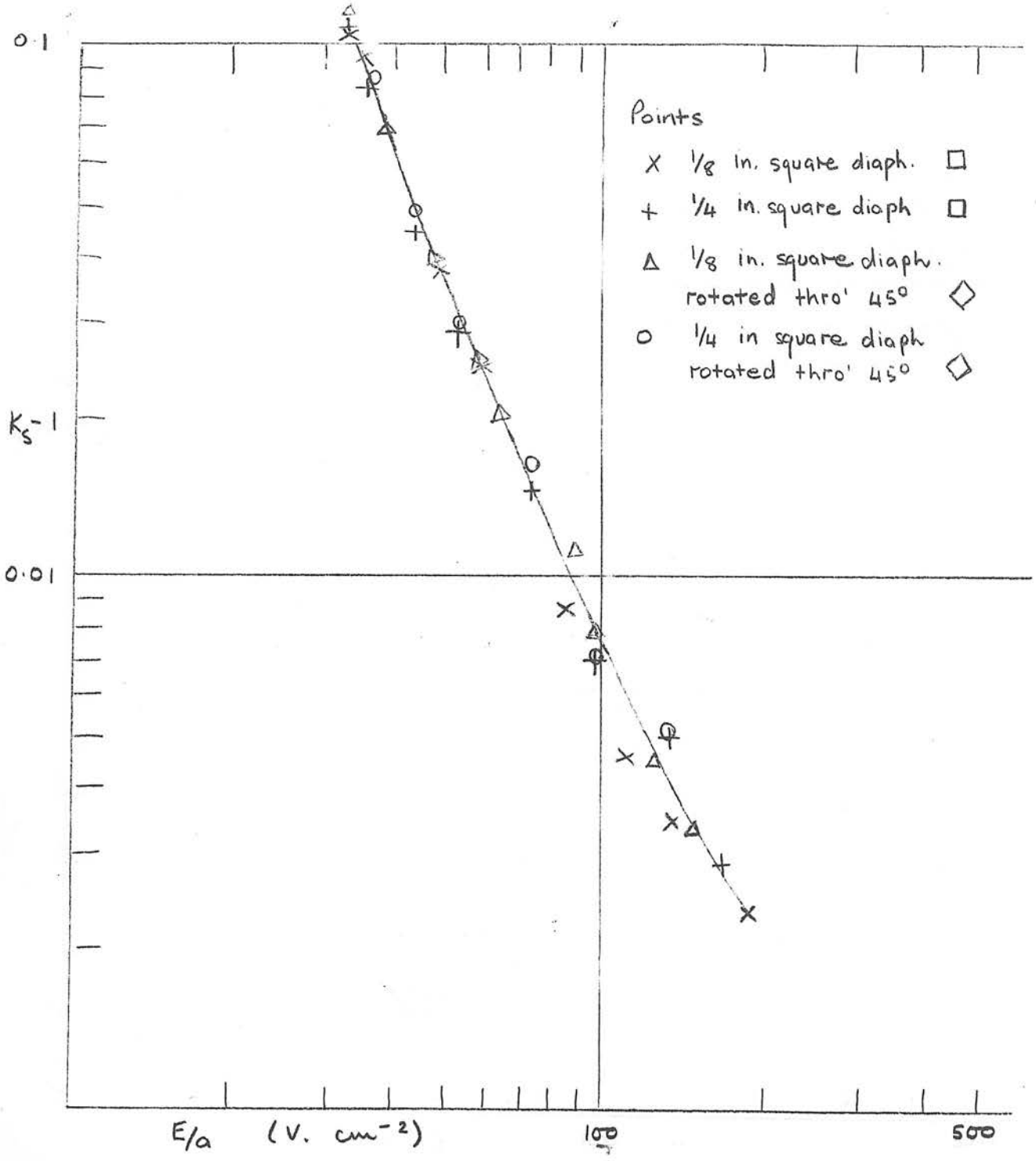

Plot of $(K_s - 1)$ against E/a for different orientations of diaphragm
Doserate approximately 20 r/min at diaphragm

4.4 Comparison of Theory and Experiment.

These values for α, k_1 and k_2 were substituted in our formula. For the majority of the results obtained using a 45 KV beam with a H.V.L. of 0.45 mm.Al. the value for c was taken as 10 mm.

In calculating K_s it must be noted that a and L are the values at the centre of the measuring electrode and so are dependent on the distance of the diaphragm from the X-ray source. Thus, for a given doserate, the values for K_s will depend on the experimental conditions, since to vary the doserate one must either change the distance and hence a, or the filtration and hence c. In Figs. (24-26), the theoretical results for $(K_s - 1)$ for the three diaphragms are drawn in as continuous curves while the experimental results are represented as points. Extremely good agreement is obtained between theory and experiment.

Experimental results on aperture shape and beam quality also bear out the theory. Values for the square apertures, 1/4 in. and 1/8.in. side, verify the choice of $a\frac{\sqrt{3}}{2}$ as parameter for circular ones, as this step brings the graphs of $(K_s - 1)$ against E/a at the same doserate into coincidence (Fig.27). Rotating the square aperture through 45 degrees makes no difference to the results (Fig.28). This is probably to be expected since the ion spread is greater than the aperture width, and so the orientation of the square will cease to matter. Measurements made with a rectangular aperture, 1/16 x 1/4 in. show only a small change in K_s when the diaphragm is rotated

Fig 29

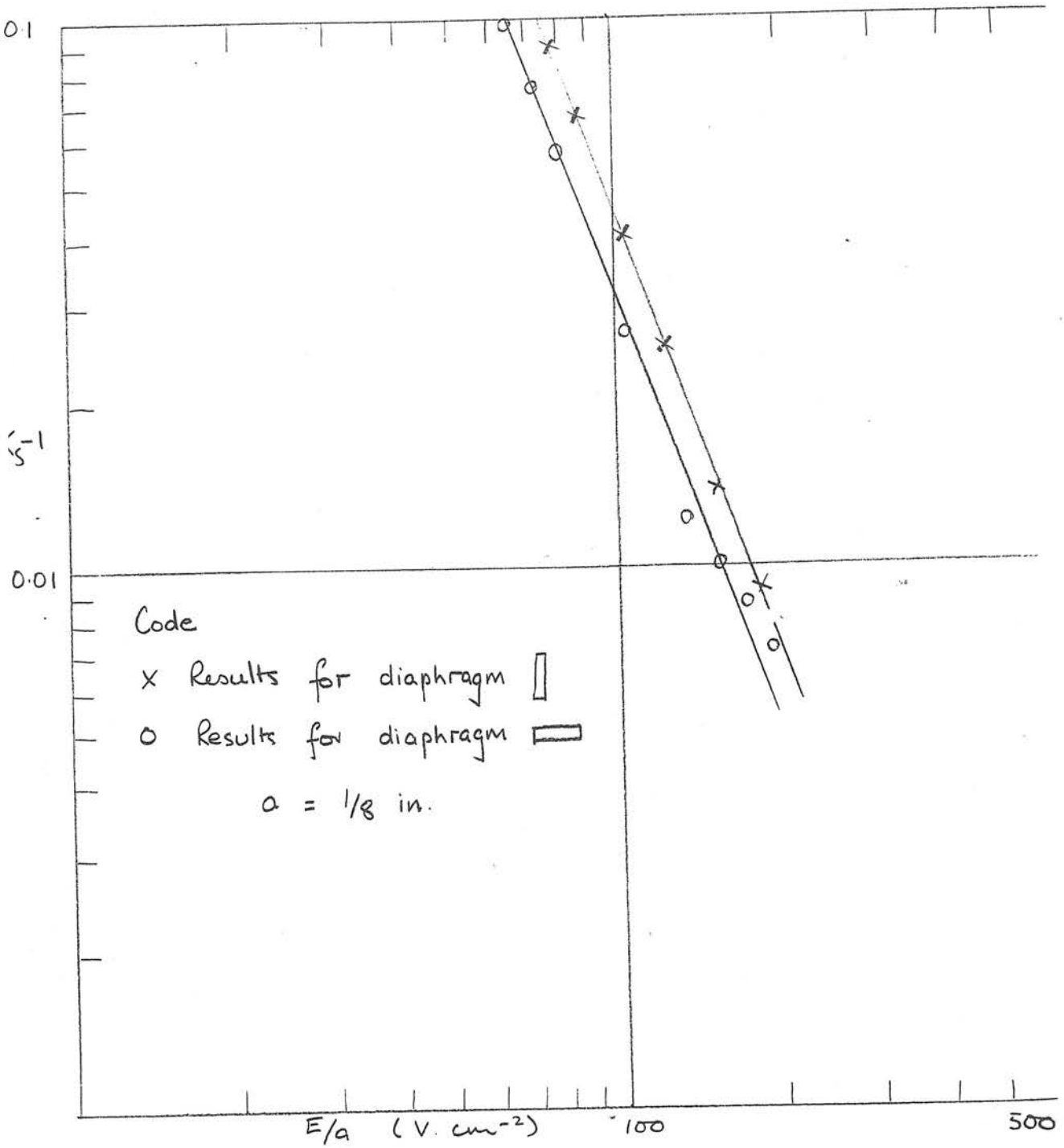

Plot of $(K_s - 1)$ against E/a for rectangular aperture at different orientations. using $a = \sqrt{\text{area}}$.

Fig 30

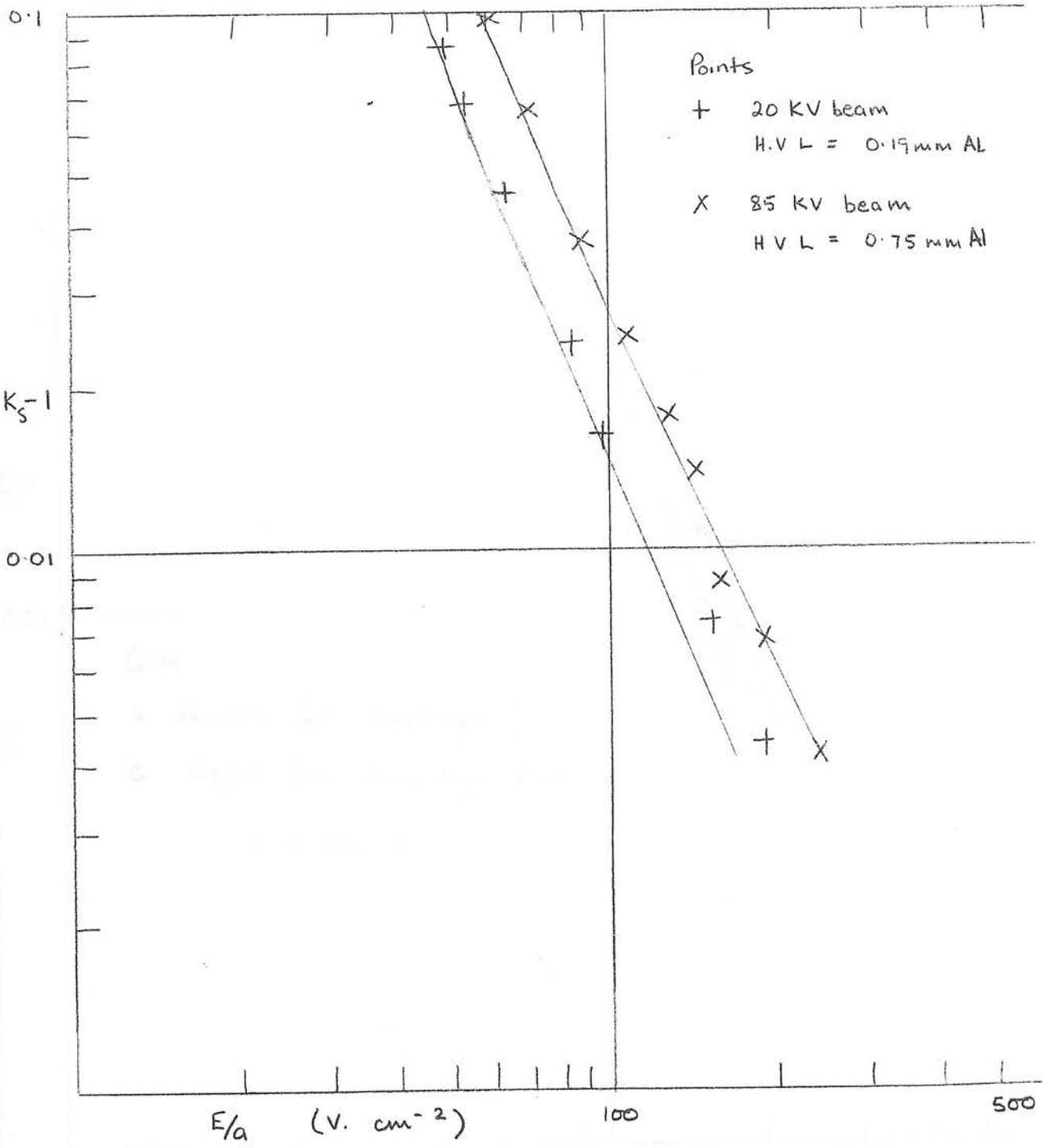

Comparison for 1/16 in diaphragm of theoretical values of $(K_s - 1)$ drawn as continuous curves with experimental results for different H.V.L represented by points. (Doserates approximately 100 r/min at diaphragm)

Fig 31

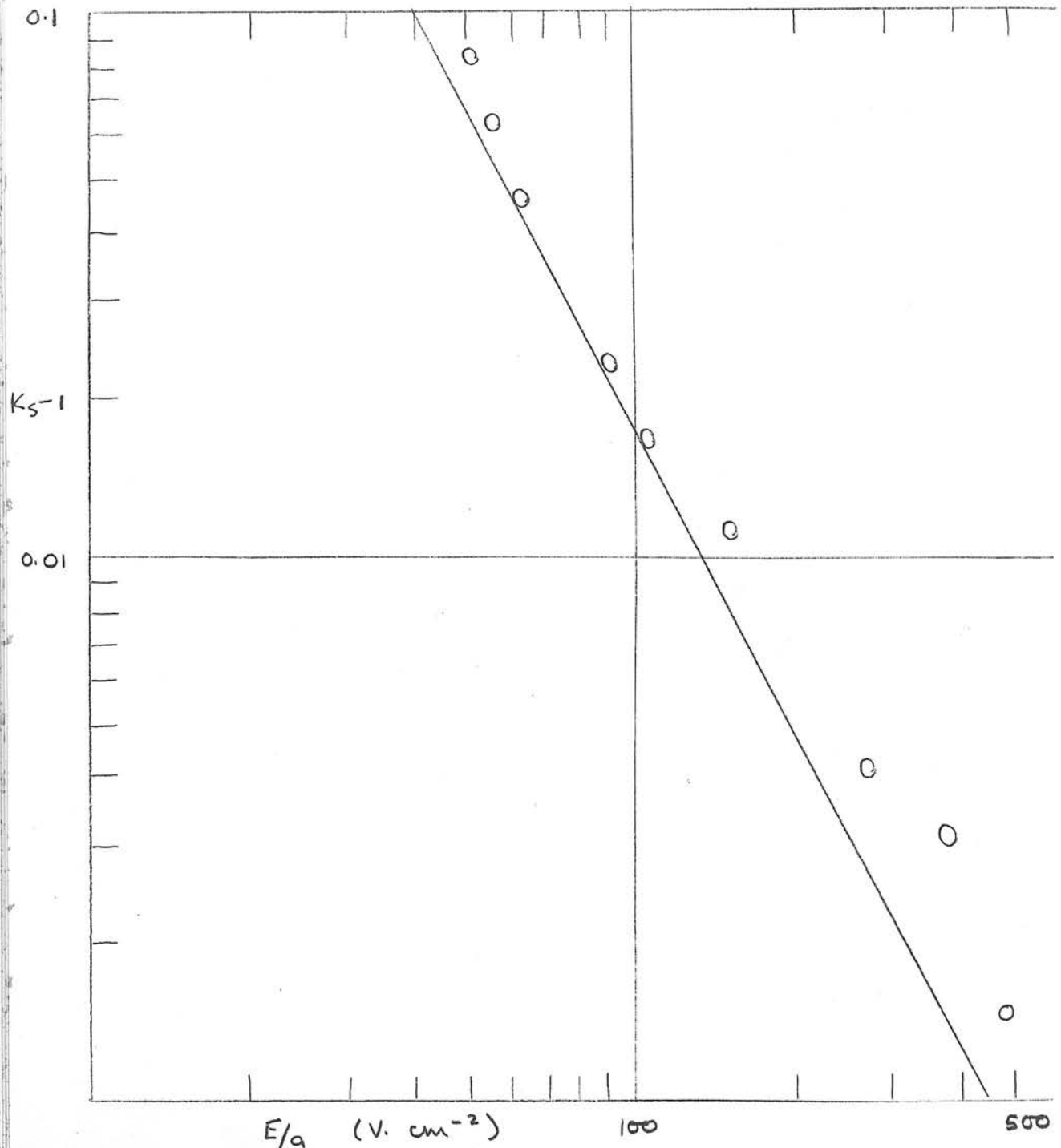

Comparison for 1/16 in diaphragm of theoretical values of (K_S-1) drawn as continuous curve with experimental results for H.V.L. = 4.46 mm Al represented as points. (Doserate approximately 100 r/min at diaphragm).

through 90 degrees (Fig.29). This also indicates that the spread of ionization beyond the beam edge results in an approximately circular distribution whatever the aperture shape provided the electron ranges are greater than the aperture dimensions.

Experiments on beam quality provide further confirmation of the theory. Fig.30 shows the experimental points and theoretical curves for a 20 KV beam with a H.V.L. of 0.19 mm.Al. and an 85 KV beam with a H.V.L. of 0.75 mm.Al. The respective values taken for C were 7 mm. and 14 mm. There is thus little change in the slope of $(K_s - 1)$ against E/a compared with the results for the 45 KV beam where c was 10 mm. The experimental results for an 85 KV beam with a H.V.L. of 4.46 mm.Al. however, indicate a definite decrease in slope. This is also anticipated by the theory. For a H.V.L. of 4.46 mm.Al. the range of the photoelectrons is 22 mm. in air. This implies that the space charge is negligible since the ion spread is sufficient to fill the space between the plates. Comparison between experiment and theory, assuming that there is no space charge, results in reasonable agreement (Fig. 31) In a way this is surprising since at this H.V.L. approximately 80 per cent of the total electron energy appears in the photoelectrons while the remaining 20 per cent appears in the recoil electrons. The mean energy of the recoil electrons in this case is 3 keV and their average range in air is 0.24 mm. We would thus expect to find some evidence of space charge arising from the recoil electrons.

4.5 Conclusions.

From an appraisal of the literature we have made a choice of values for the ionic constants α, k_1 and k_2. We have ascertained the approximate ranges $(\frac{c}{2})$ in air of secondary photo electrons at various H.V.L. On substituting these values in our formula we find good agreement with experimental results obtained in a wide field of operating conditions. The range investigated experimentally extends as follows: -

Doserate 10 - 1000 r/min. at chamber diaphragm.

Diaphragm sizes and shapes. 1/16 - 5/16. in. circles.
1/8 - 1/4. in. squares.
1/16 x 1/4. in. rectangle

H.V.L values 0.19 - 4.46 mm.Al.

CHAPTER 5.

IMPLICATIONS OF FORMULA IN THE ESTIMATION OF SATURATION CURRENT.

Synopsis.

The argument put forward in this chapter is of necessity a rather involved one. It therefore seems of use at this stage to give a brief outline of the main points.

So far we have established a formula governing the saturation losses in a free-air chamber. The current method of determining the theoretical saturation current from experimental measurements is based on an extrapolation equation due to Kara-Michailova and Lea (1940). If we now derive an extrapolation equation from our own formula, we find it involves the parameter $1/E^2$ instead of the previous I/E. which is for initial recombination.

When extrapolation plots were made using these equations, it was discovered that experimental results fitted both equations equally well although the extrapolated values of the saturation current differ by as much as 0.7 per cent.

In order to determine which was the correct method further experiments were performed with the free-air chamber at a doserate of 1 r/min. and the results compared with the original formulae, i.e. Lea's cluster theory (1934) and our equation (6). While good agreement was obtained between experimental (K_s - 1) and our formula, no evidence was found of initial recombination although it was predicted by Lea.

A possible reason for this non-confirmation of Lea's theory

lies in the value chosen for b -the radius of a cluster. This was determined empirically by Kara-Michailova and Lea by the comparison of the theoretical equation and the experimental work of Bowen. On investigation it seems to us that their value for b was an average one made over a wide range of pressures and that at low pressures a higher value of b could be taken, which would explain the lack of agreement with our results. More important is the fact that when Kara-Michailova and Lea derived b in terms of the mean free path λ and the attachment probability h of an electron, this theoretical evaluation of b was some ten times greater than the empirical one. A search in the literature for more recent measurements of λ and h did nothing to dispel this result.

We therefore conclude that our extrapolation equation should be used for free-air chambers at atmospheric pressure and doserates greater than 1 r/min.

5.1. Extrapolation Method of Determining Saturation Current.

In the handbook on the design of free-air ionization chambers published by the U.S. National Bureau of Standards, Wyckoff and Attix (1957) discuss the need to establish a practical working criterion for determining the saturation current without going to extremely high collecting potentials. They criticise the criterion most frequently found in literature, i.e. that the voltage be large enough so that the sensitivity of the electrometer system used is insufficient to detect any voltage dependence of the current as the voltage is increased further, on the grounds that it is indeterminate unless the electrometer current-sensitivity is further specified and the range of voltages is given. They recommend an extrapolation method for obtaining the saturation current. (Kara-Michailova and Lea, 1940). The extrapolation equation is of the form

$$1/j = 1/j_s + \text{const.}/E. \qquad \text{----------(7)}$$

and so a plot of $1/j$ against $1/E$, which is linear for large values of E, can be extrapolated to the $1/E = 0$ axis to give the value of j_s .

In our computations of the experimental $(K_s - 1)$ factors, we used the first criterion for determining the saturation current. Since we were trying to verify a theoretical method of estimating saturation losses, we could hardly use it or indeed equation (7) to obtain j_s . It seems worthwhile, however, to derive an extrapolation equation from our formula

and compare it with that due to Kara-Michailova and Lea which concerns initial recombination.

5.2 Estimation of Saturation Current from Present Formula.

Equation (6) can also be used to calculate saturation current by an extrapolation method. It may be written as: -

$$K_s = 1/2 + 1/2 \left\{ 1 + \frac{A_1 L}{\left[\frac{E}{a\sqrt{\frac{3}{2}}} - \frac{A_2 L}{E/2\sqrt{\frac{3}{2}}} \right]^2} \right\}^{1/2}$$

where $A_1 = 1/90 \quad \frac{\alpha}{e} \quad \frac{1}{k_1 \; k_2}$

$$A_2 = 7.75 \quad \frac{\left[d - (a + c)\sqrt{\frac{3}{2}} \right]^2}{\left[d \quad (a + c)\sqrt{\frac{3}{2}} \right]} \qquad \left(\frac{1}{k_1} + \frac{1}{k_2} \right)$$

For large values of E/a

$$K_s \doteq 1/2 + 1/2 \left\{ 1 + \frac{A_1 L}{\left[E/a\sqrt{\frac{3}{2}} \right]^2} \right\}^{1/2}$$

$$= 1 + \frac{A_1 L}{4 \left[E/a\sqrt{\frac{3}{2}} \right]^2} \qquad K_s \ll 1$$

$\therefore$ For given a and L, $K_s = 1 + \frac{A_3}{E^2} \qquad A_3 = \frac{3 A_1 L}{16 a^2}$

i.e. $j_s/j = 1 + A_3/E^2$

$$\therefore \quad \frac{1}{j} = \frac{1}{j_s} + \text{const.} \quad \frac{1}{E^2} \qquad \text{----------(8)}$$

i.e. according to our theory, the theoretical value for j_s is obtained by extrapolating a plot of $1/j$ against $1/E^2$ to the $1/E^2 = 0$ axis.

Fig 32

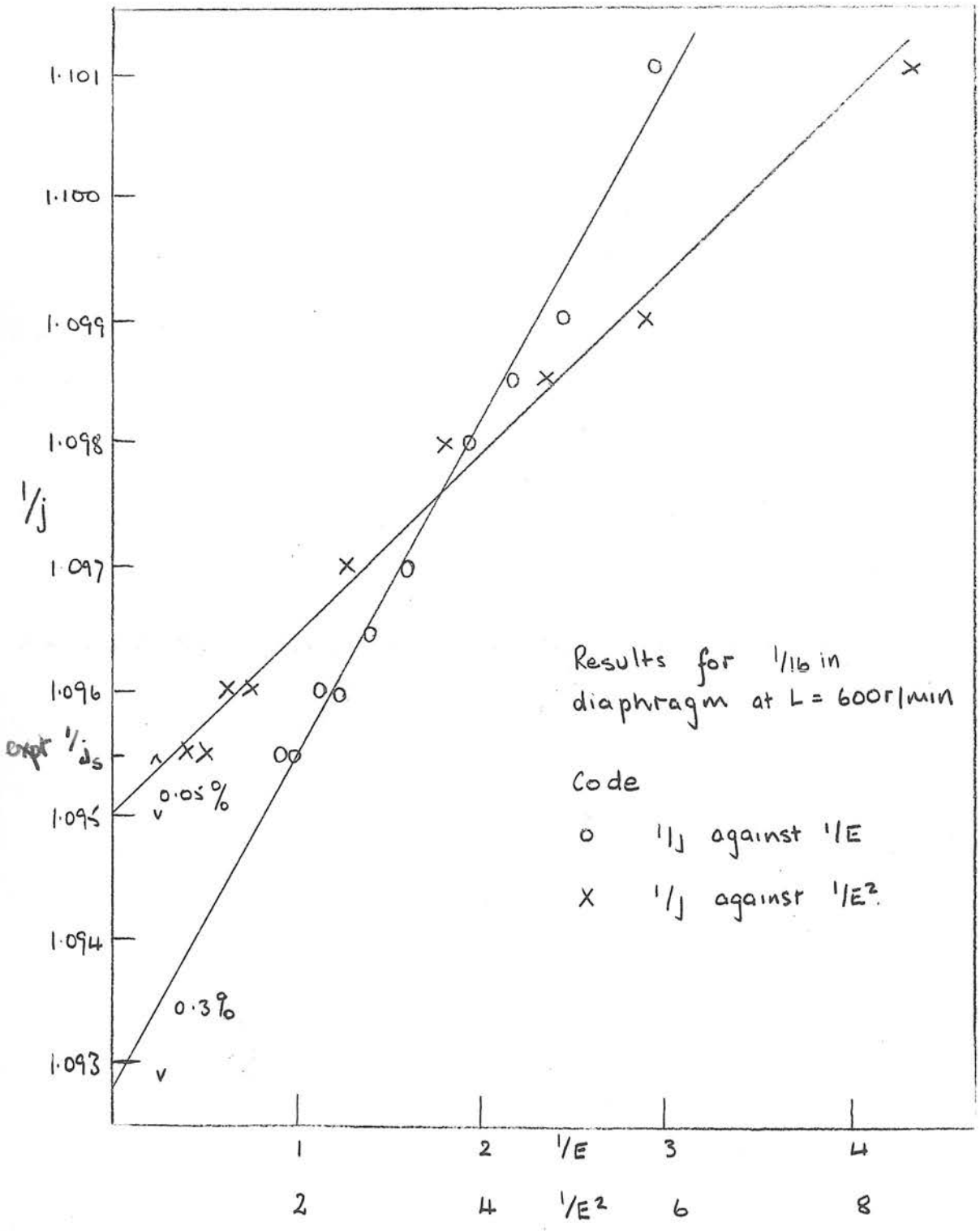

Plots of 1/j against 1/E and 1/E² in arbitrary units.

Fig 33

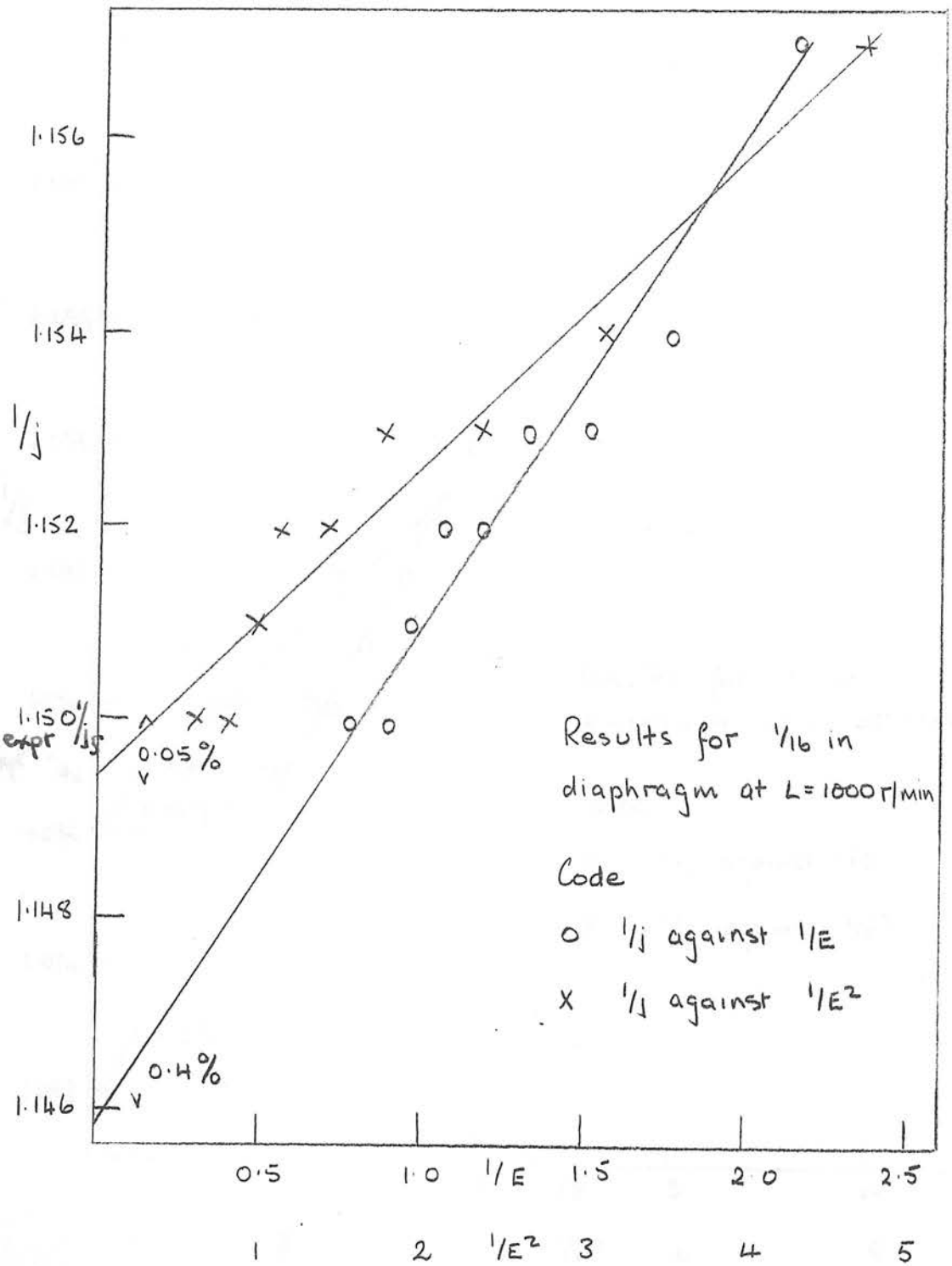

Plots of 1/j against 1/E and 1/E² in arbitrary units

Fig 34

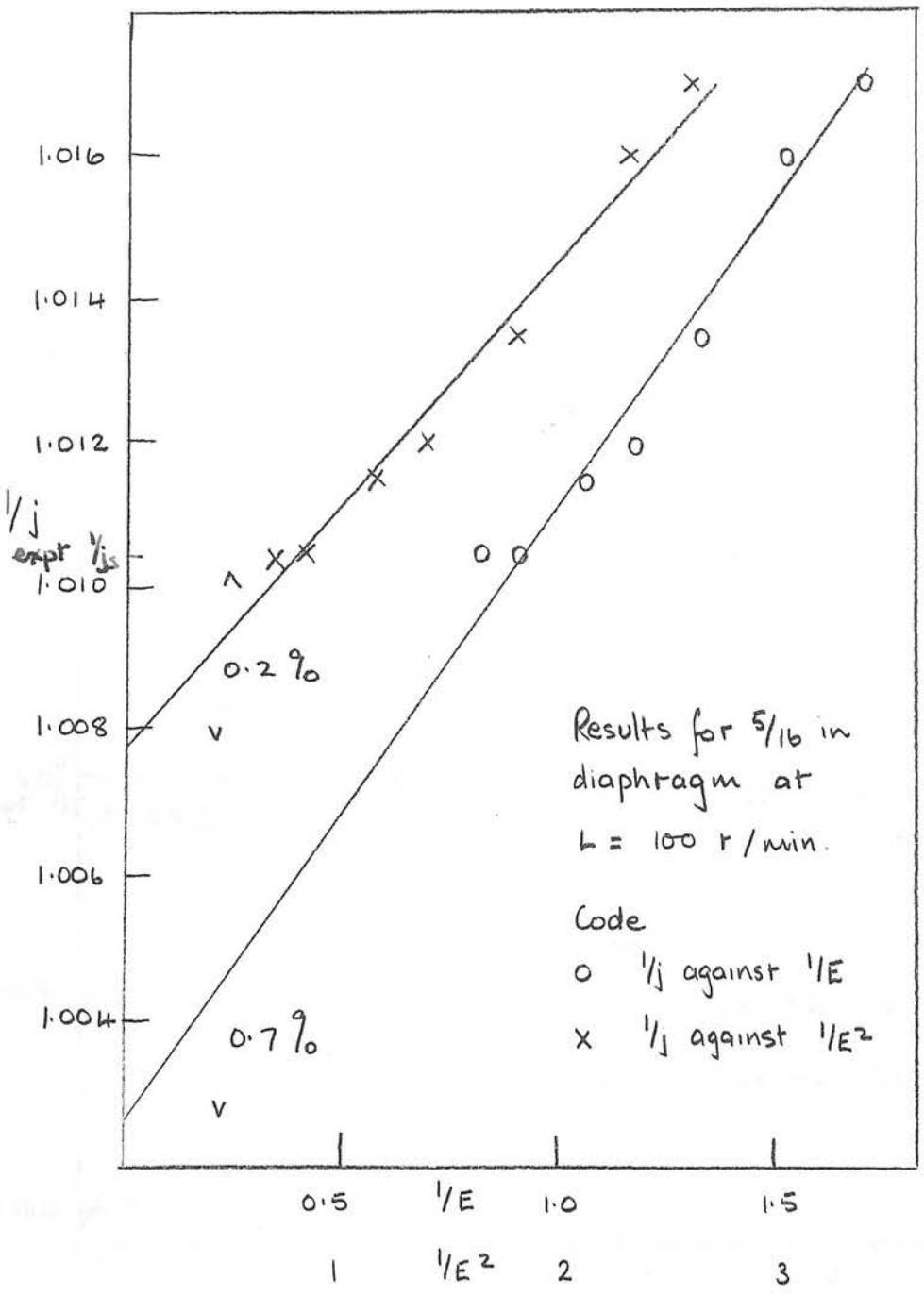

Plots of $1/j$ against $1/E$ and $1/E^2$ in arbitrary units

5.3. Comparison of the two Extrapolation Equations.

Figures 16-21 illustrated the experimental results for $(K_s - 1)$ values greater than 0.005. We did in fact make measurements of $(K_s - 1)$ at smaller values but did not portray these graphically since the point scatter of $\pm 0.001 - 0.002$ would have led to some confusion as to which point belonged to which curve. If these low values for $(K_s - 1)$ are now plotted in the form $1/j$ against both I/E and I/E^2 we find that allowing for experimental error equally good straight lines are obtained. (Fig. 32-34). There is, however, a noticeable difference between the extrapolated values for j_s. Whereas the plots of $1/j$ against $1/E^2$ show that our experimental value of j_s is usually within 0.1 per cent and never more than 0.2 per cent from the extrapolated value, the plots of $1/j$ against $1/E$ imply that the discrepancy is often 0.3 per cent and may be as much as 0.7 per cent.

Our experimental results can thus be said to satisfy both methods of plotting equally well but since the outcomes are different, careful consideration must be given to the theories on which these plots are based. Our theory has been discussed in detail and its shortcomings are pointed out in Chapter 6.2. It certainly bears close agreement with experiment even at low $(K_s - 1)$ values which would be expected to indicate the presence of any initial recombination.

It must be remembered, however, that our experimental results for $(K_s - 1)$ were calculated from our experimental value for j_s. This means that if our experimental j_s is x per cent lower than the correct value due to initial recombination, our $(K_s - 1)$ values are also x per cent smaller and so the effect of initial recombination is hidden.

5.4 Examination of Lea's Cluster Theory for Initial Recombination.

Lea (1934) was the first to apply Jaffé's columnar theory (1913) for α - particle ionization to the problem of ionization under γ - rays where the ions are formed in clusters along the tracks of the secondary electrons. He succeeded in calculating the amount of recombination occurring in a cluster from the time of its formation until it had diffused apart sufficiently to overlap with neighbouring clusters.

Lea assumed that the distribution of ions in a cluster was spherically symmetrical initially, the density at a distance r from the centre being

$$n = \frac{\nu_0}{\pi^{3/2} b^3} e^{-r^2/b^2}$$

where ν_0 is the initial number of ion pairs in the cluster and b is the parameter measuring the initial radius of the cluster. The equation representing the effects of diffusion, recombination and drift under the electric field (directed along the x axis) is

$$\frac{\partial n^{\pm}}{\partial t} = D\left\{\frac{\partial^2 n^{\pm}}{\partial x^2} + \frac{\partial^2 n^{\pm}}{\partial y^2} + \frac{\partial^2 n^{\pm}}{\partial z^2}\right\} \pm kE\frac{\partial n^{\pm}}{\partial x} - \alpha n_+ n_-$$

where k is the ionic mobility and D is diffusion coefficient. This equation is not integrable exactly but using Jaffé's method Lea obtained the number of ions ν which remain uncombined when the cluster has increased by diffusion to K times its initial radius

$$\frac{\nu}{\nu_0} = \frac{1}{1 + (\alpha\nu_0 / 8\pi^{3/2} bD) \cdot P(z)} \quad ---- (9)$$

where $\sqrt{z} = bkE/\sqrt{2D}$ and the function P (z) is described and tabulated in Lea's paper.

At this stage the clusters are overlapping and Jaffé's theory of columnar recombination can be applied, taking the column radius to be initially defined by Kb and the number of ions per cm. of column to be $No.\left(\frac{r}{r_0}\right)$ where No is the initial number of ions per cm. of electron track. The proportion finally escaping from the column is then

$$\frac{N}{No} = \frac{r/r_0}{1 + \frac{\alpha No}{8\pi D}\frac{r}{r_0}\left(\frac{\pi}{x}\right)^{\frac{1}{2}} S(x)} \qquad \text{---------(10)}$$

where $\sqrt{x} = K\sqrt{z}\sin\phi$ and the function S (x) is defined in Jaffé's paper and presented in a convenient form by Zanstra (1935).

Lea verified his theory by carrying out a series of experiments with γ- rays in nitrogen and hydrogen using ionization intensities from 200 to 1400 ions/cm.^{3} sec. He chose the cluster radius for each gas so as to give the best possible agreement with experiment and then by varying the other parameters found reasonable confirmation of his theory.

In 1940, Lea in collaboration with Kara-Michailova surveyed existing experimental data on initial recombination and from a comparison with theory, recommended values for the cluster radius for different gases. Using the experimental results obtained by Bowen (1932) they give the value for b in air as 1.05×10^{-3} cm. In an attempt to calculate the cluster radius from theoretical grounds

Kara-Michailova and Lea derived an expression for b in terms of the mean free path λ and the attachment probability h of an electron.

$$\text{i.e.} \qquad b^2 = \frac{4\lambda^2}{3h}$$

b can only be estimated roughly, however, from this equation because of uncertainties in the values of λ and h for electrons at thermal energies (V = 0.04 V). The work of Bradbury (1933) suggested the value for h is 5×10^{-5} and the value for λ on classical kinetic theory is 5.7×10^{-5} cm. The mean free path at energies of less than 1 V is known to be about one-half of the kinetic theory value thus b is approximately 10^{-2} cm. i.e. ten times the value required by the recombination theory.

5.5 Examination of Extrapolation Formula due to Kara-Michailova and Lea

Clay and Zanstra developed from Jaffé's theory an extrapolation method for the determination of the theoretical saturation current from experimental unsaturated currents. Kara-Michailova and Lea point out in their paper that the cluster theory does not lend itself to use as an extrapolation method in such a convenient manner. If, however, attention is restricted to high collecting fields and the specific ionization No of the ionizing electrons is not too high, then the recombination which occurs after the clusters have diffused into columns can be neglected. Equation (9) of the cluster theory can thus be rewritten as

$$\frac{j_s}{j} = \frac{\nu_0}{\nu} = 1 + \frac{\alpha \nu_0}{8\pi^{3/2} b D} P(z) \quad \text{--------(11)}$$

now $\sqrt{z} = bk E/\sqrt{2D}$

and for large values of z, P (z) is approximately $(\pi/z)^{1/2}$

$$\text{i.e. } P(z) \doteqdot \frac{\pi^{1/2} \sqrt{2}\, D}{bk} \frac{p}{E}$$

where the factor p takes into account the pressure dependence of b.

This approximation is valid to within 20 per cent for $\sqrt{z} \geqslant 2.5$ which, for air, means $E/p \gtrsim 80$ V. cm.$^{-1}$. atm.$^{-1}$. Thus for high fields the cluster theory (11) reduces to the extrapolation equation (7)

$$\frac{1}{j} = \frac{1}{j_s} + \frac{\text{const.}}{E}$$

5.6 Calculations of $(K_s - 1)$ based on Cluster Theory.

Under the conditions given in Chapter 5.5 (i.e. high fields and moderate specific ionizations) the cluster theory can be used to compute K_s since

$$K_s = j_s/j = v_0/v = 1 + \frac{\alpha v_0}{8\pi^{3/2} b D} P(z) \qquad \text{------(11)}$$

Kara-Michailova and Lea describe the evaluation of this formula in an appendix to their paper. They recommend the following values for the ionic constants

$$\frac{k}{D} = Ne = 40.25 \text{ at } 16^{\circ}C$$

$$\frac{\alpha}{D} = \frac{8\pi e\, k}{D} = 1.55 \times 10^{-4}$$

They point out, however, that this value for α/D is based on Langevin's formula $\alpha = 8\pi ek$ and as such may only be used at pressures above 5 atmospheres.

We have already discussed values for α, k_1 and k_2 (4.1 - 2) and for a fair comparison with our theory must use these in equation (11).

Taking $D = 0.047$ cm.^{2}/sec.

and $k = \frac{k_1 + k_2}{2} = 1.9$, $\alpha = 2.3 \times 10^{-6}$

then $\frac{k}{D} = 40.4$, $\frac{\alpha}{D} = 4.9 \times 10^{-5}$

Substituting these values for the ionic constants we find

$$\sqrt{z} = \frac{b\,k\,E}{\sqrt{2}\,D} = 28.6\,\frac{b\,E}{p}$$

and $\mathcal{L}\nu_0 / 8\pi^{3/2} bD = 1.1 \times 10^{-6}\, \nu_0\, p/b$

where b is the cluster radius at atmospheric pressure and p is the density of the gas relative to its density at 760 mm.Hg. and 16°C. The value for b recommended by Kara-Michailova and Lea for air is 1.05×10^{-3} cm.

∴ For air at 760 mm. Hg. and 22°C.

$$\sqrt{z} = 30.6 \times 10^{-3}\, E \qquad \frac{\mathcal{L}\nu_0}{8\pi^{3/2} bD} = 1.03 \times 10^{-3}\, \nu_0$$

For $E \geq 80$ V/cm., P (z) is approximately $(\pi/z)^{1/2}$

i.e. $P(z) = \frac{58}{E}$

Thus equation (11) reduces to

$$K_S = \frac{\nu_0}{\nu} = 1 + g\,\nu_0 \qquad \text{----------(12)}$$

where $g = \frac{5.97 \times 10^{-2}}{E}$

ν_0 is the initial number of ion pairs per cluster and varies from 1 to 30. As a crude approximation an average figure equal to the ratio of the total number of ion pairs produced by an electron to the number of its primary ionizations may be used for ν_0. In Lea's paper the figure $\nu_0 = 2.5$ was used but Kara-Michailova and Lea suggest a value of about 3 as being a better approximation. They state, however, that this method of determining ν_0 is only valid

when a large proportion of the ions recombine in the cluster and in other cases the effective value of ν_0 is appreciably higher than 3 and the exact value depends on the frequency of occurrence of clusters of different size.

If f is the frequency of occurrence of a cluster size ν_0 the mean value of $\frac{\nu_0}{\nu}$ is

$$\frac{\Sigma f \nu_0}{\Sigma f \nu} = \frac{\Sigma f \nu_0}{\Sigma \frac{f \nu_0}{1+g\nu_0}} = 1 + g\nu_0^* \qquad \text{-------(13)}$$

where ν_0^* is the effective mean number of ions per cluster. A graph of ν_0^* as a function of g calculated from this equation is given in Kara-Michailova and Lea's paper. It is based on the distribution of ions in clusters as given in Table 2.

Cluster Size	1	2	3	4	8	16
Cluster Frequency	0.45	0.22	0.11	0.10	0.07	0.05

Their graph is for g values between 0.01 and 10. We are interested in the range $10^{-4} - 10^{-3}$. The limit of ν_0^* as $g \rightarrow 0$ is about 7.11. Calculations for ν_0^* from equation (13) with data from Table 2 give

g	10^{-2}	10^{-3}	10^{-4}	10^{-5}	10^{-7}
ν_0^*	6.8	7.08	7.11	7.11	7.11

This indicates ν_0^* is almost constant in the range $g = 10^{-3} - 10^{-4}$ and may be taken as 7.1.

Fig 35

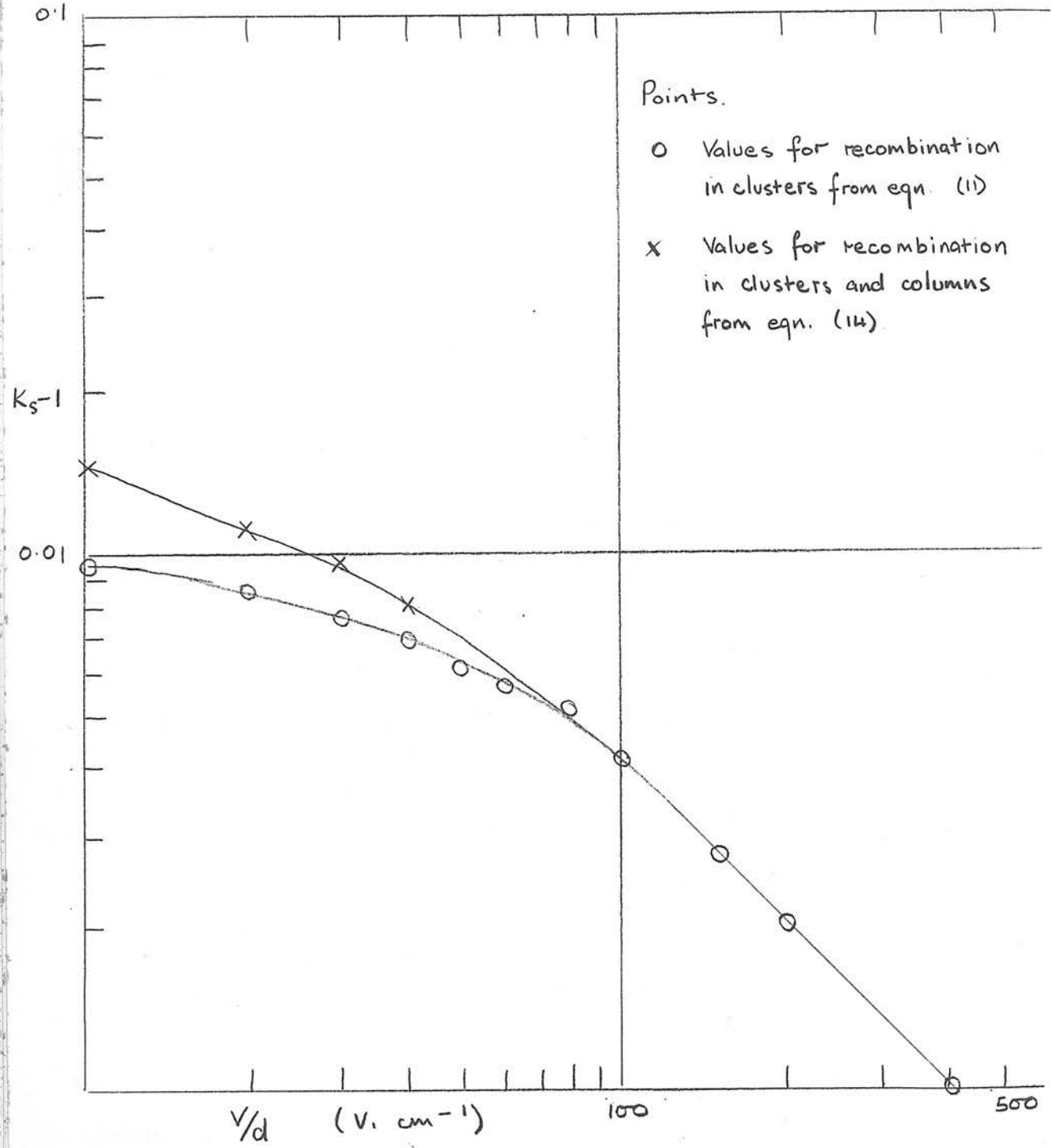

Plot of theoretical values of (K_s-1) against V/d from Lea's cluster theory

Thus for E $\geqslant$ 80V/cm. equation (12) may be written

$$K_s - 1 = \frac{0.424}{E}$$

Values for $(K_s - 1)$ calculated in this way are shown in Fig. 35

Points for E < 80 V/cm. are obtained from equation (11) using P (z) values from the graph of P (z) as a function of $\sqrt{z}$ contained in the appendix of Kara-Michailova's paper. In the evaluation of P (z) an estimate of K is necessary. Now 1/Kb is the primary specific ionization S_o and tabulated in the same appendix are figures for S_o and its mean $\overline{S_o}$ for different electron energies. For an effective electron energy of 17 KeV, K was found to be about 3.

In estimating $(K_s - 1)$ values for E < 80 V/cm., however, we must take into account the recombination occurring after the clusters have diffused into columns. This can be done using equation (10) which may be rewritten as

$$K_s = \frac{No}{N} = 1 + \frac{\alpha V_o}{8\pi^{3/2} bD} P(z) + \frac{\alpha N_o}{8\pi D} \left(\frac{\pi}{x}\right)^{1/2} . S(x) \qquad \text{----------(14)}$$

i.e. to obtain the final value for $(K_s - 1)$ we must add to the figures calculated from equation (11) the amount

$$\frac{\alpha N_o}{8\pi D} \left(\frac{\pi}{x}\right)^{1/2} S(x)$$

$\frac{\alpha N_o}{8\pi D}$ for air at 760 mm.Hg. and 22°C = 1.91×10^{-6} No

$\sqrt{x} = K\sqrt{z} \sin\phi$ where ø is the angle between the column and the field

$\therefore \quad \sqrt{x} = 9.2 \times 10^{-2} \text{ E.}$

No is the initial number of ions per cm. and its mean value $\overline{No}$ for different electron energies has also been tabulated. For an effective electron energy of 17 KeV the value for $\overline{No}$ was taken to be 1400 ions/cm. Values for $\left(\pi/x\right)^{1/2} S(x)$ for various $\sqrt{x}$ were taken from a graph in the appendix and the resulting values for $(K_s - 1)$ are shown also in Fig. 35

Fig 36

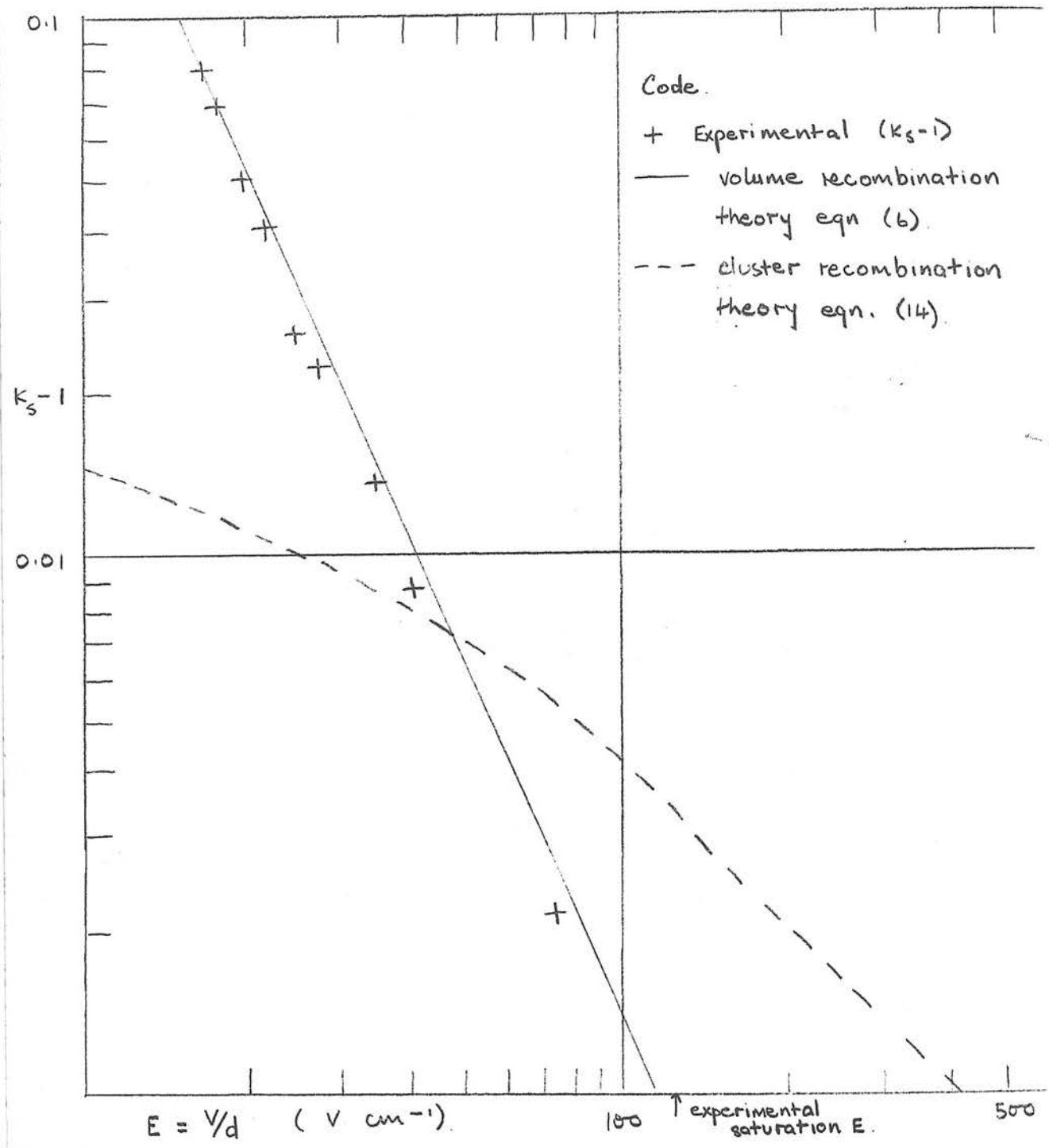

Comparison of experimental (K_s-1) for a doserate of 10r/min. at the 5/16 in. diaphragm. with cluster and volume recombination theories.

Fig 37

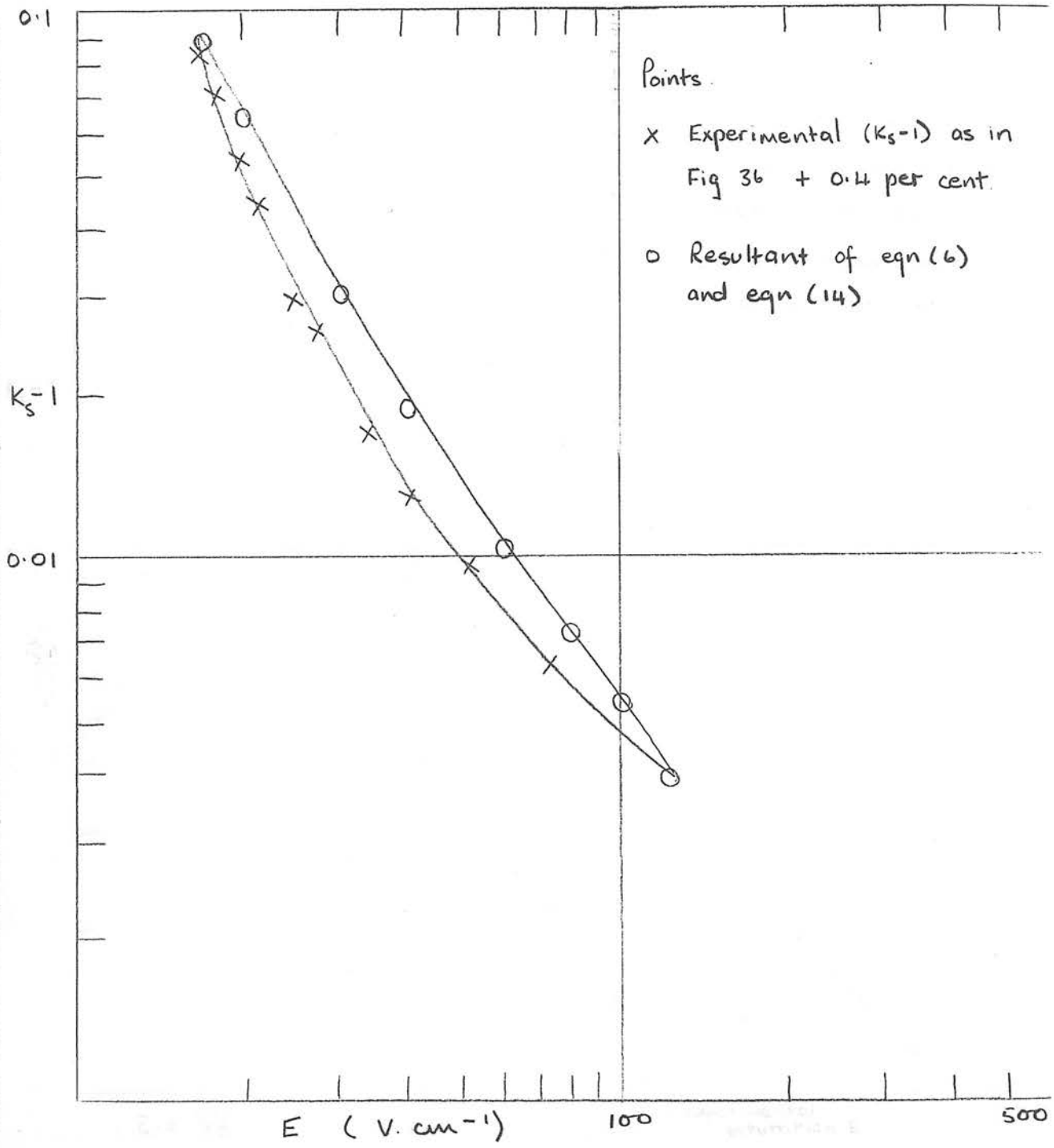

Comparison of experimental (K_s-1) corrected for initial recombination with resultant of initial and volume recombination theories.

5.7 Comparison of Experimental Results with Cluster and Volume Theories.

We are now ready to compare our experimental values of $(K_s - 1)$ with the predictions of Lea's cluster theory. Since initial recombination is most likely to be noticeable at low doserates we look first at our results for the 5/16 in. aperture at a doserate of 10 r/min. Fig. 36 shows the experimental values of $(K_s - 1)$ plotted as points against $V/d = E$. The continuous line represents $(K_s - 1)$ values as calculated from our theory (equation 6) while the broken curve is that obtained from the cluster theory (equation 14).

At first glance there appears to be no possibility of initial recombination since the experimental results agree so well with the general recombination formula. The experimental value of j_s, however, was obtained at a field strength E of 125 V/cm. At this value of E the initial recombination formula predicts a loss of 0.34 per cent, while the volume recombination formula shows a loss of less than 0.1 per cent. Thus, if the two formulae are correct our experimental value for j_s is some 0.4 per cent lower than the theoretical value and we must add 0.4 per cent to all our experimental results for $(K_s - 1)$ to allow for this.

In Fig. 37 the points represented as circles show the effect of this addition to the experimental $(K_s - 1)$, while those represented as crosses are the result of combining the theoretical losses due to the two theories. The two curves coincide

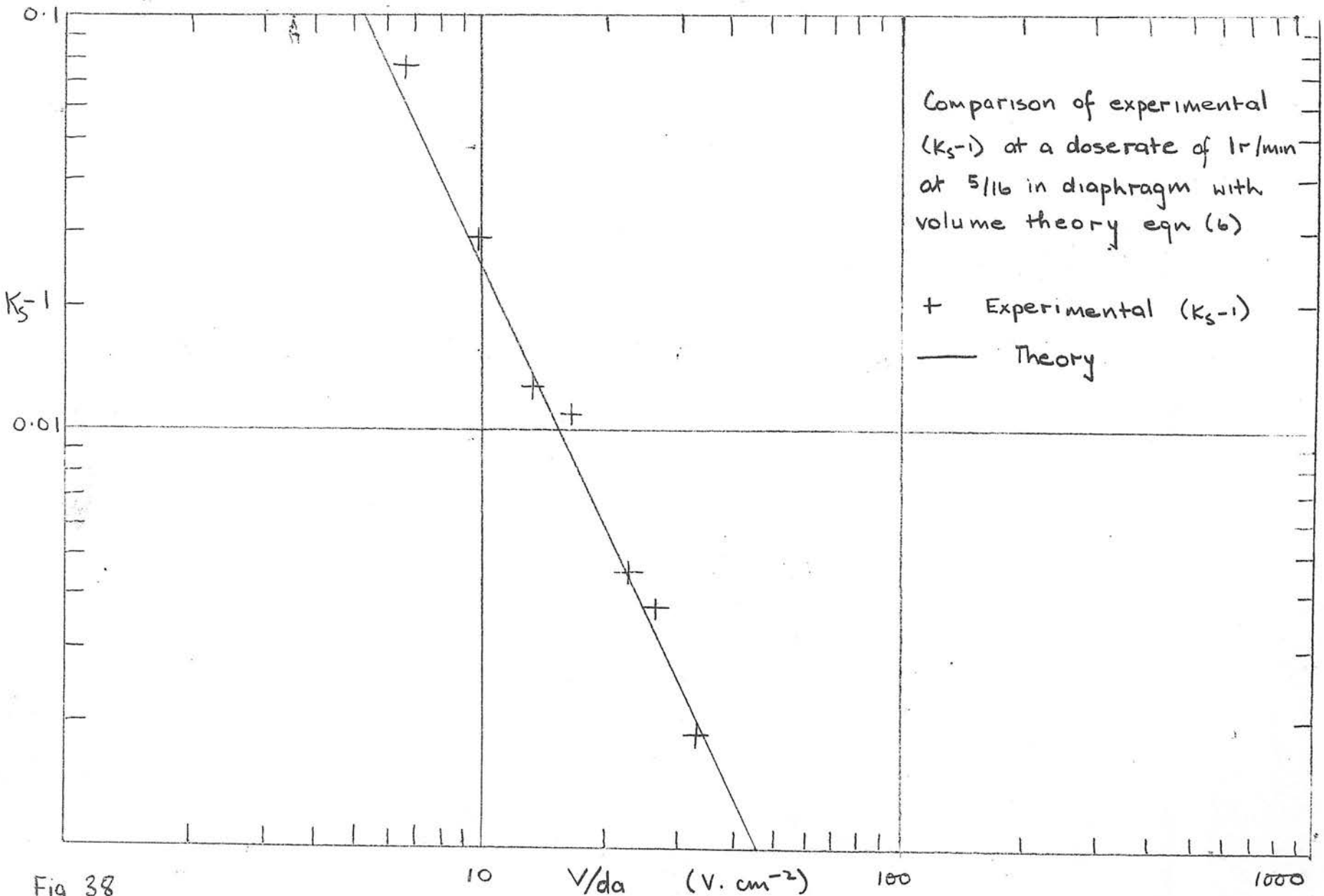
0·1
0·01
$K_S - 1$
10
V/da (V. cm^{-2})
100
1000
Comparison of experimental (K_S-1) at a doserate of 1r/min at 5/16 in diaphragm with volume theory eqn (6)
+ Experimental (K_S-1)
—— Theory

Fig 38

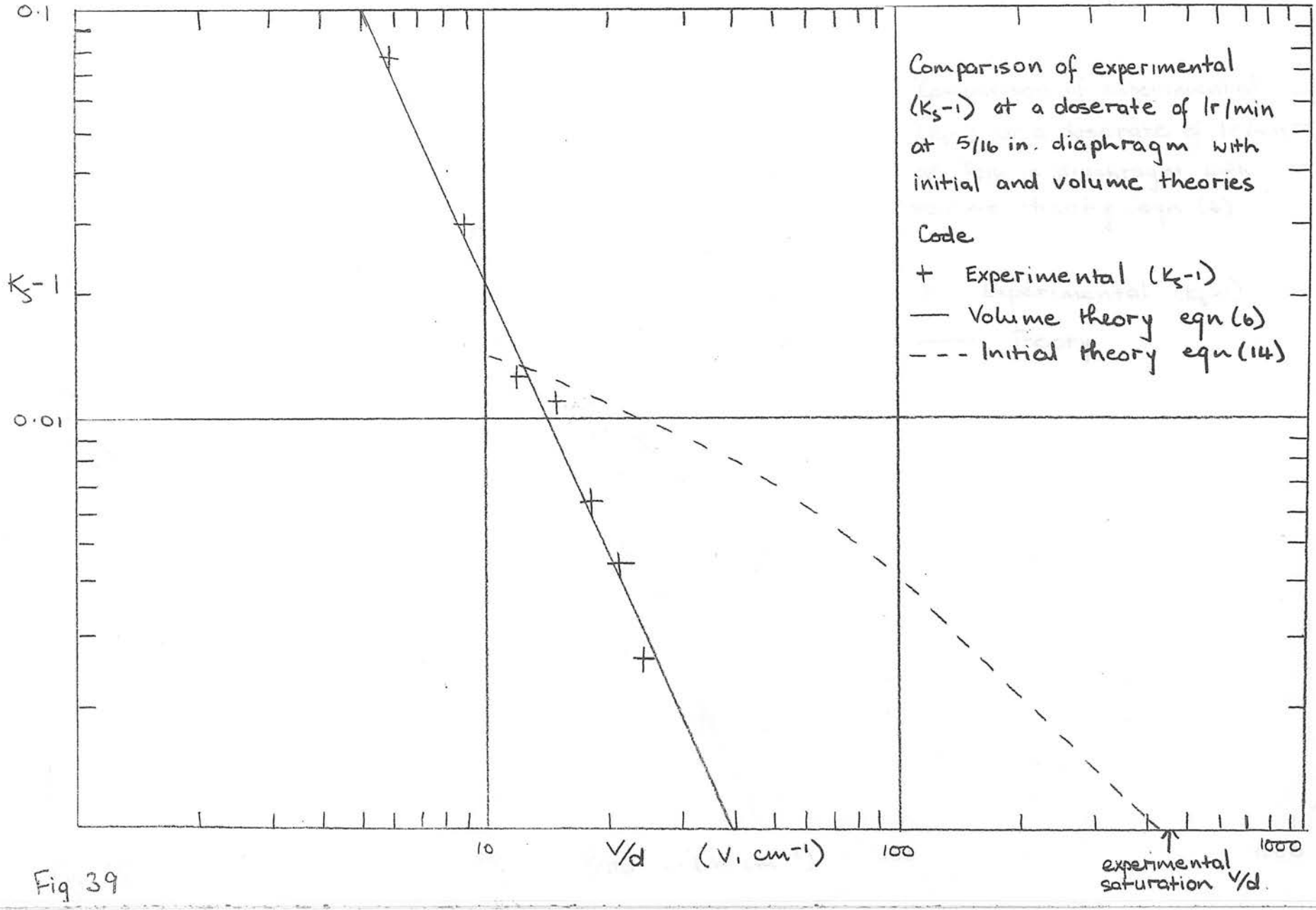
0.1
0.01
$K_s - 1$
10
V/d (V, cm^{-1})
100
1000
experimental saturation V/d.
Comparison of experimental (K_s-1) at a doserate of 1r/min at 5/16 in. diaphragm with initial and volume theories
Code
+ Experimental (K_s-1)
— Volume theory eqn (6)
- - - Initial theory eqn (14)

Fig 39

for the lowest value of (K_s - 1) as expected, then separate until high (K_s - 1) values when the initial recombination theory has little effect on the other. The maximum discrepancy between the curves is about 1.5 per cent and it seems reasonable to assume that this is outwith any experimental error. The inference is, therefore, that there is little or no initial recombination noticeable at this doserate.

In order to make quite sure of this point, a further experiment was carried out with the 5/16 in. aperture and a doserate of 1 r/min, some two years after the first experimental series was completed. The H.V.L. of the radiation was 0.36 mm.Al. and c was taken to be 9 mm. (Table 1). The experimental points and the general recombination curve for this doserate are given in Fig.38. As before, good agreement was found between theory and experiment. When these data are replotted against V/d or E and compared with the initial recombination theory (Fig. 39) it is plain that there is no evidence of any initial recombination. The saturation voltage in this experiment was 1800 V obtained from a voltage generator. At this value of E = 450 V/cm the experimental value of j_s should be within 0.1 per cent of the theoretical value for the initial theory. A drop of 0.1 per cent in the ionization current was not recorded until E was reduced to 57 V/cm. At this value of E a loss of 0.65 per cent is predicted by Lea's theory and again we must conclude that the initial recombination formula is not applicable at this doserate.

5.8 Comparison of Bowen's Measurements with Cluster Theory.

It is not the purpose of this chapter to disprove Lea's cluster theory but to show that its range of applicability is limited. Kara-Michailova and Lea referred to the work of various experimenters and quoted reasonable agreement with their theory. They pointed out, however, that before a set of experimental data could be considered suitable for comparison with a theory of initial recombination, general recombination must be low and thus ionization intensities must be small, i.e. not more than a few thousand ion pairs/cm.^{3} sec.

The experiments of Bowen (1932) illustrate this point. He studied γ-ray ionization in air from pressures from 1 to 93 atmospheres and for collecting fields from 1.55 to 1009 V/cm. Table 3 shows his results for pressures of 0.98 and 10.5 atmospheres.

Table 3.

Field V/cm.	I P = 0.98 atmos.	I P = 10.5 atmos.
1.55	112.5	79.8
6.2	118.4	86.2
23.0	118.7	89.5
91.5	120.0	94.5
367	119.7	102.1
1009	121.1	108.4

where I is the number of ions collected per cm.^{3} per sec. per atmosphere.

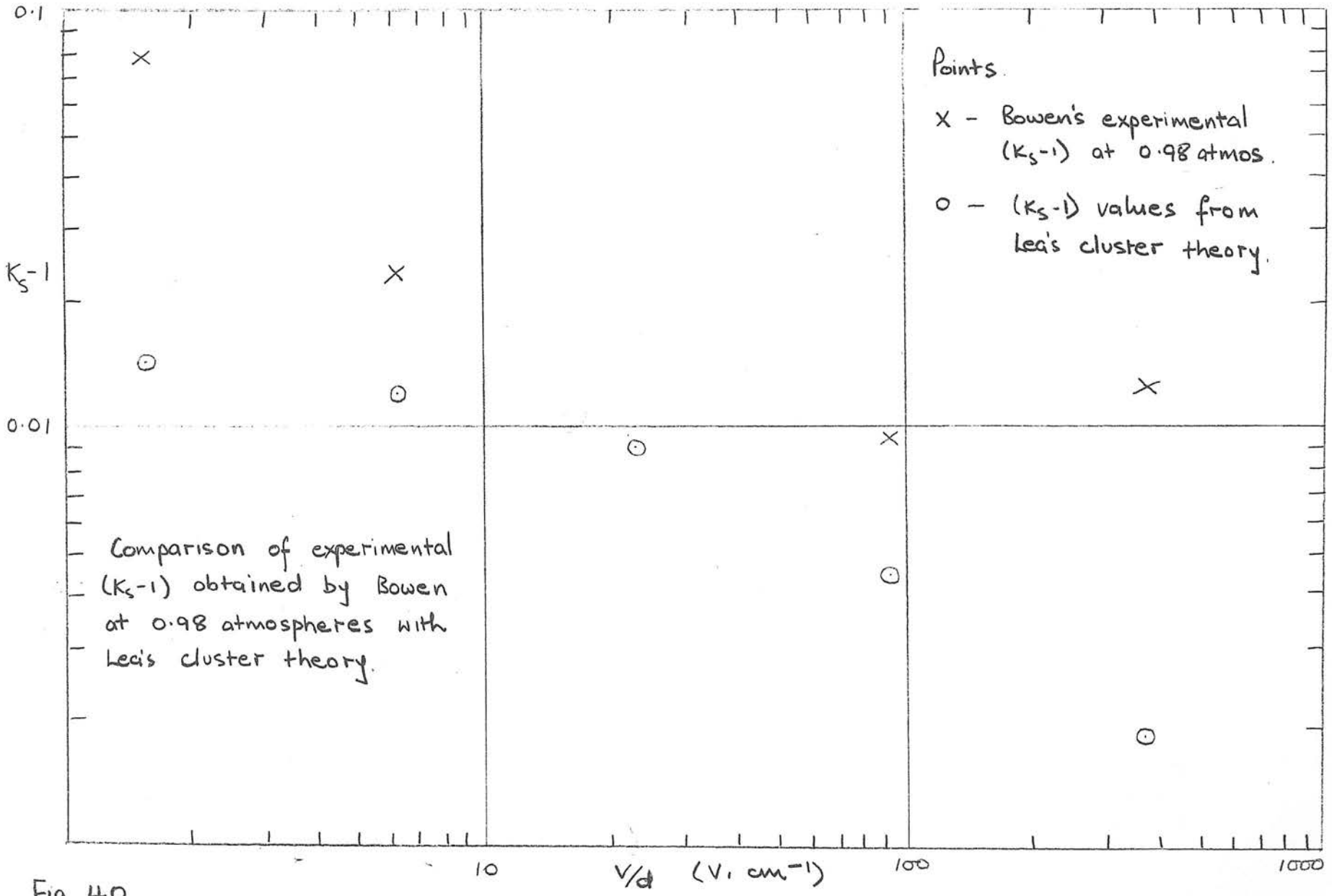
0·1
0·01
$K_s - 1$
10
100
1000
V/d (V. cm^{-1})
Points.
x - Bowen's experimental $(K_s - 1)$ at 0·98 atmos.
o - $(K_s - 1)$ values from Lea's cluster theory.
Comparison of experimental $(K_s - 1)$ obtained by Bowen at 0·98 atmospheres with Lea's cluster theory.

Fig 40

Fig. 40 portrays the experimental values for $(K_s - 1)$ at a pressure of 0.98 atmospheres obtained from Table 3. The same figure shows the theoretical $(K_s - 1)$ factors computed from equation (11) of the cluster theory using our values for the ionic constants. Bowen's source of γ - radiation was radio thorium filtered by 13 mm. of lead. The H.V.L. of this radiation is unknown to us but from data on the thorium series (Radiochemical Manual), we find the three most abundant γ -ray energies are 0.24, 0.58 and 2.62 MeV. Using mass absorption coefficient data given by Victoreen (1949) it can be calculated that a negligible proportion of 0.24 MeV and only 24 per cent of 0.58 MeV γ -rays are allowed through this filter. Since the three rays are about equally abundant it seems safe to assume that the effective γ -ray energy is considerably greater than 0.6 MeV. Tables drawn up by Lea (1946) show that 99 per cent of this γ -ray energy appears as recoil electrons with a mean energy of 220 keV.

Now the higher the electron energy the lower the primary specific ionization s_o and hence the columnar recombination factor decreases with increasing keV. Even taking 200 keV for the electron energy we find that for E = 1.55 the correction due to columnar recombination is only about 0.1 per cent. Columnar recombination can therefore be neglected in this case.

A comparison between the experimental and theoretical points shown in Fig.40 indicates discrepancies of 1 per cent for E greater than 6 V/cm. and 6 per cent for E = 1.55 V/cm. This does not

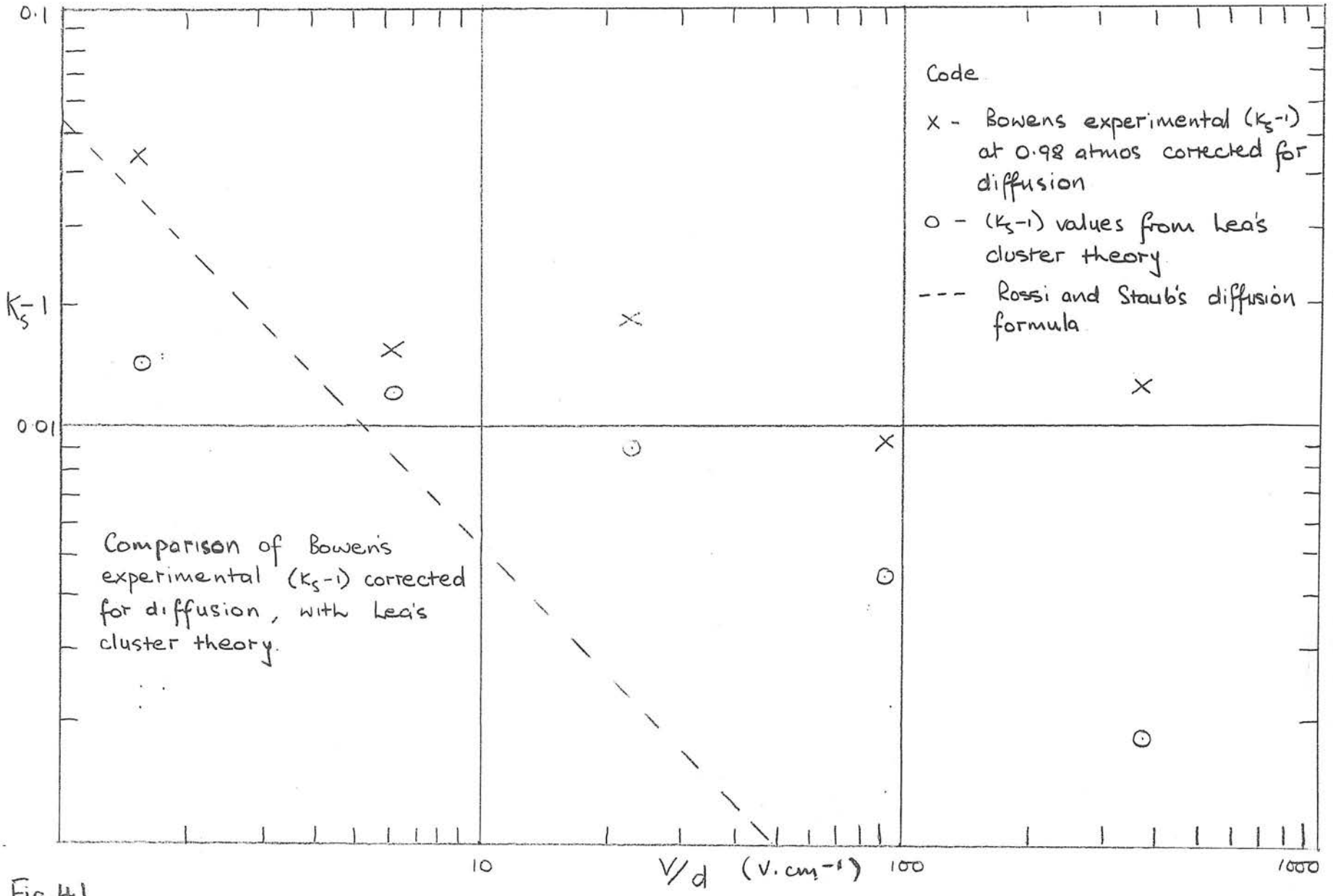
0.1
0.01
$K_s - 1$
10
100
1000
V/d (V.cm^{-1})
Code
X - Bowens experimental (K_s-1) at 0.98 atmos corrected for diffusion
O - (K_s-1) values from Lea's cluster theory
--- Rossi and Staub's diffusion formula
Comparison of Bowen's experimental (K_s-1) corrected for diffusion, with Lea's cluster theory.

Fig 41

seem unreasonable, however, when we consider that Bowen was using ionization intensities of about 120 ions/cm.^{3} sec. i.e. a value only 20 times greater than that from natural background radiation and equivalent to a doserate of 3.5×10^{-6} r/min.! The experimental values for $(K_s - 1)$ lie consistently higher than the theoretical points. A possible explanation for this is that Kara-Michailova and Lea did not specify the values for α and k they used for pressures lower than 5 atmospheres. Assuming our values for the ionic constants to be correct, however, better agreement is obtained between theory and experiment when ion losses due to diffusion are taken into account. Rossi and Staub (1949) derived a formula for the proportion of ions lost due to their diffusion to the "wrong" electrode against the electric field. This formula is discussed in detail in Chapter 9 and takes the form

$$K_s - 1 = \frac{\frac{5 \times 10^{-2}}{V}}{1 - \frac{5.10^{-2}}{V}}$$

In this case $d = 1$ cm. $\therefore K_s - 1 = \dfrac{\frac{5 \times 10^{-2}}{E}}{1 - \frac{5 \times 10^{-2}}{E}}$

Fig. 41 shows the effect of correcting Bowen's experimental points for diffusion. The maximum discrepancy between theory and experiment is now 3 per cent.

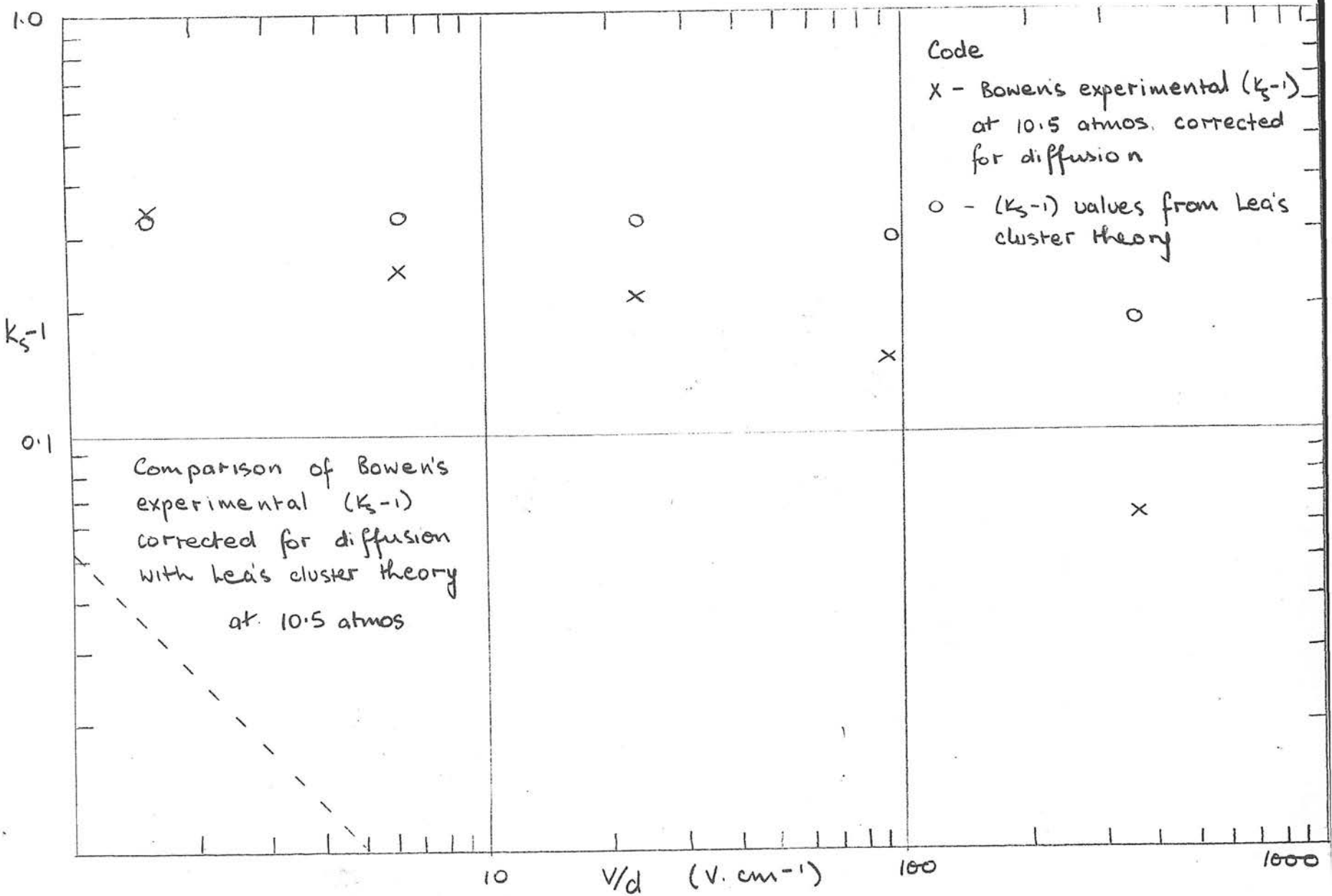
1.0
0.1
K_s-1
Code
X - Bowen's experimental (K_s-1) at 10.5 atmos. corrected for diffusion
O - (K_s-1) values from Lea's cluster theory
Comparison of Bowen's experimental (K_s-1) corrected for diffusion with Lea's cluster theory at 10.5 atmos
10
V/d (V. cm^{-1})
100
1000

Fig 42

Lea's cluster theory was primarily derived to calculate recombination in gases under high pressures where initial recombination will obviously be more important. Bowen's experimental values for $(K_s - 1)$ in air at a pressure of 10.5 atmospheres are given in Fig.42. The theoretical $(K_s - 1)$ are computed using Kara-Michailova's and Lea's values for the ionic constants. An estimation of the columnar recombination occurring at $E = 1.55$ V/cm. is about 1.5 per cent taking the electron energy to be 200 keV. The diffusion correction to the experimental $(K_s - 1)$ at this E is 3.5 per cent. This means that there is good agreement between theory and experiment at $E = 1.55$ V/cm. but differences of as much as 15 per cent arise at higher values of E.

From Kara-Michailova's and Lea's own graphical comparison of their theory and Bowen's results, it appears that at pressures of 10.5 and 24.95 atmospheres theory overestimates ion losses, but the converse is true at the highest pressure $P = 93$ atmospheres. It seems likely, therefore, that their value for b obtained by comparing theory and experiment was an average taken over this wide range of pressures. For closer agreement between theory and experiment at $P = 10.5$ atmospheres an increase in the value of b would help. After correction to the experimental $(K_s - 1)$ for diffusion at $P = 0.98$ atmospheres, the same relative values of theory and experiment would also be obtained by an increase in b.

5.9 Reasons for Lack of Agreement between Experimental Results and Cluster Theory.

It was shown in Chapter 5.4 that when Kara-Michailova and Lea attempted to calculate the cluster radius b on theoretical grounds, the result was some ten times greater than the experimental value from Bowen's work. Since this theoretical value for b was based on an extrapolation of Bradbury's measurements (1933) in order to obtain the value of the electron attachment probability h at thermal velocities, it seemed profitable to ascertain whether any further studies of h had been made at these velocities.

Although a review of the literature did not bring to light any direct measurement of h at thermal energies, it served to show that data on h obtained by various experimenters were by no means all concordant. Healey and Reed (1941) criticised Bradbury's calculations of his results since he used inaccurate values for the electron drift velocities. They advocated the values for h obtained by Bailey (1925) using a different experimental technique and drift velocity values due to Townsend and Tizard (1913). For the lowest measured electron energy (V = 0.1 V). Bailey's value for h is about ten times smaller than that of Bradbury. Since b is proportional to $1/\sqrt{h}$ this means that if Bailey is correct, the theoretical value for b is thirty times the experimental one !

In his chapter on the formation of negative ions, Loeb (1955) quoted the work of Doehring (1952) who found in the course of measuring h for oxygen that Bailey's experimental technique led to under-estimation of h. Under these circumstances Loeb believed that there was not much choice between the data from these two experimenters despite the fact they differed by a factor of 10! Recent studies by Kuffel (1958), however, have verified Bradbury's values for h at electron energies less than 1.6 V. It seems, therefore, that the value for h at thermal velocities obtained from Bradbury's results is the most accurate available. It should be noted, however, that Bradbury used dry air in his experiments and since water vapour has a higher attachment probability, it is likely that for ordinary air a slightly greater value of h should be used.

Thus both from theoretical grounds and from Bowen's experimental work at pressures less than 25 atmospheres, a larger value of b than 1.05×10^{-3} cm. is predicted. If we take b as 3×10^{-3} cm. and substitute this into the cluster theory, we find that $(K_s - 1)$ values are reduced sufficiently to avoid conflict with our experimental results at a doserate of 1 r/min. (5.7). As far as Bowen's results are concerned, this change in b at P = 0.98 atmos. does not appreciably alter the difference between theory and experiment if the latter has been corrected for diffusion, while at P = 10.5 atmos. theory underestimates experimental $(K_s - 1)$ by as much as it previously over-estimated them.

On the other hand this choice of b means that as the pressure is increased, the cluster theory will progressively underestimate Bowen's experimental results. It is also greater than the value for the radius of an α - particle column, i.e. 1.79×10^{-3} cm. which satisfies Jaffé's theory.

In view of this doubt as to the correct value for b and on the basis of our experiments it is tempting to state categorically that at atmospheric pressures there is no evidence of initial recombination occurring at doserates greater than 1 r/min. and therefore that $1/j$ is proportional to $1/E^2$.

Later experimental studies with an extrapolation chamber, however, showed that at doserates of as much as several thousand r/min, $1/j$ was proportional to $1/E$ for very small plate separations (less than 0.2 cm.) This will be discussed in detail in Chapter 9 but it seems that the dependence of ionization current on the applied field is a complex function of doserate and plate separation. Conditions most favourable for initial type recombination are low ionization intensities and small plate separations. This is borne out by all the experimental work quoted by Kara-Michailova and Lea. In each case, the ionization intensity was only a few thousand ion pairs/cm.^{3} sec. at most and, although in Lea's experiments (1934) he used a cylindrical chamber in which the distance between the collecting rod and outer electrode was 5 cm, investigators operating parallel plate chambers used spacings of not more than 2 cm.

5.10 Conclusions.

Since our free-air chamber was specifically designed for measurements of low energy radiation its geometry is very compact and its plate separation is several times smaller than in free-air chambers for use in medium and high energy ranges. It thus appears safe to assume that in all free-air chambers operating at atmospheric pressure, recombination losses will be entirely due to volume recombination for doserates greater than 1 r/min. In the theoretical determination of saturation currents, therefore, an extrapolation plot of $1/j$ against $1/E^2$ is recommended. At high pressures and low ionization intensities where initial recombination is predominant, j_s is obtained from plotting $1/j$ against $1/E$.

CHAPTER 6.

COMMENTS AND CONCLUSIONS

ON

CHAPTERS 2 - 5.

6.1 Conclusions.

After a critical survey of existing theories we chose Boag and Wilson's formula (1952) as the most suitable expression for volume recombination losses in a parallel-plate ionization chamber. We then adapted their formula to suit a free-air chamber using Hübner's method (1958) and carried out a series of further modifications. Consideration was given to the effective width of a circular cross-section X-ray beam and to the influence of space charges. Finally the effect of ion spread and distribution on both recombination and space charge was investigated.

The modified formula was checked experimentally with a small free-air chamber by varying field strength, dose-rate, beam quality and size and shape of the X-ray beam. Good confirmation was obtained over a wide range of operating conditions.

It has been shown that the current practice of estimating the theoretical saturation current from an extrapolation equation due to Kara-Michailova and Lea (1940) is incorrect for free-air chambers at atmospheric pressures and doserates greater than 1 r/min. For these conditions a different extrapolation equation, based on our formula, has been suggested.

It is hoped that the formula will be an aid to calculating saturation losses in many experimental situations and that its extrapolation equation will provide a method for the quick determination of saturation currents. It should also prove useful in fundamental free-air chamber design since it emphasises the importance of adequate chamber dimensions and the choice of suitable aperture sizes.

Fig 43

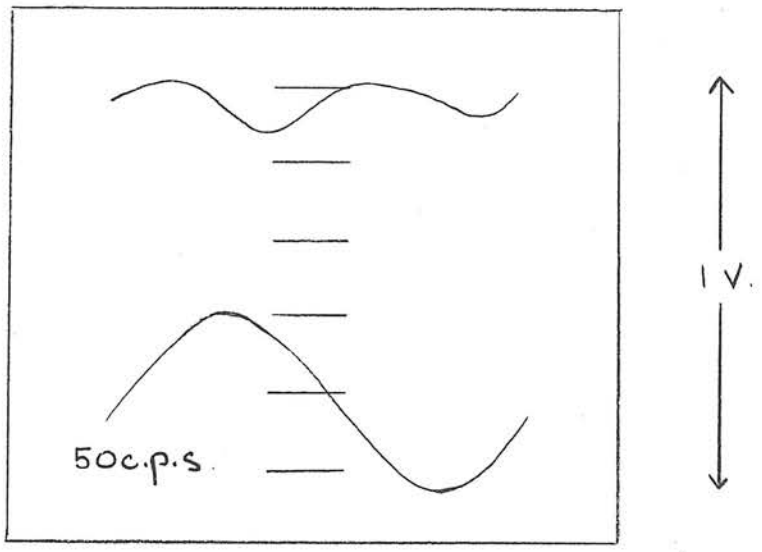

Trace taken from an oscilloscope showing variation in output from X-ray machine at 45 kV.

6.2 Criticisms of Present Formula.

Although our formula gives adequate representation of experimental findings, there is still room for improvement. No account has been taken of the effect of non-uniformity of ionization on recombination. We have estimated that the reduction in recombination due to this is less than 14 per cent but we did not calculate this accurately. The space charge correction chosen is only an approximation and again no allowance is made for the non-uniform distribution of ionization.

Another point to be considered is the dose-rate "waveform" provided by the X-ray machine. The dose-rate variation with time in our experiments was investigated using a large multiplate ionization chamber (Greening 1959) in conjunction with an oscilloscope. Traces taken showed that the output from the tube was constant to within 15 per cent (Fig. 43). We therefore assumed that it was not necessary to modify our theory to allow for fluctuations in dose rate. Normal unsmoothed half- or full-wave rectification would lead to pulses of ionization and in any particular case, consideration would need to be given to the extent to which the space charge produced by one pulse of radiation had been collected before the next pulse occurred.

Thus a completely satisfactory theory could only be evolved from a rigorous mathematical treatment of these points. It is doubtful, however, whether this is in fact necessary since the formula would become too cumbersome to be of any practical use. In any case the exact spacial distribution of ionization is rarely known.

CHAPTER 7.

DESIGN AND CONSTRUCTION OF AN EXTRAPOLATION CHAMBER

Fig 44.

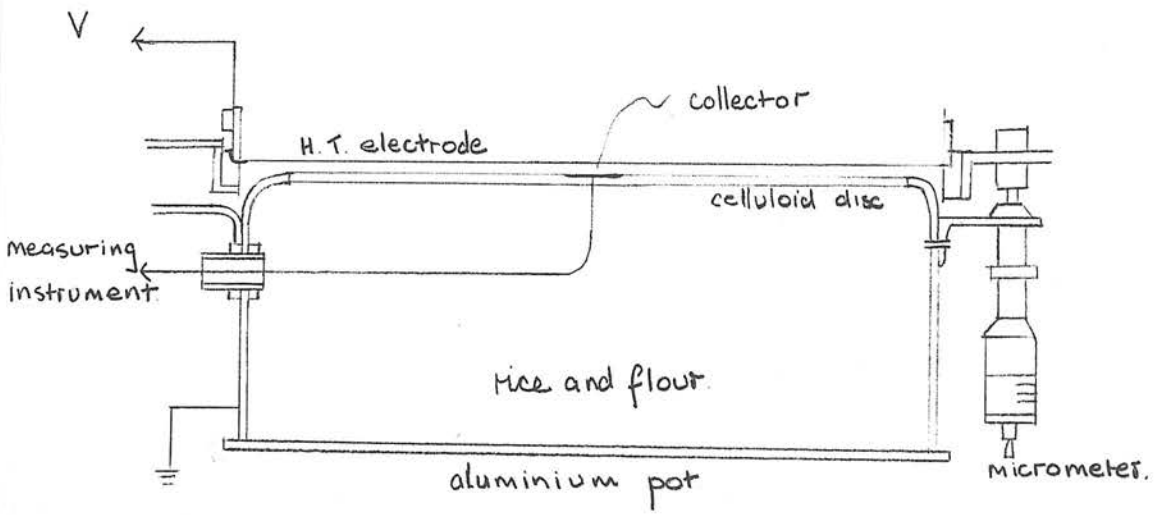

Schematic view of extrapolation chamber designed by Failla.

7.1. Prototype Extrapolation Chamber due to Failla.

In radiation therapy the dose received at the skin surface from the primary beam is augmented by radiation scattered back from underlying tissue.

The extrapolation chamber was first devised by Failla (1937) in order to estimate skin and tissue dosages. His aim was to construct a chamber with tissue equivalent walls and by measuring the ionization current for decreasing plate separations, to determine the relation between the ionization per unit volume and the air layer thickness. By extrapolating these results to zero air thickness he planned to obtain the ionization per unit volume at the surface of the skin.

Failla found that it was not practicable to construct a chamber with entirely tissue equivalent walls and his compromise is shown schematically in Fig.44. The base of the chamber was an aluminium pot with the bottom turned out and a celluloid disc screwed on in its place. The top of the disc was coated with Indian ink to make it conducting and a small circle was scribed at the centre with a sharp compass. This small circular area constituted the collecting electrode while the remainder of the disc formed the guard ring and was connected to the aluminium pot. When a null method of current measurement was used the scratch made by the compass was sufficient to provide good insulation between the collector and guard plates. The

space below the celluloid disc was filled with rice and flour to simulate tissue and the connection between the collecting electrode and the current measuring instrument was made through a fine rubber insulated wire.

The upper electrode consisted of ink soaked chiffon stretched over an aluminium hoop. This was mounted on three micrometer screws which were fixed rigidly to the base of the aluminium pot. These micrometers provided both the means for measuring the plate separation and ensuring the parallelism of the electrodes. Failla pointed out, however, that in practice he found that the celluloid disc did not remain plane and that it was difficult to determine the absolute spacing with great precision.

7.2 Design Considerations.

The basic mechanical arrangement of an extrapolation chamber must be such that the two electrodes always remain parallel and that their separation may be measured to a high degree of accuracy. Some recent papers on the design of extrapolation chambers have suggested mounting the upper electrode on a movable shell threaded internally and marked externally in micrometer drum style (Bortner, 1951, Loevinger, 1952 and Scarboro and Silverman, 1959). This type of chamber demands a high degree of precision in construction and it was felt that a simpler improvement on Failla's design could be made by ensuring that the collecting surface remained plane and checking the micrometer readings by capacity measurements.

A solid perspex base was therefore envisaged with the top surface graphited and a collecting area scribed in the centre. The upper electrode was to be mounted on three micrometer heads resting in closely fitting holes drilled into the periphery of the base at equal intervals. By placing a steel ball bearing at the bottom of each hole this method of supporting the micrometer heads ensures positive points of contact and prevents any rotation of the upper electrode whilst its height is being altered.

The most important dimension of the chamber is the diameter of the collecting electrode. The choice of this factor

is influenced by the general size of the chamber since in order to eliminate field distortion a wide guard ring is desirable. Another point to bear in mind is that while a large collector has the advantage of high sensitivity it also demands greater requirements on the degree of parallelism between the two surfaces. We wanted a fairly compact chamber, e.g. a base width of about 6 in. and we therefore chose 3 cm. as a suitable collecting diameter.

Fig 45.

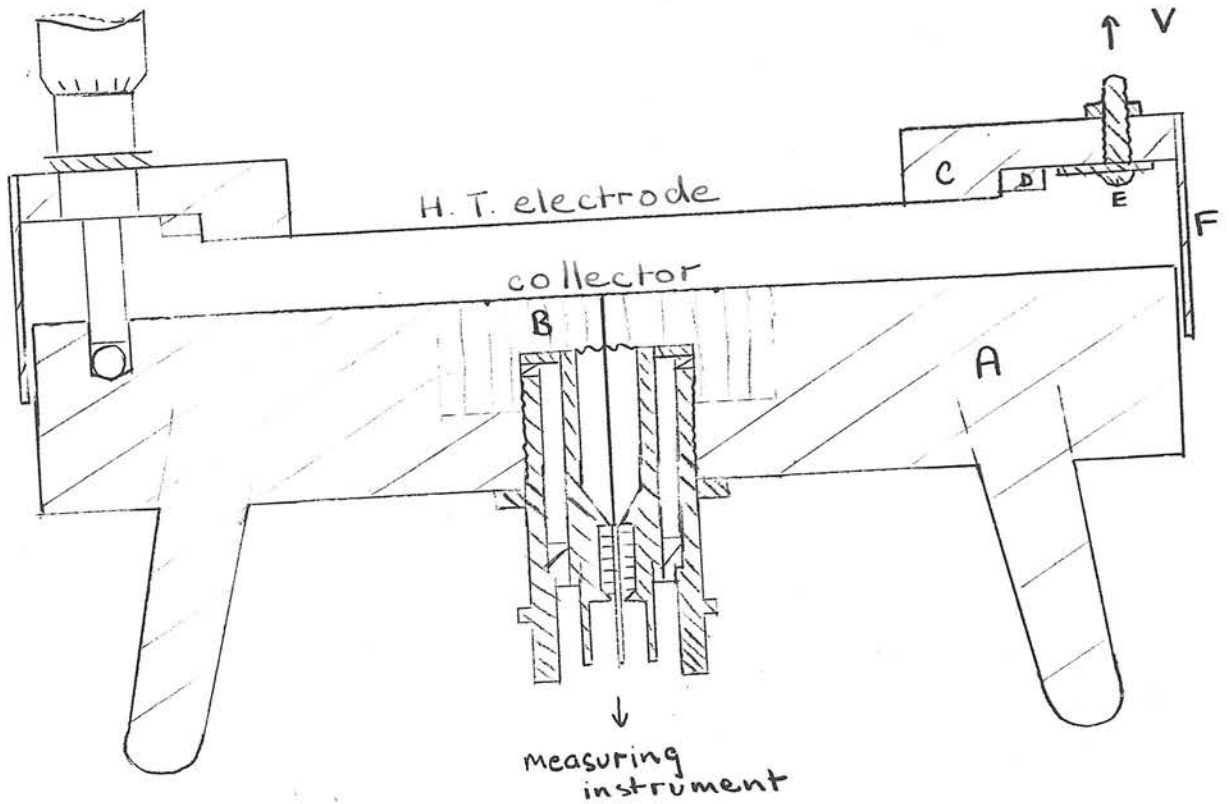

Cross-section of extrapolation chamber drawn to scale

brass perspex polythene polystyrene

A - block ; B - inset ; C - annulus ; D - ring ; E - H.T connection ; F - dust shield

7.3. Construction.

A cross-section of the extrapolation chamber is given in Fig. 45 . Since ionization currents were to be measured by an I.D.L. vibrating reed electrometer, the chamber base was built round a plug which would fit directly into the head amplifier. The base was a perspex block, A, 6 in. in diameter and 1 in. deep, standing on three legs. High insulation is required between the collector and the guard ring and since perspex tends to absorb water which lowers its surface resistivity, an inset of polystyrene, B, 2 in. in diameter was let into the centre of A. The surface of the base was carefully machined flat and rendered conducting by spraying on colloidal graphite ("Dag") and then scraping it off with a scalpel until a smooth bonded conducting surface was obtained. The collecting plate was an area 3 cm. in diameter scribed at the centre. Connection between the collector and the centre pin of the plug was made by a length of pencil lead while the guard ring was connected to the inner socket via a graphite trail.

The upper electrode consisted of aluminised Melinex stretched over the perspex annulus C. Melinex was chosen because of its thinness (10^{-3} in.)., toughness and stretch characteristics. Some difficulty was encountered in procuring a flat taut surface. The first idea was to hold the foil in position by means of a rubber "O" ring as suggested by Scarboro and Silverman (1959), but it proved impossible to obtain a wrinkle-free surface in

Fig 46

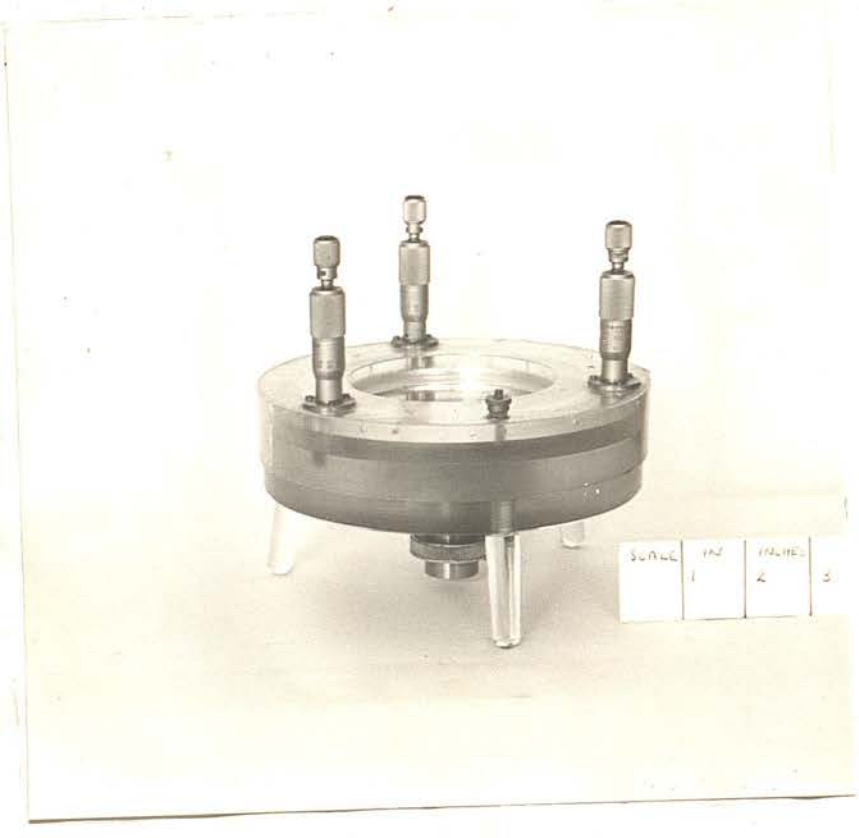

Extrapolation Ionization Chamber

this way. The problem was eventually solved by pre-stretching a piece of the foil on a 7 in. embroidery hoop, placing the hoop over C and then ramming the electrode home with a tightly fitting perspex ring D. The excess foil round the edges was trimmed off with a scalpel except for a small piece which made contact with the screw E leading to the H.T. supply.

In order to prevent dust reducing the insulation across the groove separating the collector and guard ring, a dust shield F was fitted round the top of the chamber. A small clearance was deliberately left between F and A to allow free access from the collecting volume to the atmosphere and so avoid pressure sensitivity. It also proved necessary to keep the top of the chamber covered, since dust particles falling on the H.T. electrode were able to work their way between the foil and the perspex (C) and hence reduce the effective plate separation.

A view of the completed chamber is shown in Fig.46.

Fig 47

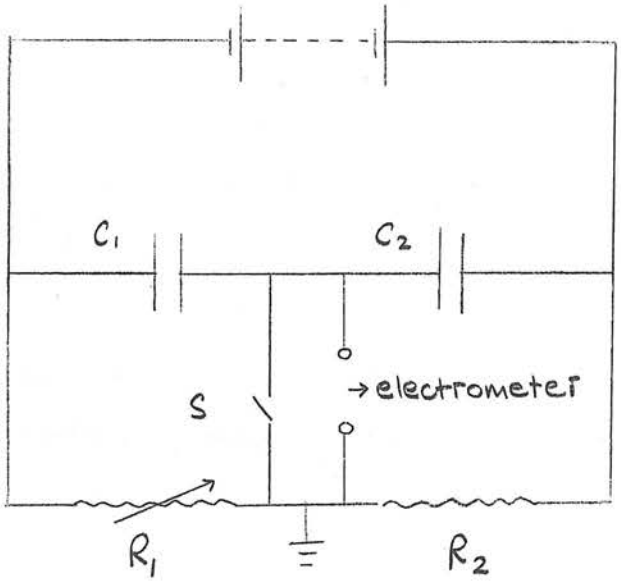

Townsend balance circuit for capacity measurement.

7.4. Measurement of Insulation and Plate Separation.

The insulation between the collector and guard plates of the chamber was tested by the resistance measuring unit of a Vibron electrometer Model 33B. The insulation resistance was found to be $\sim 10^{13}$ ohms which is sufficiently high for our purposes since both plates are operated at earth potential. Throughout the experimental series periodic checks were made to ensure that the insulation was maintained at this level. If dust was present in the groove it was removed by a fine camel-hair brush viewed through a travelling microscope.

Zero setting of the micrometer heads was first carried out by hand and the nominal plate separations were then verified using a resistance - capacity bridge (Fig. 47). This is another Townsend balance circuit in which C_1 represents a known capacitor and C_2 the chamber capacity at a given plate spacing. A voltage is applied across AB and when the earthing switch S is opened, the variable resistance R_1 is altered to keep the point P at earth potential. As before the null detector is a Lindemann electrometer. When the bridge is balanced

$$\frac{C_2}{C_1} = \frac{R_1}{R_2}$$

In making measurements with the extrapolation chamber C_1 was chosen to be 99.5 pF, $R_1 = R_2 = 100$ K and the fraction of R_1 for balance was given by a dial reading.

Table 4 shows a comparison between the nominal plate separation μ and the spacing d obtained from substituting for capacity in the formula for a parallel plate condenser.

i.e. $d = A/4\pi C$

where A is the area $= \pi (1.5)^2$ $(cm.^2)$

C is the capacity in e.s.u.

Expressing C in pF we find $d = \frac{0.625}{C}$

Table 4.

μ	C	d	μ -d
cm.	pF.	cm.	cm.
0.05	12.6	0.0495	0.0005
0.04	14	0.0447	0.0003
0.03	21	0.0298	0.0002
0.02	50.3	0.0199	0.0001
0.01	64.8	0.00975	0.00025

Agreement between μ and d is thus within 1 per cent except for the lowest μ.

CHAPTER 8.

OPERATION OF EXTRAPOLATION CHAMBER AND EXPERIMENTAL RESULTS.

Fig 48

I.D.L. Vibrating Diaphragm Electrometer with Extrapolation Chamber in position.

8.1. Current Measuring System.

Our extrapolation chamber was designed to plug directly into the head amplifier of an I.D.L. vibrating diaphragm electrometer type 1880A (Fig. 48). This instrument has a voltage measurement range from 10 to 2,000 mV, i.e. it is capable of measuring currents within the range 10^{-14} - 10^{-6} A depending on the value of the input resistor. The input sensitivity is continuously variable so that any value of voltage or current within these limits may be represented at full scale on the front panel meter. The response-speed is also continuously variable, thus critical damping may be achieved over a wide range of signal sources and input arrangements. A relay in the head amplifier, remotely actuated from the indicator unit, short circuits the input so that zero checking and setting can be carried out from the indicator unit without need to disconnect the signal. Another useful feature of the instrument is an internal polarising voltage supply available up to 200 positive or negative volts and monitored by the meter.

During the initial operation of this electrometer several snags were encountered. The zero setting was found to drift quite appreciably but fortunately this stopped after several days continual running of the instrument. A more irritating feature was that changing the response speed control caused a

marked and undesirable shift of the zero setting. This was discovered to be due to pick up in the response speed line from the modulator coils. The insertion of decoupling condensers in both the head amplifier and the indicator unit and of extra screening round the inter-connecting cables corrected this fault.

It was decided to use an external polarising supply, viz. several 120 volt Winner dry batteries in order to attain finer voltage control than that given by the electrometer supply. Voltage variation was obtained by connecting two variable rheostats in parallel with the batteries thus giving coarse and fine control. Voltage measurements were made on an A.V.O. meter except for values of less than 1.8 volts where the volts were provided and measured by a standard potentiometer.

The input resistor supplied by the manufacturers was nominally 10^{10} ohms. Its value was checked by the Vibron 33B and found to be 0.9×10^{10} ohms.

Fig 49

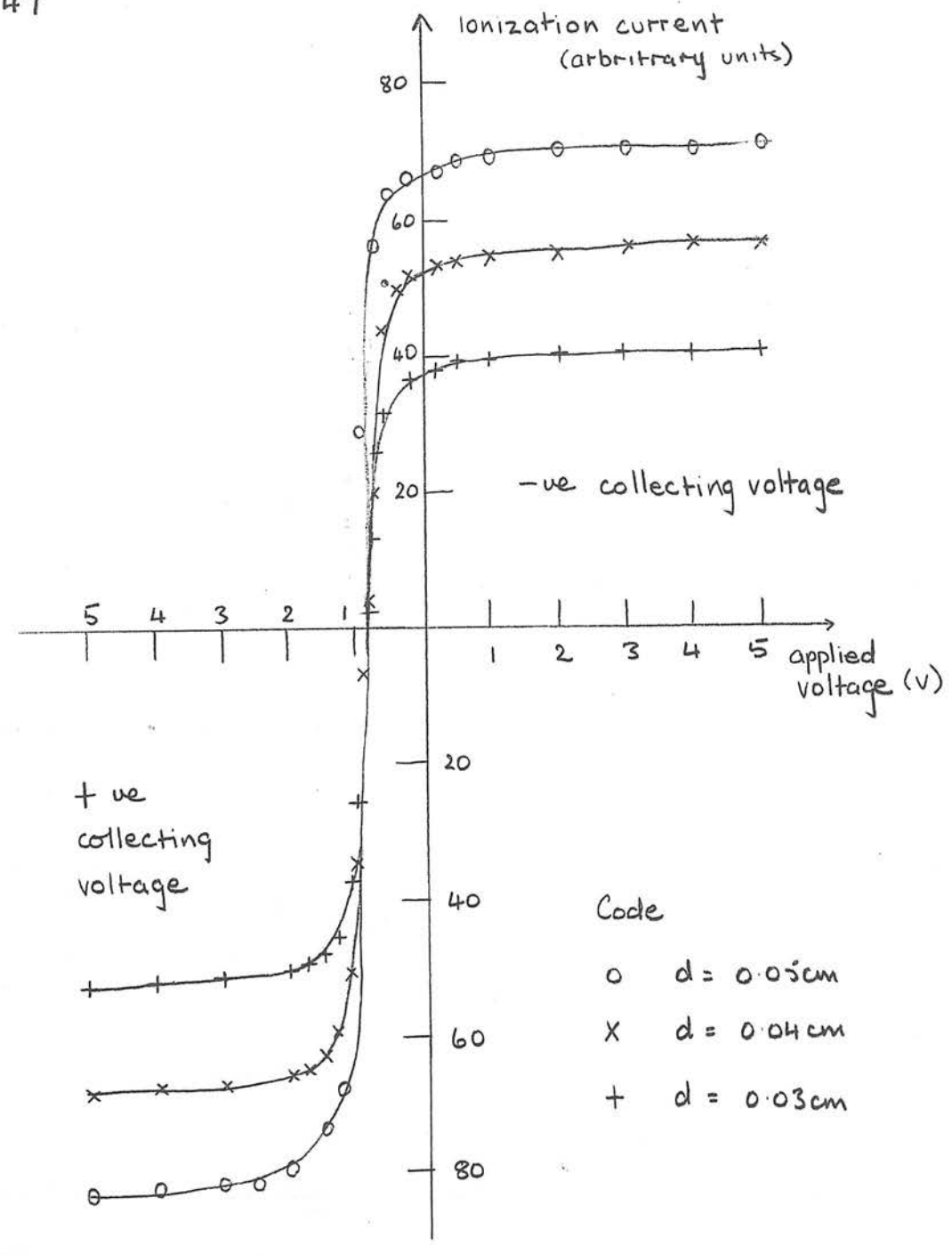

Plots of ionization current against applied voltage for various d using 1mC source

8.2 Preliminary Experiments.

Some trial measurements were made with the extrapolation chamber under β-irradiation. Two sources of about 1 mC and 5 mC respectively were available. These were in the form of silver discs with a thallium 204 compound of high specific activity bonded firmly within the metal resulting in an active diameter of 3 cm. The required source was mounted on a steel plate which was then screwed down into position on the top of the chamber. The steel plate thus acted as a dust shield for the thin electrode and a radiation shield for the experimenter.

The first trial was carried out using the 1 mC source and saturation runs were made for plate separations ranging from d = 0.05 cm. to d = 0.03 cm. using "saturation" field strengths of several KV/cm. Readings were taken for both positive and negative collecting voltages so as to observe the charge carried by the primary β-particles. Fig.49 illustrates the ionization current-applied voltage relationships for various d. These results indicated that there was a contact potential of about one volt in the circuit since at a positive collecting voltage of this value the ionization current was zero and it reversed direction when the voltage was decreased further. It was also noted that after the current had changed direction it tended to drift slowly back towards zero. This proved puzzling until a search in the literature revealed a possible

explanation. During an investigation into the saturation curve of a similar type of ionization chamber, Boag, Pilling and Wilson (1951) noticed exactly the same effect. After many experiments they concluded that it was due to a property of the oxide layer on the surface of the aluminium foil forming their electrodes. They found that the apparent contact potential could be eliminated by painting the aluminium surfaces with a very thin coating of colloidal graphite.

We tried this remedy with considerable success since the "contact potential" was reduced to approximately 0.2 volts by spraying a thin layer of "Dag" on the aluminium surface of the H.T. electrode. Due to the difficulty in obtaining a sufficiently thin and even layer of graphite, it was decided to use gold as the conducting surface. A sample of clear melinex was obtained from the manufacturers and a piece some 9 in. square was mounted on a metal frame and placed in a large bell jar. The pressure inside the jar was reduced to less than 10^{-4} mm.Hg. by means of a diffusion pump and then a small amount of gold was evaporated on a hot filament. Provided care was taken in mounting the melinex so that there were no "shadows" between it and the gold, and that it was not allowed to overheat and therefore shrink, this proved an excellent method for obtaining a conducting surface which was only about 500 A° in thickness.

The H.T. electrode was made from the gold coated melinex in exactly the same way as for the aluminised melinex. Results

showed that with this electrode the "contact potential" was reduced still further and indeed appeared in the opposite polarity at a value of 0.05 volts. This was probably a true contact potential and had a negligible effect on the saturation characteristics of the chamber.

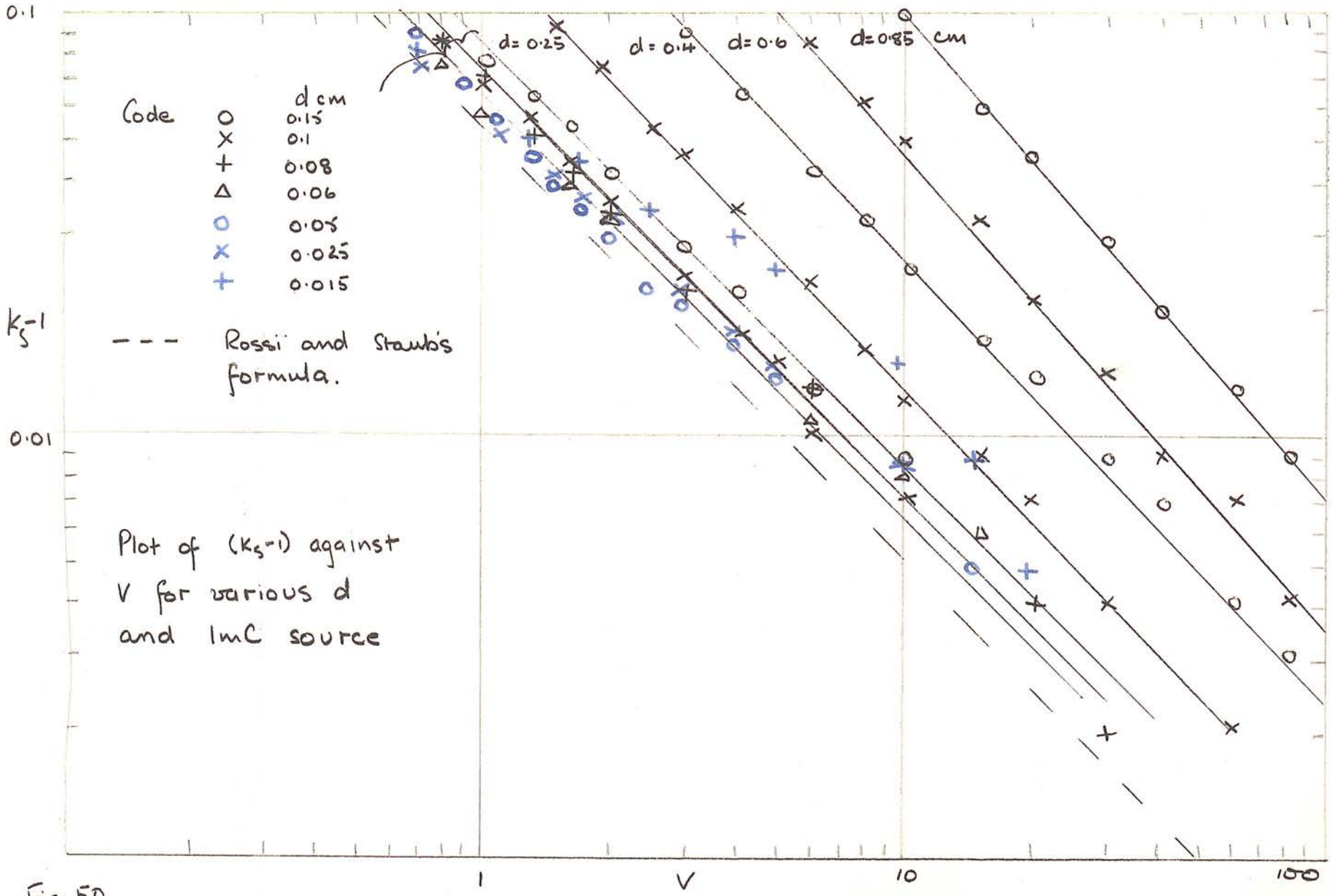
0·1
0·01
K_S-1
d = 0·25
d = 0·14
d = 0·6
d = 0·85 cm
Code
d cm
○ 0·15
× 0·1
+ 0·08
△ 0·06
○ 0·05
× 0·025
+ 0·015
– – – Rossi and Staub's formula.
Plot of (K_S-1) against V for various d and 1mC source
1
V
10
100

Fig 50

8.3. Saturation Curves for Various Plate Separations under Irradiation.

The use of the gold coated electrode and hence the elimination of the "contact potential" effect proved a valuable time-saver during our experimental investigations since the ionization current at any applied voltage was then simply the mean of the values for positive and negative collection. This meant that it was only necessary to measure current losses of up to 10 per cent for each polarity.

A series of saturation runs was made for plate separations ranging from d = 0.015 cm. to d = 0.85 cm. The source of radiation was the 1 mC disc held in position at a fixed distance of 0.8 cm. above the H.T. electrode. The effective doserate at these various d is discussed in Chapter 8.4. $(K_s - 1)$ values were calculated as before and are shown plotted on a double log. scale against the applied voltage in Fig.50. These measurements were made using the 10^{10} ohms input resistor and the saturation current readings varied from about 750 mV for d = 0.85 cm. to 25 mV for d = 0.015 cm. This meant that the accuracy of measurement ranged from $\pm$ .02 per cent to $\pm$ 1.0 per cent. The results for the lowest d values must be therefore considered as possessing a wide point scatter.

From Fig. 50 it appears that plotting log $(K_s - 1)$ against log V with d as parameter, results in a family of approximately parallel straight lines with a slope of -1.0.

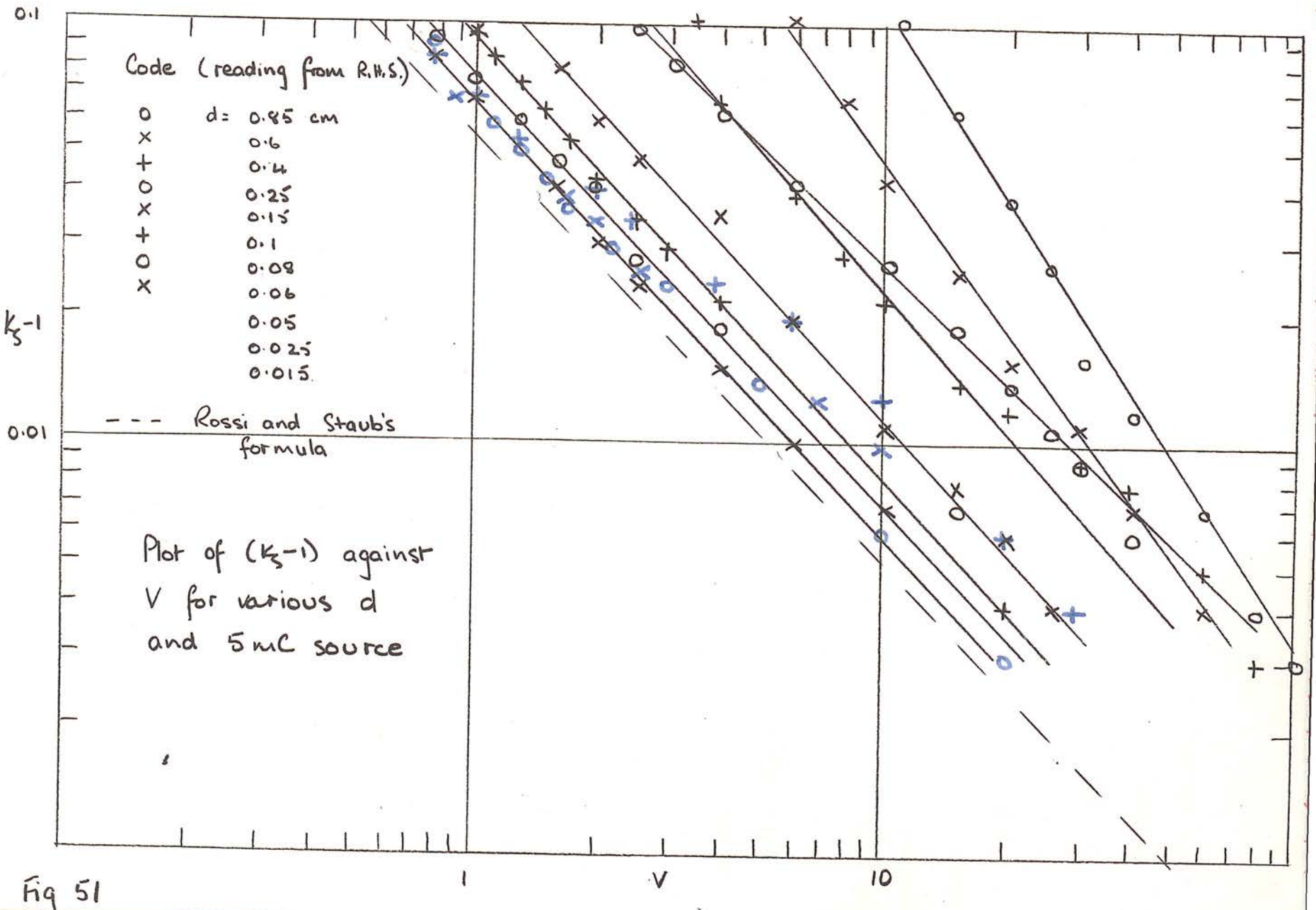
0.1
0.01
$k_s - 1$
Code (reading from R.H.S.)
o d = 0.85 cm
x 0.6
+ 0.4
o 0.25
x 0.15
+ 0.1
o 0.08
x 0.06
0.05
0.025
0.015
--- Rossi and Staub's formula
Plot of $(k_s - 1)$ against V for various d and 5 mC source
1
V
10

Fig 51

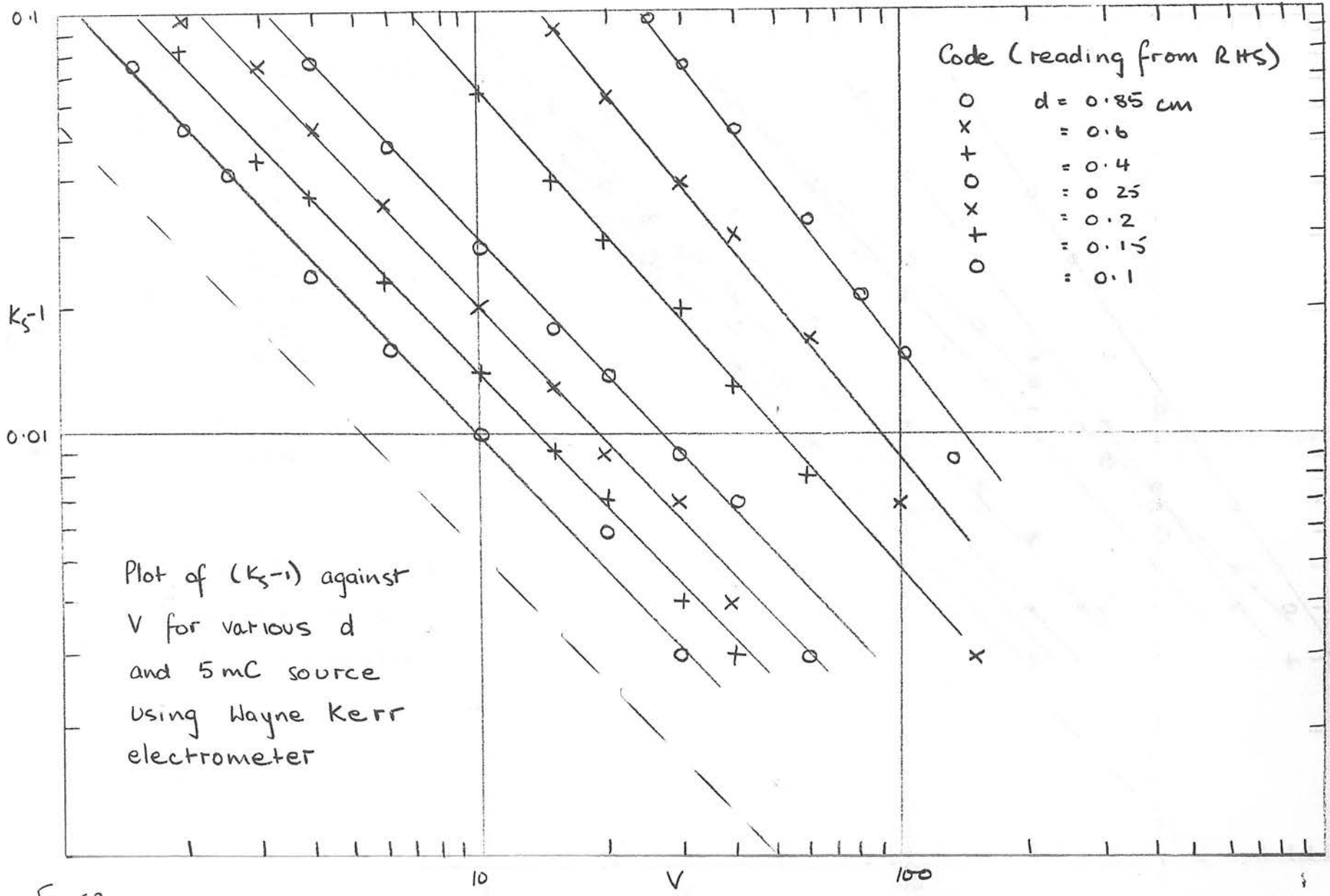
0·1
K_s-1
0·01
10
V
100
Code (reading from RHS)
o d = 0·85 cm
x = 0·6
+ = 0·4
o = 0·25
x = 0·2
+ = 0·15
o = 0·1
Plot of (K_s-1) against V for various d and 5 mC source using Wayne Kerr electrometer

Fig 52

The broken curve in the diagram represents the losses caused by diffusion of ions to the "wrong" electrode from the formula due to Rossi and Staub (1949). As might be expected the results for low d values indicate that losses are almost entirely due to diffusion. At larger values of d the slope of -1.0 suggests that recombination is probably initial.

The same series of experiments was performed for the 5 mC source and these results are shown in Fig. 51 . The overlap which occurs between (K_s - 1) values for d = 0.25 and d = 0.4 cm. coincided with changing the 10^{10} ohm resistor for one of 10^9 ohm. Since the (K_s - 1) factors for the other plate separations coincided quite well with those for the 1 mC source, it was thought at first that (K_s - 1) was independent of doserate and that the results for d = 0.25 cm. and the 5 mC source were faulty in some way.

The situation was clarified by the fortuitous loan to the Department of a Wayne Kerr Electrometer type M.141. This proved an exceedingly satisfactory instrument to operate. Measurements were made by transferring the first digit of the reading to a decade control and a meter then indicated the second and subsequent digits. Since the voltage measurement range was 1 mV to 10 V all the 5 mC results for d greater than 0.1 cm. were repeated, using the one input resistor, i.e. 10^{10} ohm. (Fig. 52). A comparison between the measurements made on the two electrometers revealed that the Wayne Kerr gave higher estimates of saturation losses than did the I.D.L.

with the 10^9 ohm input resistor. Unfortunately the period of loan was too short to allow all the experiments to be repeated on the Wayne Kerr electrometer but a few measurements made for d less than 0.1 cm. sufficed to confirm the I.D.L. results using its 10^{10} ohm resistor. The inference was therefore that the measurements made with the 10^9 ohm resistor in the I.D.L. electrometer were incorrect. This was possibly because of some contamination on the glass surface of the resistor although it had been carefully cleaned with alcohol before use.

We were thus forced to conclude that $(K_s - 1)$ was not dose-rate independent since at the largest d values there was a definite increase in $(K_s - 1)$ when the 1 mC source was replaced by 5 mC.

Fig 53

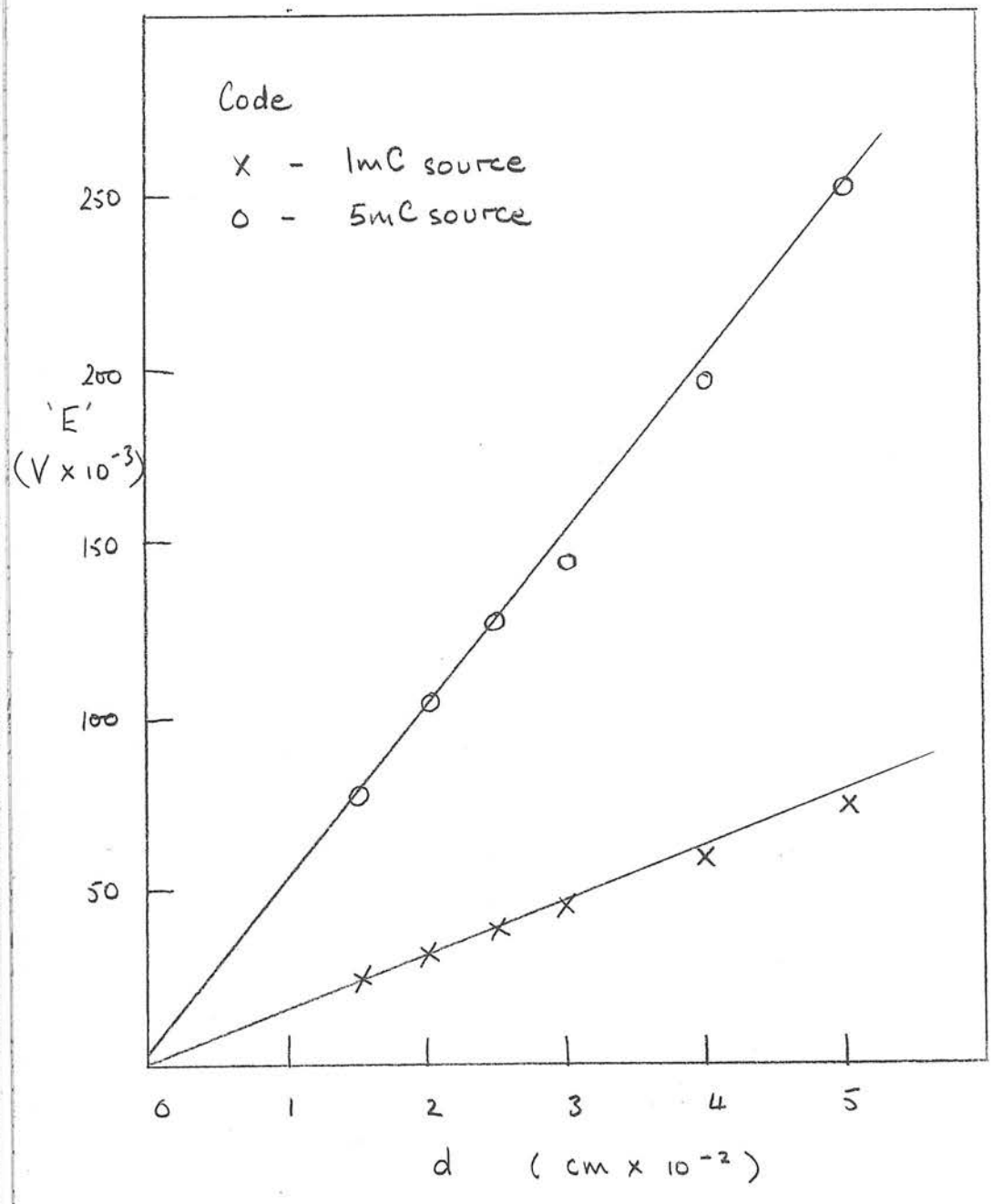

Plots of electrometer potential 'E' against d

Fig 54

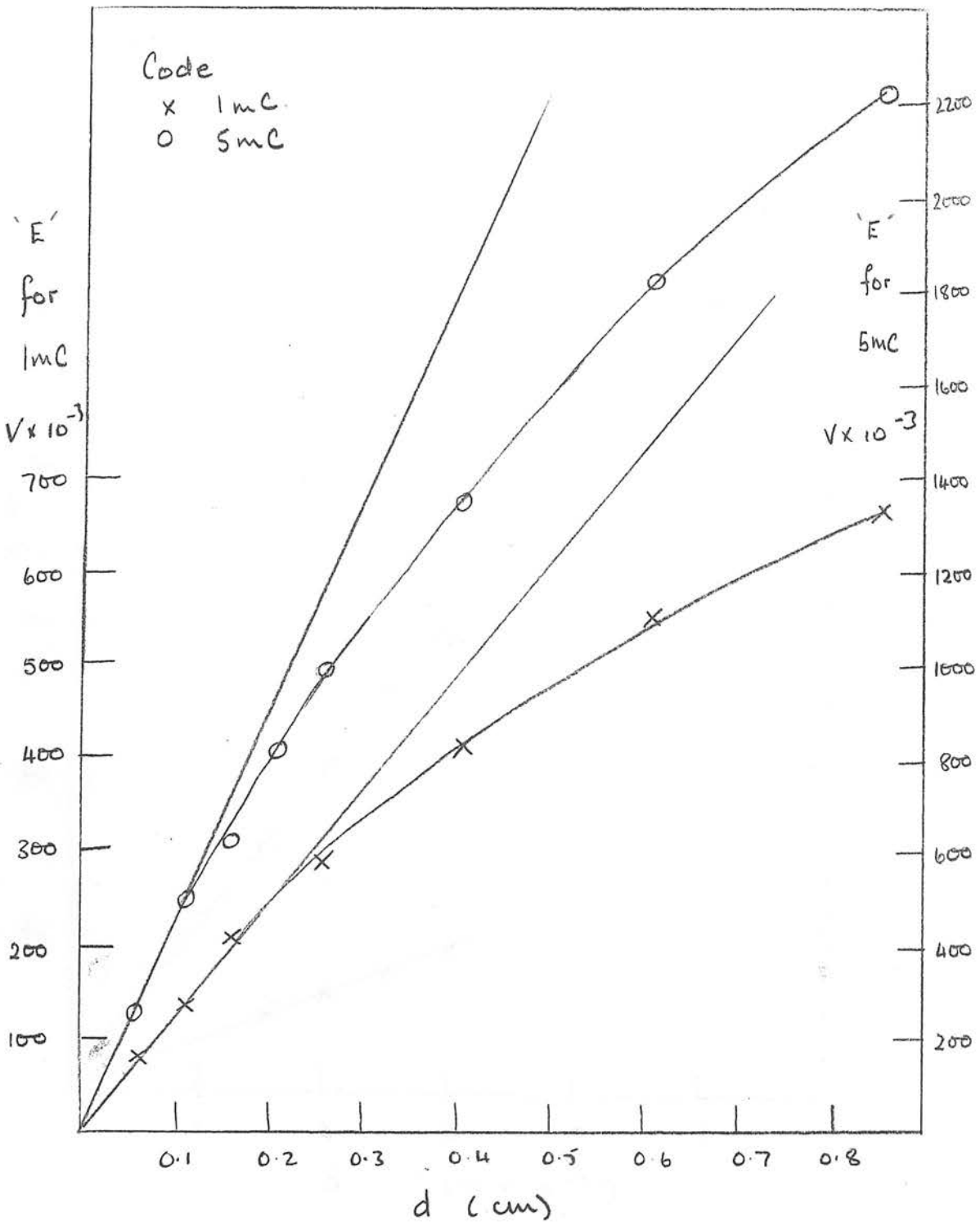

Plots of electrometer potential against d

Fig 55

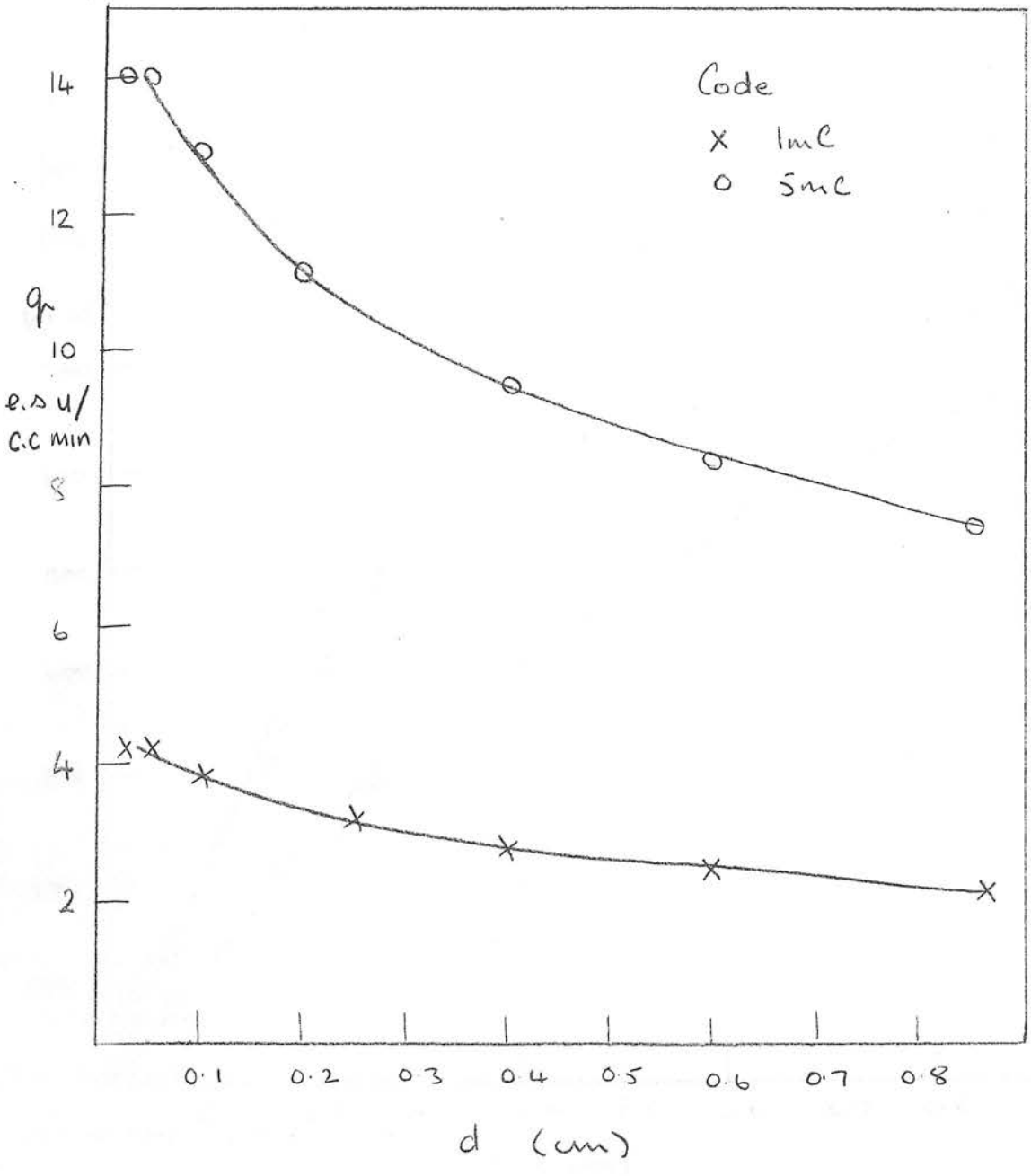

Plots of ionization intensity against plate separation

8.4. Saturation Curves at Various Doserates under β-Irradiation.

The doserate measured by an extrapolation chamber can be calculated from an equation due to Bortner (1950).

$$I = 3 \times 10^{9} \times \frac{E'T}{PRV} \times K$$

where I = doserate in e.s.u./cm.^{3} sec.

P = barometric pressure in mm.Hg.

T = absolute temperature

E' = electrometer potential (V)

R = resistance of electrometer circuit (ohm)

K = 760/295

V = vol. of air from which ions are collected (cm.^{3})

$= \pi r^2 d$ (r = radius of collecting electrode)

This formula predicts that a plot of electrometer potential against plate separation should result in a straight line. Fig. 53 illustrates our results for the 1 mC and 5 mC sources and shows that straight lines are obtained when E' is plotted against d of less than 0.05 cm. If electrometer readings for larger plate separations are graphed, however, curves of gradually decreasing slopes are found (Fig. 54). This means that the effective doserate falls off with increasing plate separation (Fig. 55). This is to be expected since the back scattered radiation from the collecting electrode and the forward scatter from the H.T. electrode will maximise the ionization intensity at the smallest plate separations.

In order to investigate further the effect of doserate

Fig 56

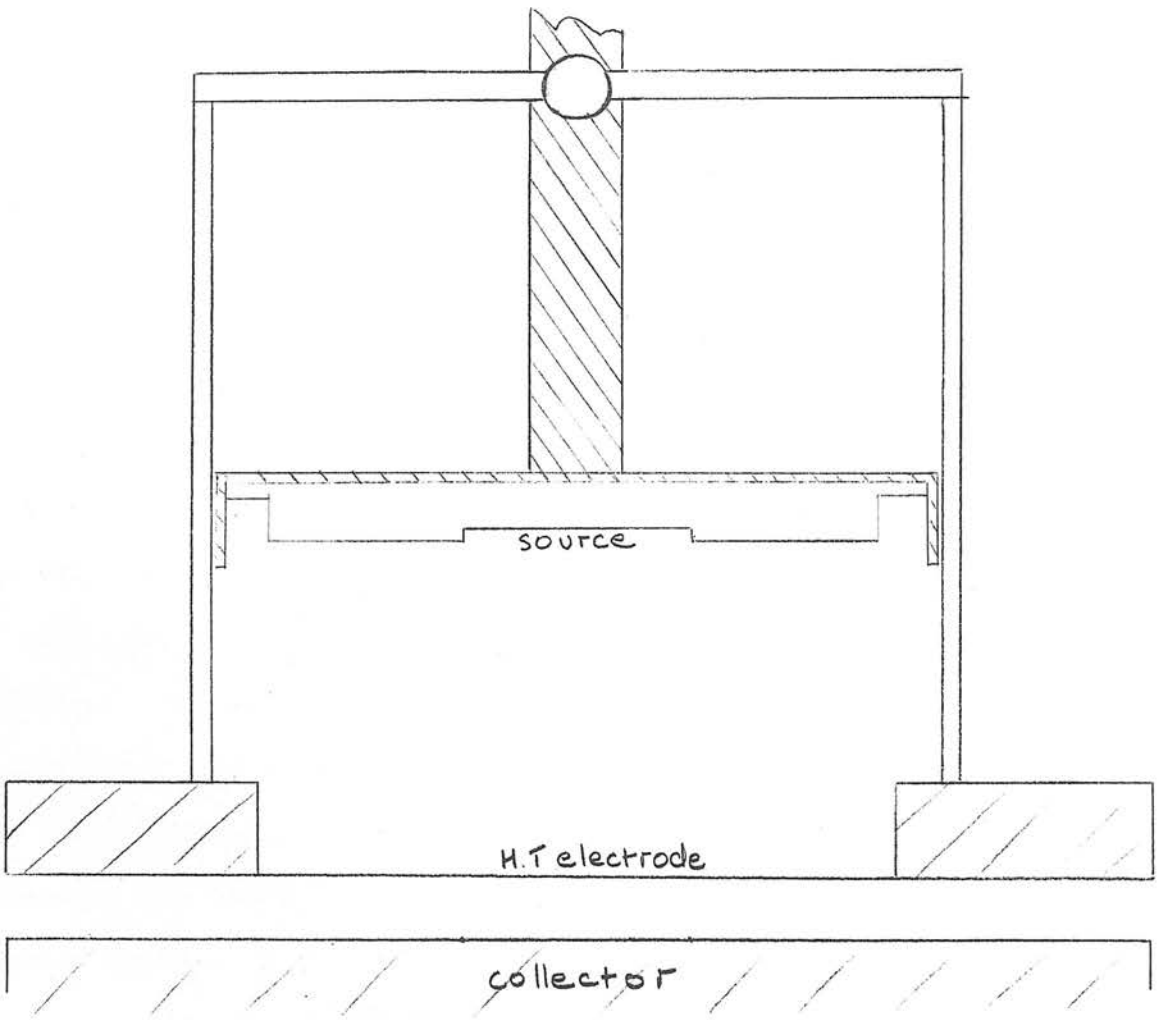

Experimental arrangement for altering source heights.

brass perspex steel

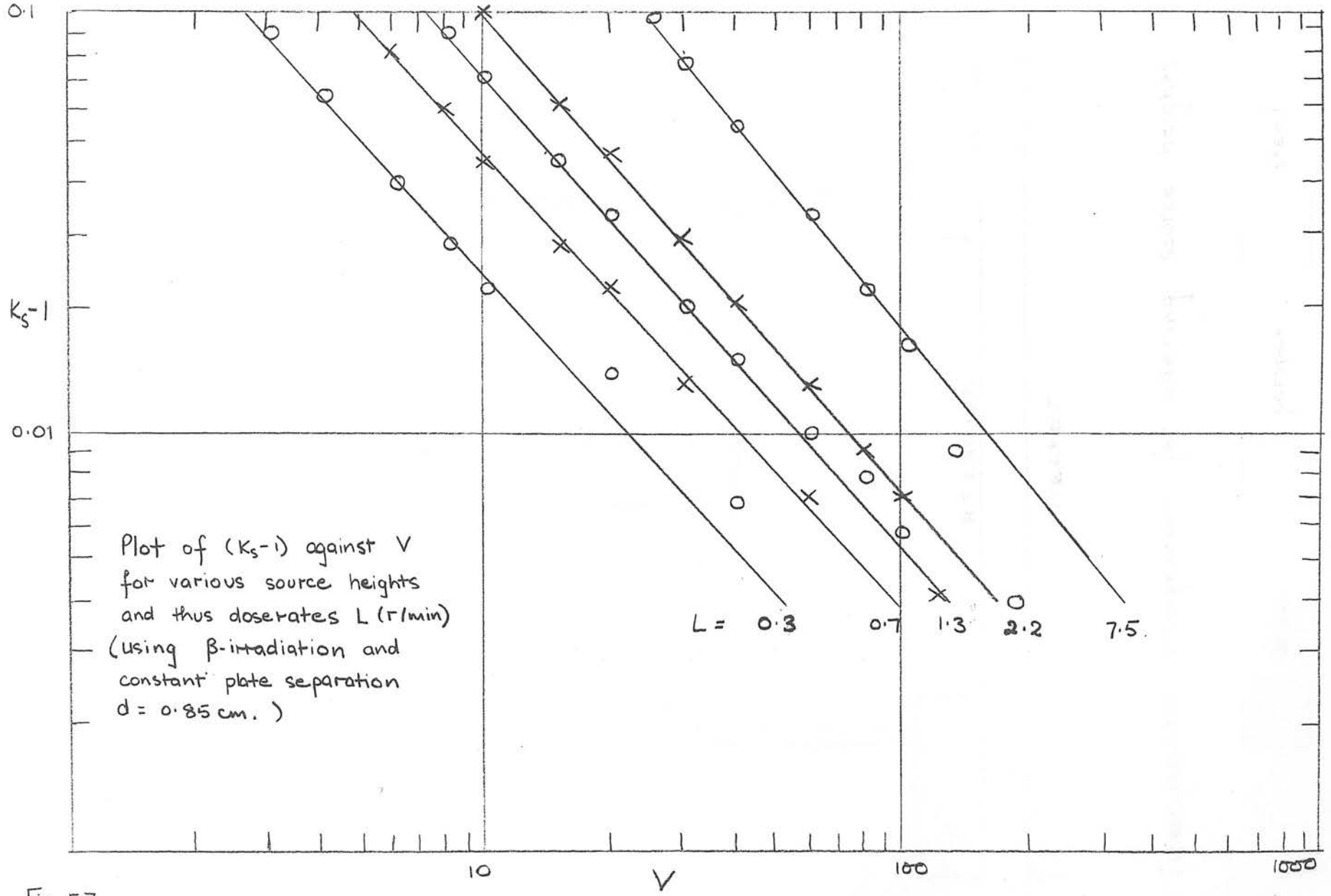
0·1
$K_s - 1$
0·01
Plot of $(K_s - 1)$ against V
for various source heights
and thus doserates L (r/min)
(using β-irradiation and
constant plate separation
d = 0·85 cm.)
L = 0·3
0·7
1·3
2·2
7·5
10
V
100
1000

Fig 57

on the saturation characteristics of the extrapolation chamber, measurements were made with the β-ray source at various heights above the collecting electrode. Fig.56 shows the experimental arrangement. A steel cylinder was screwed down to the top of the chamber. The steel holder of the β-ray source was screwed to one side of a brass plate which had a brass rod soldered to the centre of the other side. The brass plate fitted exactly inside the steel cylinder and the rod could be clamped to any desired height by a bracket fixed to the top of the cylinder.

The $(K_s - 1)$ factors at various source heights are plotted against the collecting voltage in Fig.57 and show a definite decrease with decreasing doserate.

N.B. In an attempt to measure very low ionization currents a 10^{11} ohm resistor was used in the I.D.L. electrometer. When the $(K_s - 1)$ factors were graphed a strange increase in slope was found compared to similar results for the 10^{10} ohm resistor. Again this was thought to be due to contamination on the surface of the resistor since both the 10^{9} and the 10^{11} ohms had been stored for some time. This emphasises the importance of eliminating surface leakage of the input resistor in making measurements of this type.

8.5. Investigation of Possible Losses due to Lateral Diffusion.

It was thought possible that the increase in saturation losses as the source was brought nearer the collector was not only due to the increase in dose rate but also to the effect of lateral diffusion. Rossi and Staub's formula (1949) deals only with losses due to ions diffusing to the "wrong" electrode and presupposes an experimental situation where the radiation field extends far enough beyond the collecting region to eliminate any losses due to a net movement of ions outwards from the collecting volume. Since our Thallium discs were the same diameter as the collector and the minimal distance (at which the majority of our experiments had been carried out) between the two was (0.8 + d) cm. it seemed possible that ions had been lost because of lateral diffusion.

An identical chamber base, but for the collector plate which was 1 cm. in diameter, was therefore constructed. The zero setting of the micrometer screws and the nominal plate separations were checked as before. An inter-comparison of the two collecting electrodes for several plate separations and the 1 mC source in its nearest position, showed that no losses due to lateral diffusion could be observed.

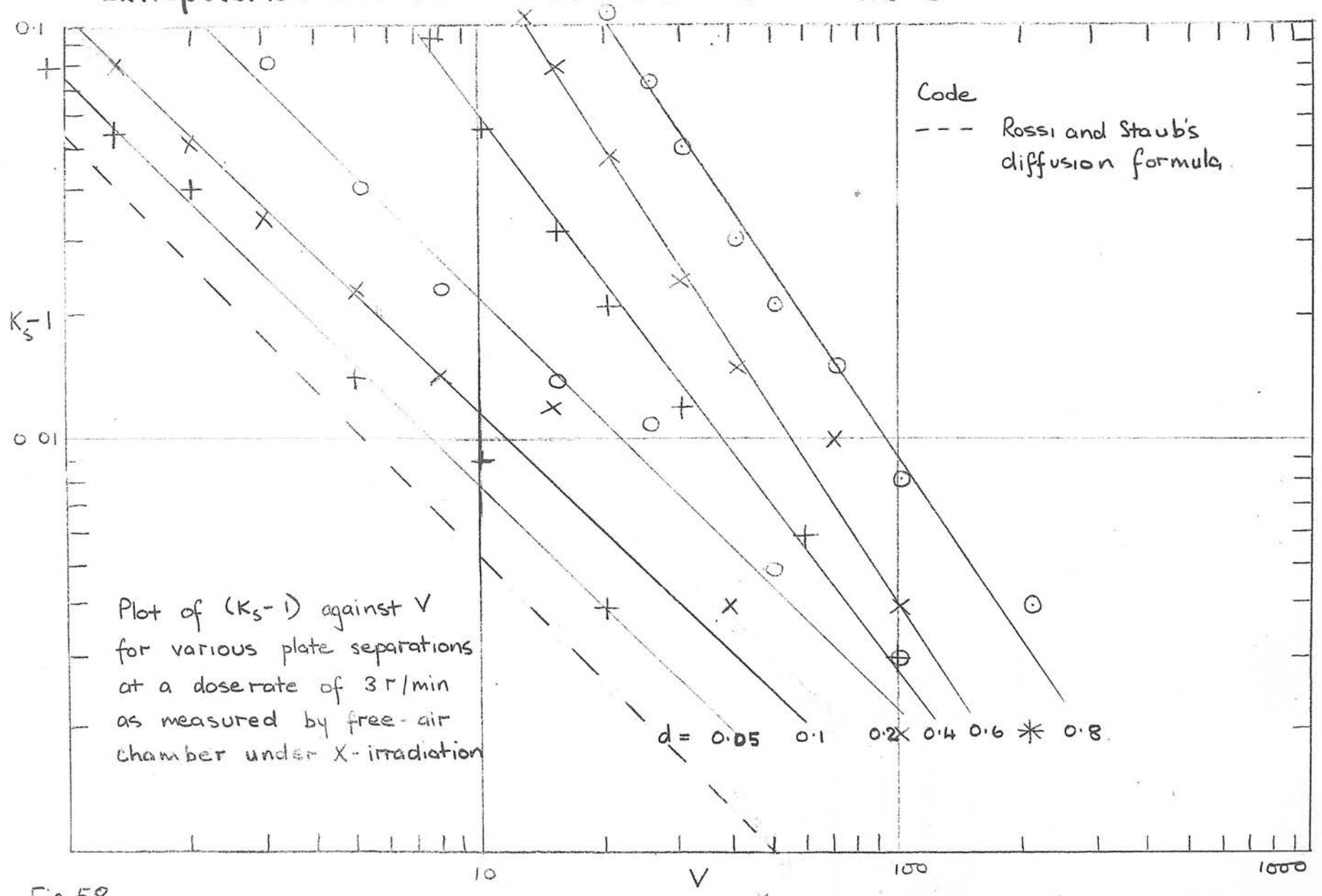
Extrapolation Chamber Results under X-irradiation.
0·1
0·01
$K_s - 1$
10
V
100
1000
Code
--- Rossi and Staub's diffusion formula
Plot of $(K_s - 1)$ against V for various plate separations at a doserate of 3 r/min as measured by free-air chamber under X-irradiation
d = 0·05 0·1 0·2 0·4 0·6 0·8

Fig 58

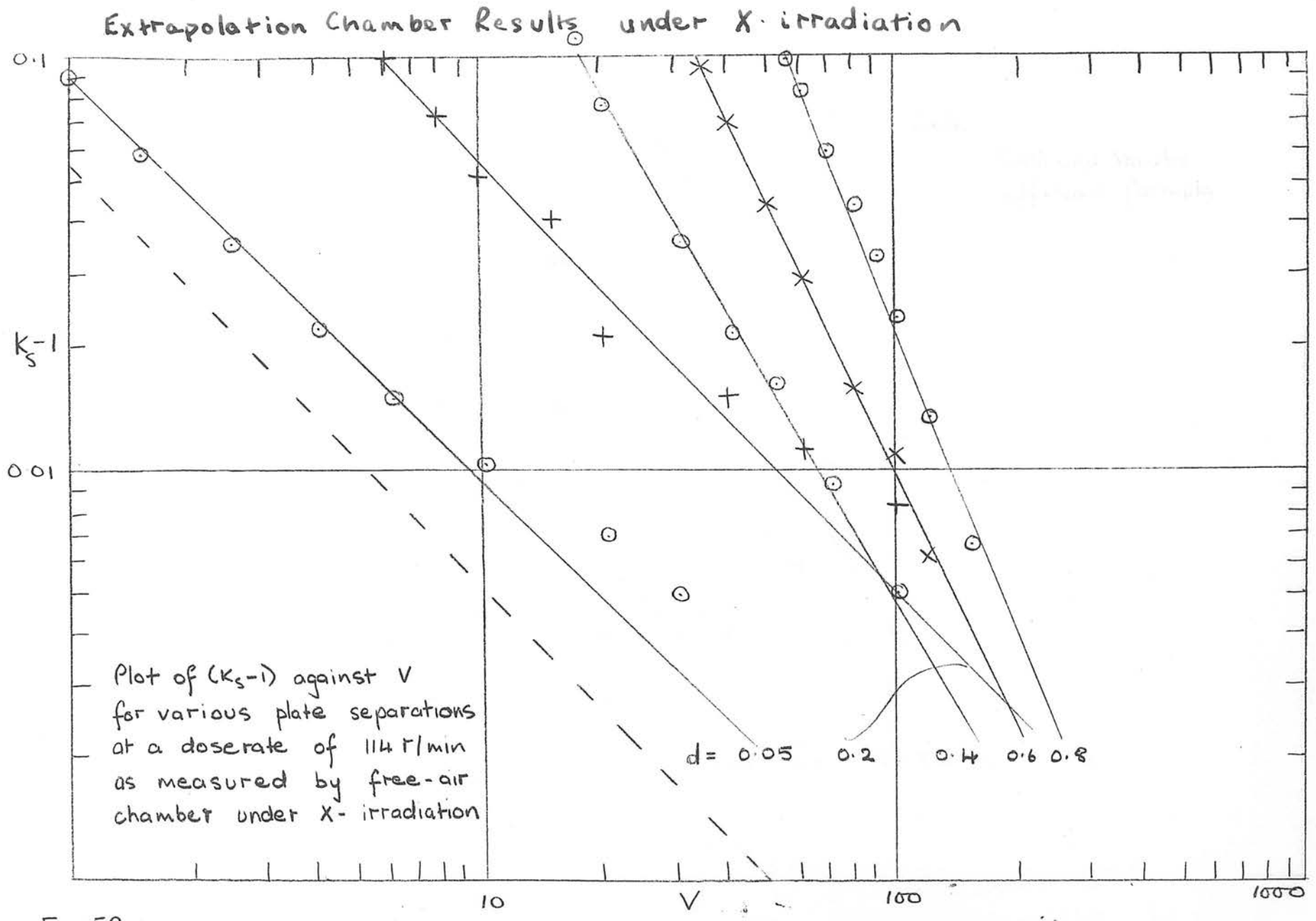
Extrapolation Chamber Results under X-irradiation
0·1
0·01
$K_s - 1$
10
V
100
1000
d = 0·05
0·2
0·4
0·6
0·8
Plot of $(K_s - 1)$ against V
for various plate separations
at a doserate of 114 r/min
as measured by free-air
chamber under X-irradiation

Fig 59

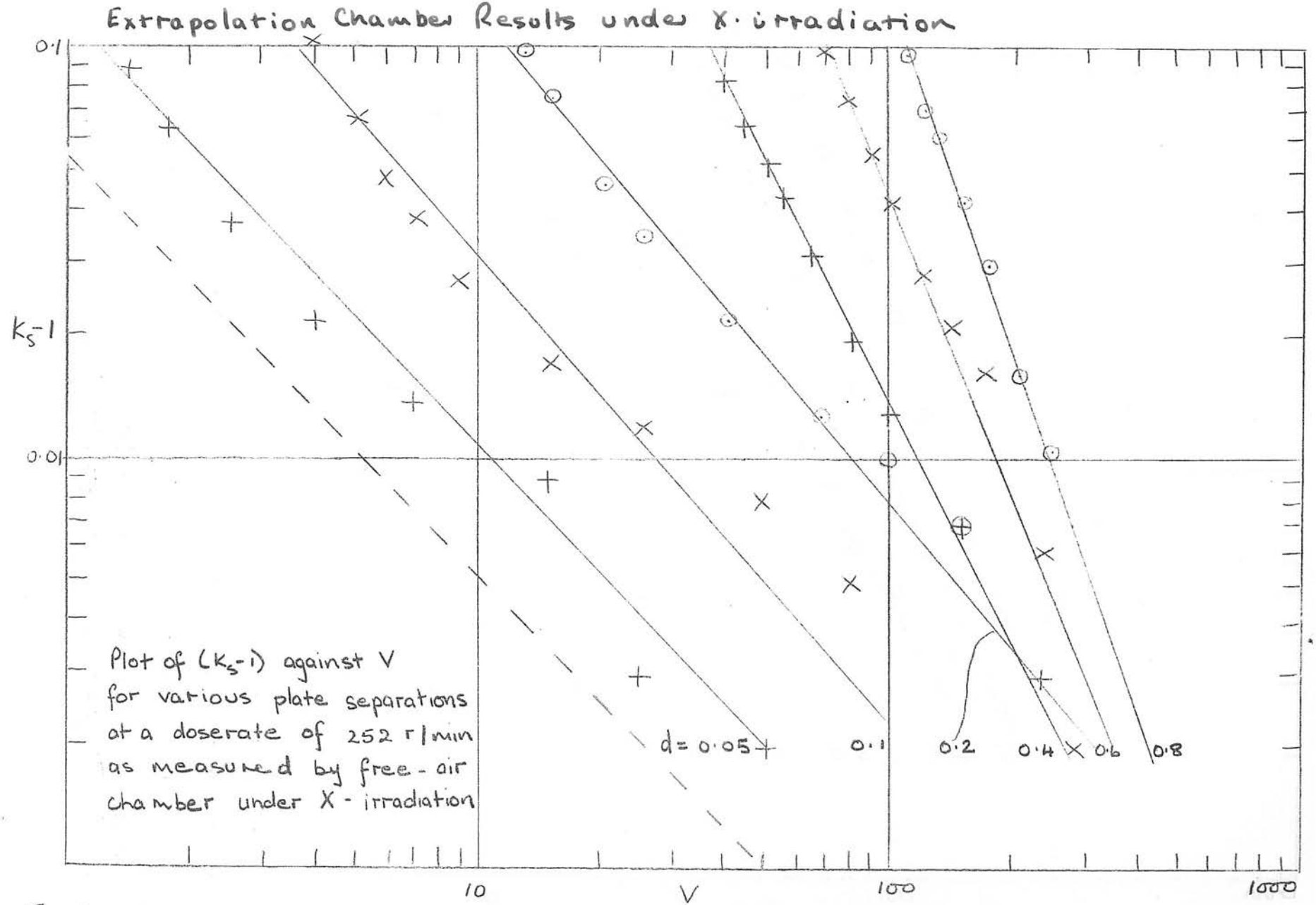
Extrapolation Chamber Results under X-irradiation
0·1
0·01
$K_s - 1$
Plot of $(K_s - 1)$ against V
for various plate separations
at a doserate of 252 r/min
as measured by free-air
chamber under X-irradiation
d = 0·05
0·1
0·2
0·4
0·6
0·8
10
V
100
1000

Fig. 60

8.6 Behaviour of Extrapolation Chamber under X-irradiation

Some measurements were made with the extrapolation chamber under irradiation by X-rays. The experimental arrangement was similar to that described in Chapter 3. The source of X-rays was again the Müller superficial therapy set but this time the tube head was clamped into position vertically above the chamber and centred on the collecting electrode by means of a plumb-line. The monitor chamber was placed at the edge of the beam and the two ionization currents were balanced as before on the Kemp comparator.

Saturation runs were made for several plate separations ranging from d = 0.05 to d = 0.8 cms. at three doserates (Figs. 58-60). Results at low d indicate a slope of 1.0 for log (K_s - 1) against log V while at high d the slope is as much as 2.0 as for volume recombination. The doserates were measured by an Ionex thimble chamber placed in exactly the same position as the collecting plate and later calibrated against the free-air chamber in conjunction with the E.I.L. electrometer to establish the quality correction. The various qualities and doserates are given in Table 5: -

Table 5.

Distance of Tube head from Collector. cm.	Filter at 45 KV mm.Al	H.V.L. mm.Al.	Ionex Reading. r/min.	Calibration factor.	Doserate r/min.
90	1.7	1.3	2.6	1.15	3
90	-	0.07	72	1.59	114
30	0.25	0.19	192	1.31	252

The extrapolation chamber was then connected to a V.R.E. type 1079C electrometer and it was found that doserates measured on this instrument proved very different from those in Table 5. As a check, the V.R.E. meter scale was calibrated against the standard potentiometer and the value of the chosen input resistor was determined by a free-air chamber measurement. Measurements were then made of the saturation currents at the various beam qualities and plate separations, and doserates were calculated from Bortner's equation.

Table 6 compares the extrapolation chamber results with the corrected Ionex readings over the range of d.

Table 6.

	Corrected Ionex Doserates in r/m.			
d in cm.	2.95	114	252.	
0.8	37	309	1270	Extrapolation chamber readings in e.s.u./c.c.min.
0.6	46	374	1522	
0.4	63	489	2160	
0.2	87	774	3485	
0.1	122		5310	
0.05	152	1775	7075	

The increases in doserate as measured by the extrapolation chamber are thought due to ejected photo electrons from the gold electrode and must raise doubts as to the use of this particular chamber under radiation by X-rays. Since the chamber walls rather than the air volume are contributing most of the secondary electrons, the ionization intensities have been expressed in e.s.u./cc.min. rather than r/min.

CHAPTER 9.

INTERPRETATION OF EXPERIMENTAL RESULTS.

It appears a difficult if not impossible task to set up a formula governing the saturation characteristics of an extrapolation chamber since diffusion, initial and volume recombination all play their parts to such varying extents according to the experimental conditions. In this chapter we shall discuss the role of each of these factors in turn, making quantitative evaluations where possible.

9.1 Rossi and Staub's Formula for Diffusion Losses.

The best theoretical treatment of ion losses arising from diffusion in ionization chambers is due to Rossi and Staub (1949).

They considered an ionization chamber under uniform irradiation and assumed that

n_o = number of ion pairs produced per unit volume and time

n_+ = density of positive charge carriers.

n_- = density of negative charge carriers.

$\vec{w}_+$ = drift velocity of positive carriers.

$\vec{w}_-$ = drift velocity of negative carriers.

Current vectors for positive and negative particles are given by

$$\left.\begin{aligned} \vec{j}_+ &= n_+ \vec{w}_+ - D_+ \operatorname{grad} n_+ \\ \vec{j}_- &= n_- \vec{w}_- - D_- \operatorname{grad} n_- \end{aligned}\right\} \quad \ldots\ldots\ldots (15)$$

and $\operatorname{div} \vec{j}_+ = \operatorname{div} \vec{j}_- = n_o - \alpha n_+ n_- \quad \ldots\ldots\ldots (16)$

The density of the electric current is given by

$$e\vec{j} = e(\vec{j}_+ - \vec{j}_-)$$

Due to diffusion, however, j is not parallel to the lines of electric force and the total electric current is not the same across every surface intercepted by the lateral boundary of the sensitive volume.

For a negative collecting electrode, the current I through the measuring system is

$$I = e\int_{S_-}(jn_+ - jn_-)\ dS$$
$$= e\int_A n_o.dA - e\int_A \alpha\ n_+\ n_-.dA - e\int_{S_-} jn_-\ dS - e\int_{S_+} jn_+\ dS$$
$$- e\int_{S_1} j_{n_+}.dS$$

where A is the sensitive volume of the chamber

S_1 is the lateral boundary of the sensitive volume

S_+ is the boundary at the positive electrode

In order to determine the boundary conditions at the electrodes, Rossi and Staub assumed that every charged particle which impinged on an electrode was captured. Since n_+ and n_- are thus zero at S_+ and S_-, and w_n is zero at S_1, then substituting for j_+ and j_- from equations (15), we get

$$I = e\int_A n_o.dA - e\int_A \alpha\ n_+\ n_-.dA + e\int_{S_-} D_-\ (\text{grad}\ n_-)_n.dS$$
$$+ e\int_{S_+} D_+\ (\text{grad}\ n_+)_n\ dS + e\int_{S_1} D_+\ (\text{grad}\ n_+)_n\ dS \quad \ldots\ldots(17)$$

The physical interpretation of this equation is as follows: -

The number of positive charges entering the collecting (negative) electrode equals the number of positive ions formed in the active

volume (first term) minus the number of positive ions that recombine (second term) minus the number of positive ions that diffuse back to the positive electrode (fourth term always negative), minus or plus the number of positive ions that diffuse out of or into the sensitive volume through its lateral boundary (fifth term). To obtain the current in the measuring instrument from the number of positive charges entering the collecting electrode, subtract the number of negative charges that diffuse back to this electrode (third term, always negative).

The solution of these equations can be determined for a parallel plate chamber of separation d uniformly irradiated over its active volume and beyond it for some distance. Assuming first that there is negligible recombination and taking the x axis as the direction of the field, Equations (15) becomes

$$\left.\begin{aligned} j_+ &= n_+ w_+ - D_+ \frac{dn_+}{dx} \\ j_- &= n_- w_- + D_- \frac{dn_-}{dx} \end{aligned}\right) \quad \ldots\ldots\ldots\ldots \quad (18)$$

while Equation (16) gives

$$\frac{dj_+}{dx} = -\frac{dj_-}{dx} = n_o = \text{const.} \quad \ldots\ldots\ldots\ldots (19)$$

Integration of equation (19), substitution in equation(18)and integration of the resulting equations with the boundary conditions $n_+ = n_- = 0$ at $x = 0$ and $x = d$ yields

$$\left.\begin{aligned} n_+ &= \frac{n_o}{w_+} x - \frac{n_o}{w_+} d \cdot \frac{e^{(w_+)x/D_+} - 1}{e^{(w_+)d/D_+} - 1} \\ n_- &= -\frac{n_o}{w_-} x + \frac{n_o}{w_-} d \cdot \frac{1 - e^{-(w_-)x/D_-}}{1 - e^{-(w_-)d/D_-}} \end{aligned}\right\} \quad \ldots\ldots(20)$$

Equation (20) can be simplified by assuming that $w_+ d/D_+$ and $w_- d/D_-$ are usually very large numbers. Substitution in equation (18) gives

$$j_+ = n_o x - \frac{n_o}{w_+} D_+$$

$$j_- = n_o (d - x) - \frac{n_o}{w_-} D_-$$

But $I = eS(j_+ + j_-)$

$$= eS\, dn_o - e S \left(\frac{n_o}{w_+} \cdot D_+ + \frac{n_o}{w_-} \cdot D_- \right)$$

$$\therefore \frac{I}{I_s} = 1 - \left(\frac{D_+}{w_+ d} + \frac{D_-}{w_- d} \right)$$

where I_s = saturation current = $eS\, dn_o$

It can be proved that $w = \frac{D}{\mathcal{E}\, kT}\, e\, E$

where $\mathcal{E}$ is the average agitation energy of the ions and k is Boltzmann's constant

$$\therefore \quad \frac{wd}{D} = \frac{eEd}{\mathcal{E}\, kT} = \frac{V}{2.5 \times 10^{-2}} \cdot \frac{1}{\mathcal{E}}$$

$$\therefore \quad \frac{1}{K_s} = 1 - \frac{2.5 \times 10^{-2}}{V} (\mathcal{E}_+ + \mathcal{E}_-)$$

$$\text{i.e. } K_s - 1 = \frac{\frac{2.5 \times 10^{-2}}{V} (\mathcal{E}_+ + \mathcal{E}_-)}{1 - \frac{2.5 \times 10^{-2}}{V} (\mathcal{E}_+ + \mathcal{E}_-)} \qquad \text{.....(21)}$$

The agitation energy $\mathcal{E}$ is practically 1 for ions, while it may be much higher for electrons. Assuming that the negative charge carriers are ions

$$K_s - 1 = \frac{\frac{0.05}{V}}{1 - \frac{0.05}{V}} \qquad \text{.....(22)}$$

9.2 Comparison of Results and Rossi and Staub's Formula.

Measurements made with β-rays (Figs. 50-51) indicated that at plate separations $d \leqslant 0{\cdot}05$ cm. saturation losses were almost entirely due to diffusion as predicted by Rossi and Staub's equation (22). Lateral diffusion had been proved experimentally to be of negligible effect despite the frequently narrow radiation field for the 3 cm. collecting electrode.

Results for X-irradiation, however, showed that $(K_s - 1)$ factors for $d = 0.05$ cm. were somewhat higher than predicted by diffusion theory. This was particularly evident at the highest doserate (Fig.60) where the plot of $(K_s - 1)$ against voltage at $d = 0.05$ cm, although parallel to equation (22), was some 5 per cent higher at the low voltage end. The possible explanation for this, which will also be borne out in Chapter 9.4, is that at this high ionization intensity (118 e.s.u./cc.sec.) a considerable proportion of the electrons are crossing the air gap without attachment. If this is so, then the effective value of ε_- will be greater than unity and $(K_s - 1)$ for a given voltage will be correspondingly larger (equation (21)).

9.3 Evidence of Electron Attachment.

Boag and Wilson (1952) discussed Thomson's formula (1928) for the estimation of electron attachment to molecules. Thomson showed that if $1/n$ is the fraction of all collisions between free electrons and molecules which result in the formation of a negative ion by electron capture, the probability of an electron drifting a distance d in a uniform electric field E without becoming attached to a molecule is

$$P(d) = e^{-vd/n\lambda kE} = e^{-\psi} \quad \text{say}$$

where v is the velocity of agitation and λ the mean free path of the electron. If electrons are liberated uniformly in the space between two plane electrodes at a distance d apart, then the proportion crossing unattached will be

$$P'(d) = \frac{1}{d}\int_0^d P(x)\,dx = (1 - e^{-\psi})/\psi$$

Boag and Wilson used data on n, v, λ and kE from tables compiled by Healey and Reed (1941). Their values for n ($= 1/\bar{n}$) are based on Bailey's measurements (1925) while the other quantities are obtained from the studies of Townsend and Tizard (1913). Each factor is tabulated as a function of the ratio of the field strength E to the gas pressure p in mm.Hg.

Fig 61. (taken from Loeb (1955))

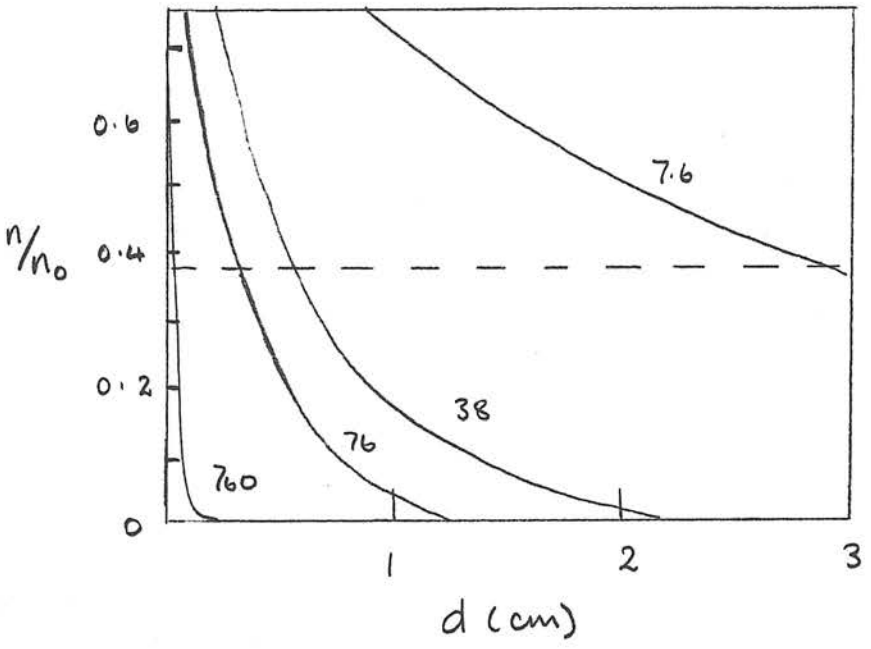

Plot of n/n_0 = number of electrons getting to various distances d at various pressures p (mm Hg.)

h = assumed constant = 2.5×10^{-6}

V = 10 Volts.

e.g. at the lowest E/p = 0.5

$$n = 3 \times 10^{5} \qquad v = 3.3 \times 10^{7} \text{ cm./sec.}$$

$$\lambda = 4.2 \times 10^{-5} \text{ cm,} \quad kE = 9 \times 10^{5} \text{ cm./sec.}$$

$$\therefore \quad \psi = \frac{vd}{n \lambda kE} = \frac{3.3 \times 10^{7} \times d}{3 \times 10^{5} \times 4.2 \times 10^{-5} \times 9 \times 10^{5}}$$

$$\therefore \quad \psi = 2.88\, d$$

For $d = 0.05$ cm. and $p = 760$ mm.Hg, $E/p = 0.5$ for $V = 20$ V.

and $P'(d) = (1 - e^{-\psi}) / \psi = 0.94$

i.e. only 6 per cent of electrons form ions in crossing the gap.

We have previously (Chapter 5.9) supported Bradbury's measurements of h in preference to Bailey's. The former's value for n at E/p = 0.5 is 5.5×10^{4} and using this we find

$$\psi = 15.7\, d$$

i.e. for $d = 0.05$ $P'(d) = 0.69$

and some 30 per cent of electrons form ions.

Loeb (1955) presents a graph (Fig.61) illustrating the formation of negative ions in air at several pressures as a function of distance x in the direction of the field. He computed rough values of the proportion of electrons getting to various distances d from Thomson's formula assuming n = constant = 4×10^{5} and V = 10 volts.

Since the presence of moisture in the air is likely to increase the probability of attachment, it seems impossible to make any accurate estimate of the number of free electrons present in any

experimental situation.

We can say, however, that this number will be maximum for the smallest plate separations and the highest fields. Loevinger (1960) has in fact reported oscilloscope observations of the current pulses from various ion chambers showing that an appreciable fraction of electrons escaped negative ion formation. This fraction varied from a few per cent for large dimensions and low collecting voltages to a major amount for small dimensions and large collecting voltages.

The value for ε_- for electrons in air is a function of E/p and is 6 for E/p = 0.5. We would thus expect an increase in $(K_s - 1)$ factors computed from Rossi and Staub's formula, verifying the experimental findings for X-rays. Since $\varepsilon_- = 1$ fits the results obtained with β - rays, however, it would appear that the proportion of free electrons rises with increasing doserate. This is not predicted by theory and a possible explanation lies in the fact that if a considerable proportion of the negative charge carriers are free electrons then the negative space charge becomes negligible compared to the positive space charge. The field strength is therefore no longer constant between the plates and the diffusive losses will be affected.

Boag and Wilson (1952) considered the case of a gas in which no electron attachment occurs, i.e. the negative carriers are solely electrons. They defined a dimensionless variable

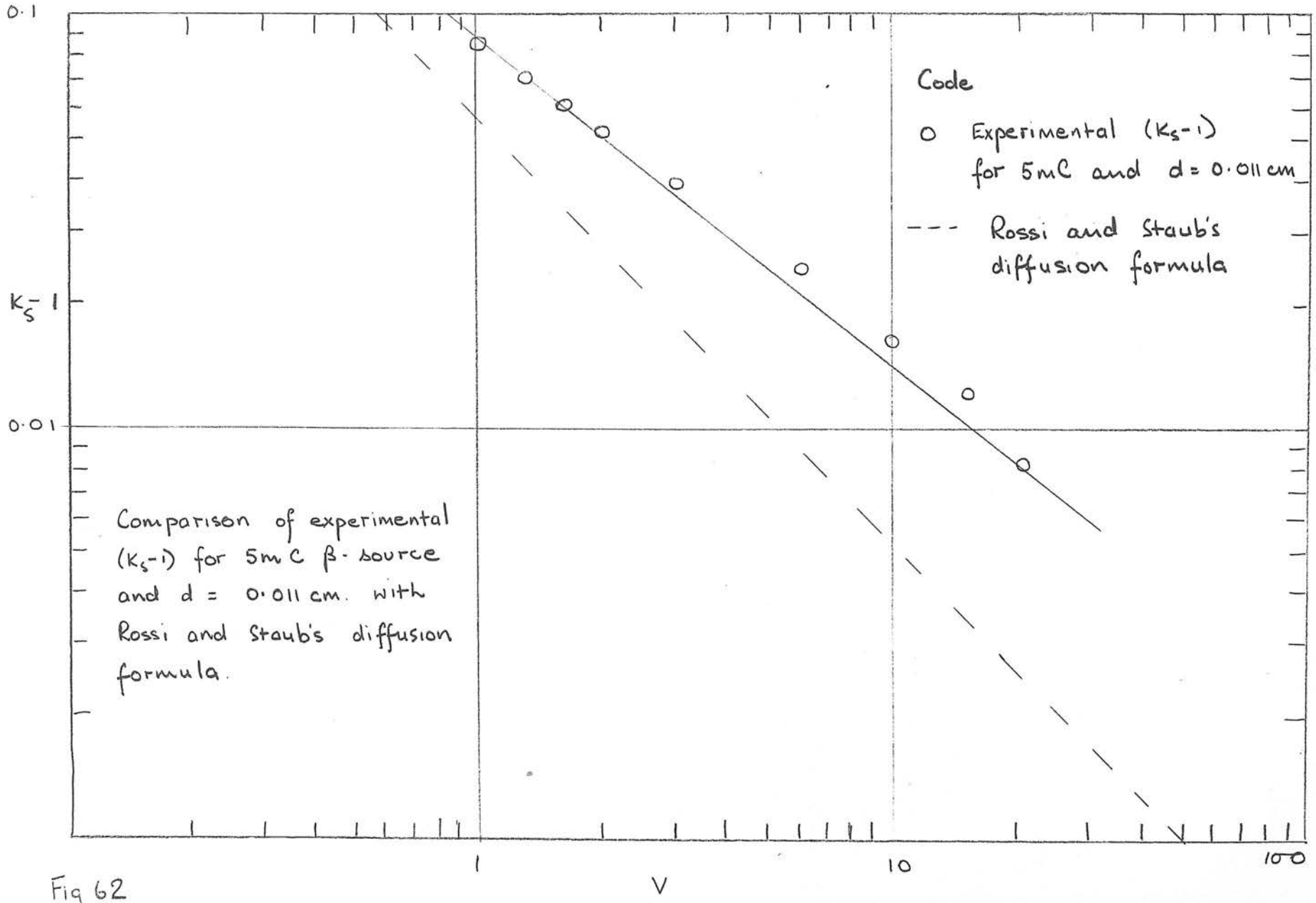
0·1
$K_s - 1$
0·01
Code
o Experimental $(K_s - 1)$ for 5mC and d = 0·011 cm
--- Rossi and Staub's diffusion formula
Comparison of experimental $(K_s - 1)$ for 5m C β· source and d = 0·011 cm. with Rossi and Staub's diffusion formula.
1
10
100
V

Fig 62

$$\xi' = \sqrt{\frac{4\ \pi\ (k_1 + k_2)}{k_1\ k_2}} \qquad \frac{d^2\ \sqrt{q}}{V}$$

and showed graphically the variation of field strength across the gap for several values of ξ'. The minimal value of ξ' at which a change in the field distribution became apparent was

$$\xi' = 0.5$$

Under our experimental conditions, however, space charge effects seem to be negligible

e.g. for $V = 20$ V, $d = 0.05$ cm., $k_2 \doteq 10^3$

$$\xi' = 0.012 \text{ for } q = 118 \text{ e.s.u./c.c.sec.}$$

Further discussion on the relationship between the proportion of free electrons and doserate is given in the next section.

There is some evidence for the presence of free electrons under β - radiation at the smallest plate separation used - $d = 0.011$ cm. (Fig.62). This was not graphed previously as it would have led to confusion with results for larger d. At the low voltage end, $(K_s - 1)$ for this d are some 3 per cent higher than given by equation (22).

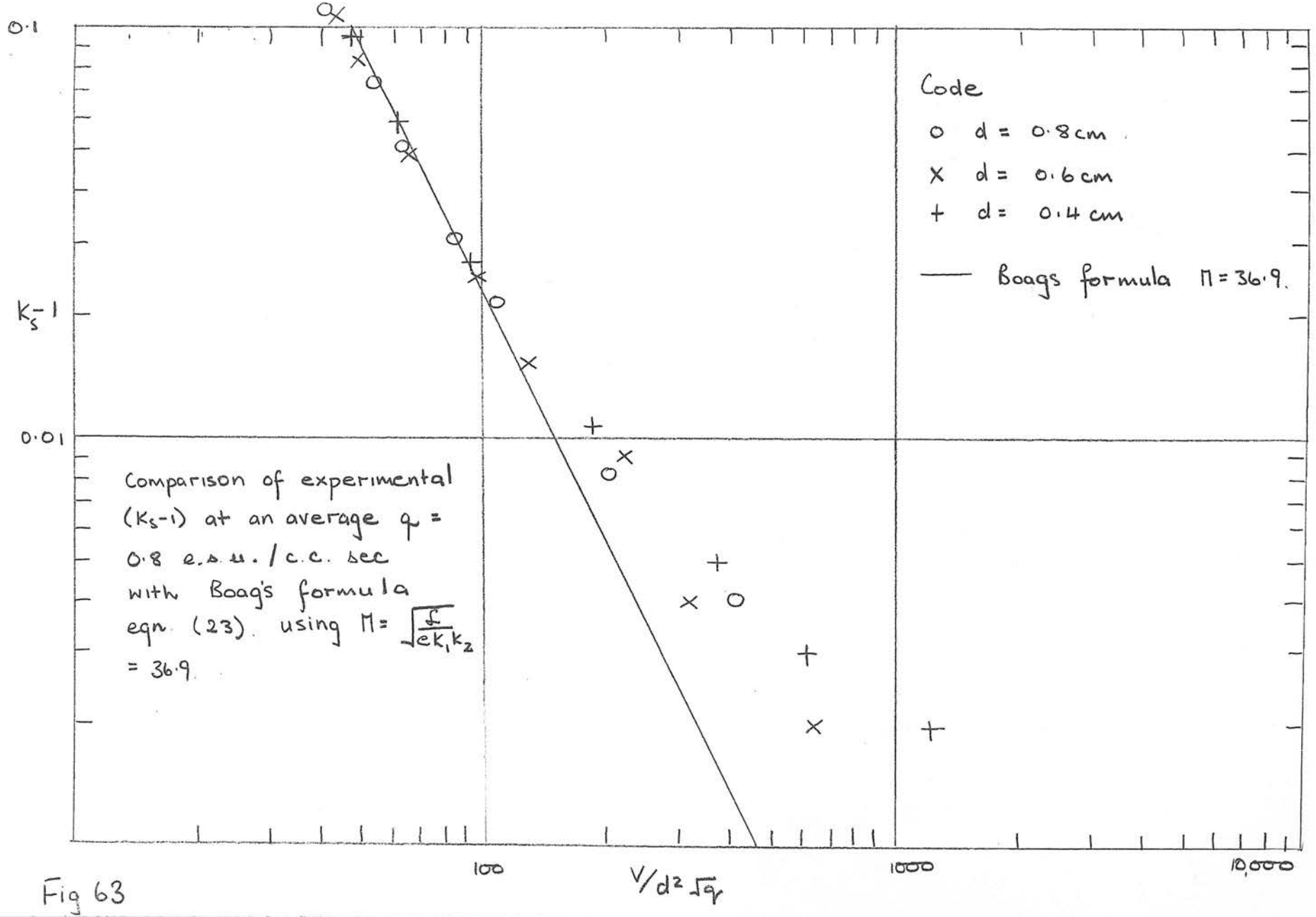
0·1
0·01
$K_s - 1$
100
1000
10,000
$V/d^2\sqrt{q}$
Code
o d = 0·8 cm
x d = 0·6 cm
+ d = 0·4 cm
—— Boags formula Π = 36·9.
Comparison of experimental (K_s-1) at an average q = 0·8 e.s.u./c.c. sec with Boag's formula eqn (23) using $\Pi = \sqrt{\frac{f}{ek_1k_2}}$ = 36·9.

Fig 63

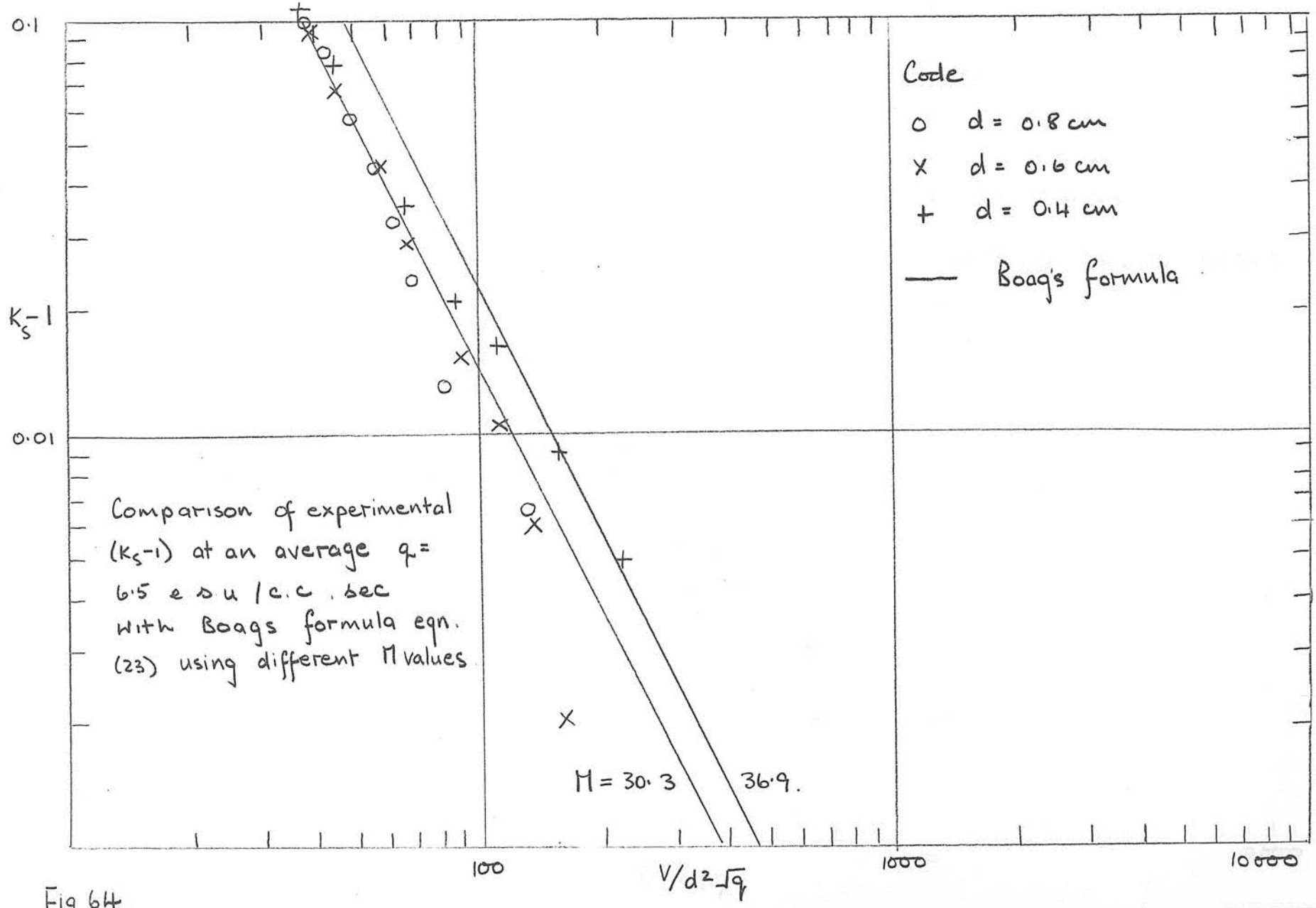
0.1
0.01
$K_s - 1$
100
1000
10000
$V/d^2\sqrt{q}$
Code
o d = 0.8 cm
x d = 0.6 cm
+ d = 0.4 cm
Boag's formula
Comparison of experimental (K_s-1) at an average q = 6.5 e s u / c.c. sec with Boags formula eqn. (23) using different M values
M = 30.3
36.9.

Fig 64

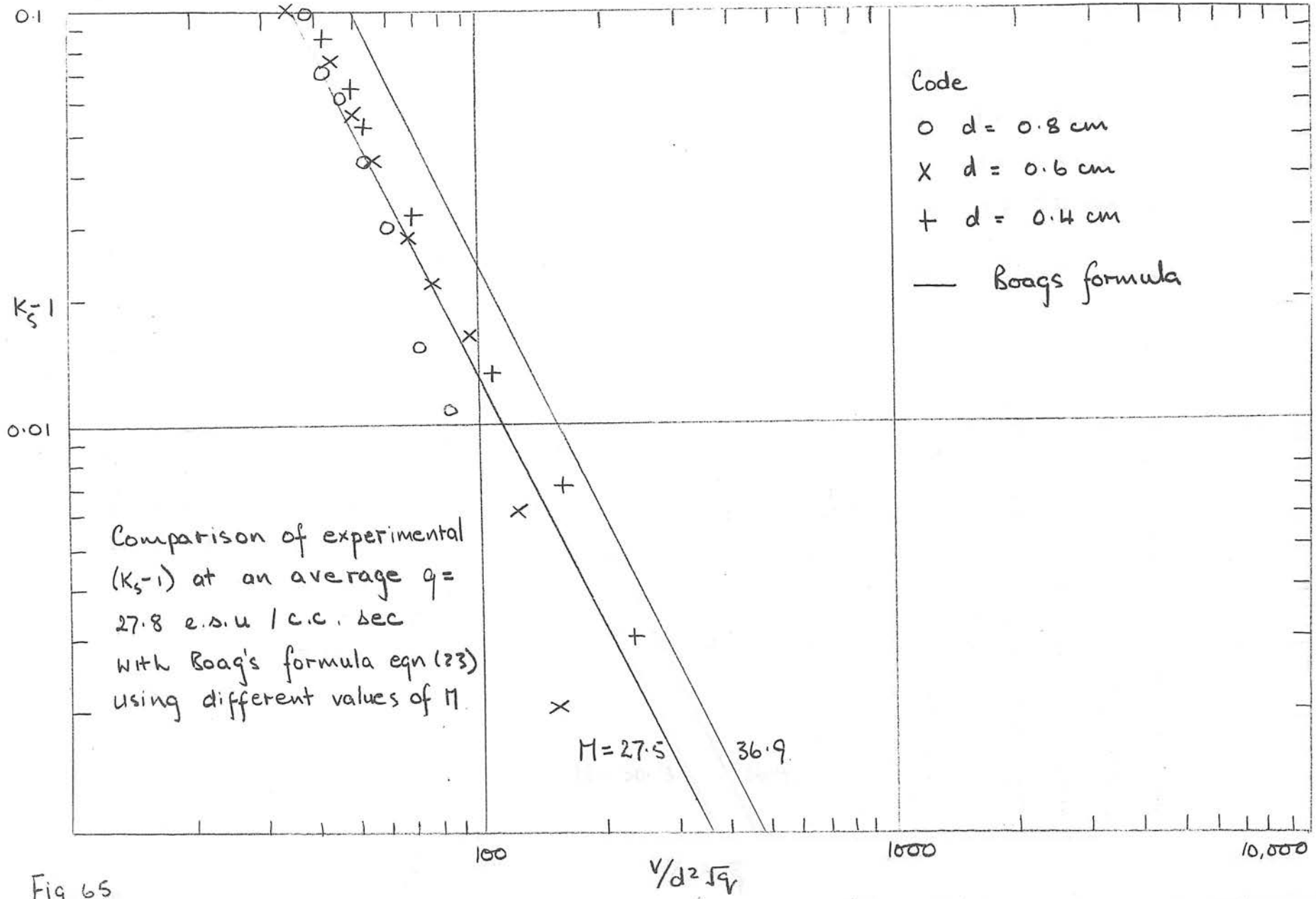
0·1
0·01
$K_s - 1$
100
1000
10,000
$V/d^2\sqrt{q}$
Code
o d = 0·8 cm
X d = 0·6 cm
+ d = 0·4 cm
— Boags formula
Comparison of experimental $(K_s - 1)$ at an average q = 27·8 e.s.u / c.c. sec with Boag's formula eqn (23) using different values of M
M = 27·5
36·9

Fig 65

9.4 Saturation Losses due to Volume Recombination.

Shevyrev (1960) agreed with Boag and Wilson's assumption (1952) that space charge effects could be neglected in the calculation of volume recombination losses in a parallel plate chamber under uniform irradiation provided that these losses did not exceed 10 per cent. Their formula may be written in the form

$$K_s = 1/2 + 1/2 \sqrt{1 + \frac{2}{3} M^2 \left(\frac{d^2 \sqrt{q}}{V} \right)^2} \quad \ldots\ldots(23)$$

where $M = \sqrt{\frac{\alpha}{e\, k_1\, k_2}}$

Using the same values for α , k_1 and k_2 as before, we find

$$M = 36.9 \text{ and } K_s = 1/2 + 1/2 \sqrt{1 + 907 \left(\frac{d^2 \sqrt{q}}{V} \right)^2}$$

From this formula a plot of log $(K_s - 1)$ against log $\left(\frac{V}{d^2 \sqrt{q}} \right)$ results in a straight line of slope - 2.0. Figs (63-65) compare this theoretical plot with experimental $(K_s - 1)$ for d = 0.4, 0.6 and 0.8 cm. under the three types of X-radiation described in Chapter 8.6. The values for $\sqrt{q}$ for each plate separation and beam quality were taken from Table 6. The average q for the three spacings are 0.8, 6.5 and 27.8 e.s.u./c.c. sec. Good agreement between theory and experiment

is obtained for $\bar{q}$ = 0.8 e.s.u./c.c. sec. (Fig.63). Theory overestimates losses by as much as 3 per cent at $\bar{q}$ = 6.5 and 4 per cent at $\bar{q}$ = 27.8 e.s.u./c.c. sec (Figs. 64-65). The experimental results for each of these two $\bar{q}$ do, however, group round straight lines which are obtained from equation (23) using values for M = 30.3 and 27.5 respectively.

This is a similar situation to that described in Boag and Wilson's paper where they found that M = 19.4 satisfied their experimental results at ionization intensities of (1 - 118). 10^3 e.s.u./c.c. sec. and plate separations of 0.0625 to 0.253 cm. They attributed their low value for M to the lack of electron attachment since the presence of free electrons would raise the value of k_2 and hence reduce M. Again the amount of electron attachment appears to decrease with increasing q but this time there is a simple explanation.

For small values of K_s equation (23) can be re-written as

$$K_s = 1 + \frac{1}{6} M^2 \left(\frac{d^4 q}{V^2} \right)$$

thus for constant M and d, $(K_s - 1) \propto \frac{q}{V^2}$

and therefore an increase in q means that the voltage must also be increased to give the same value for $(K_s - 1)$. The proportion of free electrons present, however, increases with the field strength and hence M does not remain constant as the voltage rises but diminishes

leading to lower values of $(K_s - 1)$ than before.

The observed change in M is therefore due to an increase in the proportion of free electrons caused by the use of higher field strengths rather than higher ionization intensities. This argument does not explain, however, the increase in diffusive losses described previously as the diffusion formula is dose-rate independent. Part of the answer may lie in the differing degree of action of the two types of radiation. It has already been shown that under X-irradiation an appreciable number of photo electrons are released from the upper electrode. These secondary electrons from gold are more energetic than from air or polystyrene and are thus more likely to reach the "wrong" electrode.

Shevyrev's experimental results for volume recombination also indicated that an increase in ionization intensities led to a shift of the saturation curve towards lower values of $\left(\frac{V}{d^2 \sqrt{q}} \right)$. He compared his results with Mie's theory and found that increasing q from 10^3 r/hr. to 10^5 r/hr. involved changing M from 39 to 33, i.e. a change of some 20 per cent. This is similar to the change in M of 25 per cent. we obtain if we take $M = 34.6$ as best fitting our experimental results for $\bar{q} = 0.8$ e.s.u./c.c. sec. $\doteq 3 \times 10^3$ r/hr. and $M = 27.5$ for $\bar{q} = 27.8$ r/sec. $\doteq 10^5$ r/hr.

Since Shevyrev's experiments for $q = 10^5$ r/hr. were carried out in an extrapolation type chamber for $d = 0.3$, 0.5 and 1 cm. we would expect his results to be comparable to ours. He gives

M = 33 as the parameter for substitution in Mie's equation which he quotes as

$$f = 1/K_s = 0.48 + \sqrt{0.231 + \frac{1.95}{M\left(\frac{d^2\sqrt{q}}{V}\right)}} \quad \ldots\ldots\ldots(24)$$

From Fig. 65 $(K_s - 1) = 0.0125$ for $\frac{V}{d^2\sqrt{q}} = 100$

substituting $M = 33$ and $\frac{d^2\sqrt{q}}{V} = 10^{-2}$ in (24)

$$1/K_s = 0.48 + \sqrt{0.231 + \frac{1.95}{33 \times 10^{-2}}}$$

$$= 0.48 + \sqrt{6.14}$$

$$\doteq 3.$$

i.e. $K_s = 0.33$ and $K_s - 1 = -0.66!$

Yet from Shevyrev's graph $f = 0.98$, i.e. $(K_s - 1) = 0.02$ for $\frac{d^2\sqrt{q}}{V} = 10^{-2}$

It thus appears that in Shevyrev's paper his formula based on Mie's theory is quoted incorrectly since it does not agree with its graphical form. Shevyrev gives no details as to how he transformed Mie's equations which as mentioned in Chapter 1 contained a parameter R - the apparent resistance of the ionized gas at very low collecting voltage. This makes it difficult to compare the two sets of results.

Fig 66 (Taken from Shevyrev (1960)).

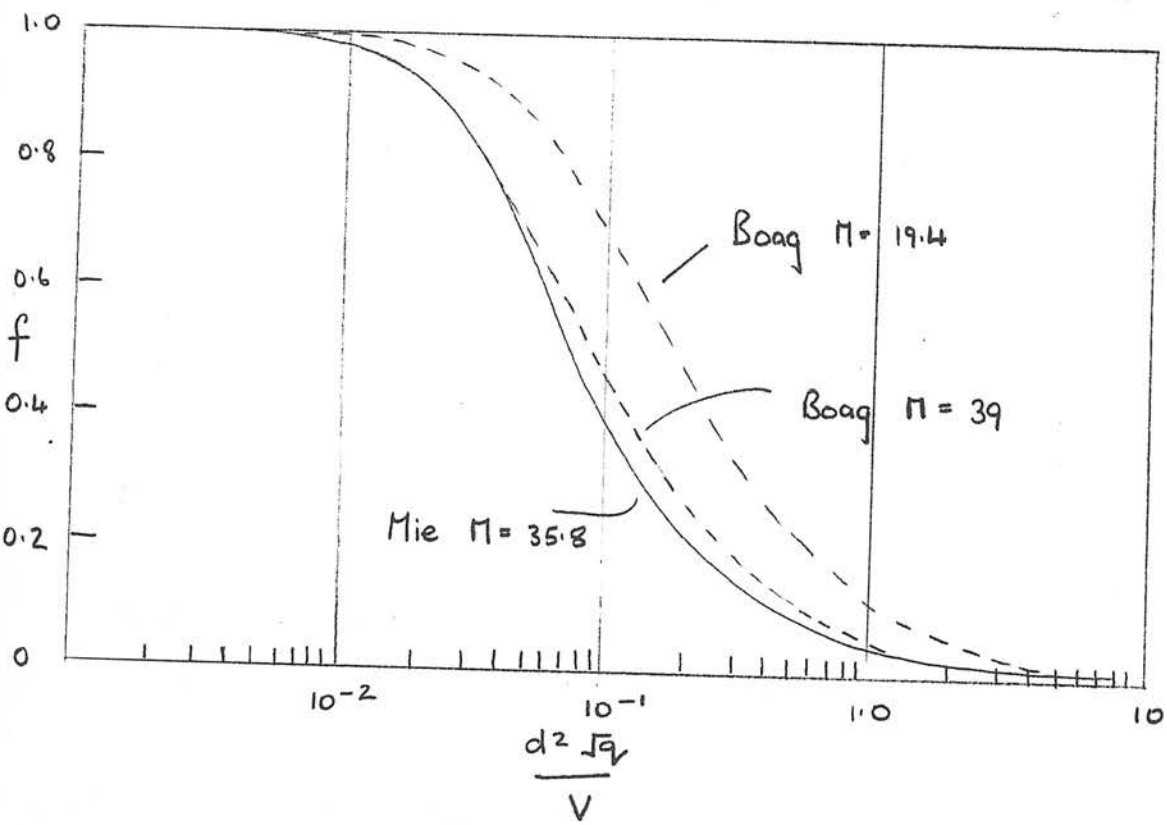

Theoretical plots of $f = 1/K_s$ against $d^2\sqrt{q}/V$ based on theories of Boag and Mie for various M.

Fig.66 taken from Shevyrev's paper does show, however, Mie's formula for $M = 35.8$ and Boag's formula for $M = 39$ and 19.4. This implies that if Shevyrev's results had been compared to Boag's theory a value of M at least as high as 39 would be required for $q = 10^5$ r/hr. Shevyrev thus seems to have obtained larger $(K_s - 1)$ values than ours. On the basis of his results he stated that he found it hard to believe that Boag's experimental parameter of 19.4 was correct. He suggested that this low value for M was due to additional ionization created by scattered electrons outside the limits of the assumed active volume and diffusion of ions into non-irradiated regions of the chamber. This certainly seems plausible since the chamber used by Boag and Wilson did not have a guard ring and the collecting volume was defined purely by the geometrical shape of the beam after it passed through an aluminium "stop". Any collection of ions from outside the assumed active volume would effectively increase the value of q to be substituted in the formula and hence M would be reduced.

Our experimental results agreed well with Boag's theory for

$$M = \sqrt{\frac{\alpha}{e\, k_1\, k_2}} = 36.9 \quad \text{for} \quad \bar{q} = 0.8 \text{ e.s.u./cc. sec.}$$

and the decrease in M with increasing q does seem to indicate an increasing amount of free electrons. We have already noted (Chapter 8.6) the surprising increases in q measured by the extrapolation chamber compared to the free-air chamber. This was

supposed due to photo-electrons being ejected from the upper electrode thus the ionization intensity is hardly likely to be uniform. Probably the only conclusion we can draw from this section is that our results tend to support Boag's findings, and that,under these operating conditions, it is impossible to make exact comparisons of saturation losses measured by different chambers.

9.5 Complexity of Remaining Results.

So far we have established that for plate separations $d \leqslant 0.05$ cm. saturation losses can be predicted by a diffusion formula and for $d \geqslant 0.4$ cm. and ionization intensities $q \geqslant 0.8$ e.s.u./c.c. sec. losses can be described by a theory based on volume recombination. The intermediate range of $d \geqslant 0.05$ cm. and $q \leqslant 0.2$ e.s.u./c.c. sec. does not appear amenable to description by any single theory.

Loevinger (1960) discussed an experimental method for determining the range of validity of available theories on recombination losses in ionization chambers. He suggested that the relationship between the ionization current j and the applied voltage V should first be observed experimentally. j can then be expressed as being proportional to $(1 - \text{const.}V^{-n})$ If measurements are made at a number of radiation intensities, the constant is found to be a function of the intensity and the results may be expressed in the form

$$j = j_s (1 - x\, q^{y}\, V^{-z}) \quad \ldots\ldots\ldots\ldots (25).$$

By considering $f = j/j_s$ and comparing equation (25) with: -

1. Boag's formulae

$$f = 1 - \text{const.}\, q\, d^4\, V^{-2} \qquad \text{(steady radiation)}$$

$$= 1 - \text{const.}\, \frac{q}{n_p}\, d^2\, V^{-1} \qquad \text{(pulsed radiation at } n_p \text{ pulses /sec.)}$$

2. Lea's cluster theory

$$f = 1 - \text{const.}\ d\ V^{-1}$$

3. Formula based on Loevinger's measurements (1953) with an extrapolation chamber and β-particle sources

$$f = 1 - 0.014\ d^{-1/2}\ V^{-1/2}$$

Loevinger concluded that values of z lay between 0.5 and 2, and values of y between 0 and 1. The constant x is a function of the chamber geometry, the nature of the radiation field and sometimes the polarity of the collecting voltage. He used the term "recombination slope" for the various factors governing recombination losses depending on which parameter was being taken as the independent variable. By plotting j values against the various parameters he obtained values for the recombination slopes and hence information on the degree of saturation. He ascertained y and z values by the use of log - log graphs. Loevinger's experimental measurements have little relevance here, however, as they all concerned pulse radiation.

We have in fact already used a graphical method (Figs. 50,52) for determining the power of V and it seems worth while to extend it to d and q. Let us first summarise the relationship between $(K_s - 1)$ and these parameters according to the three theories available.

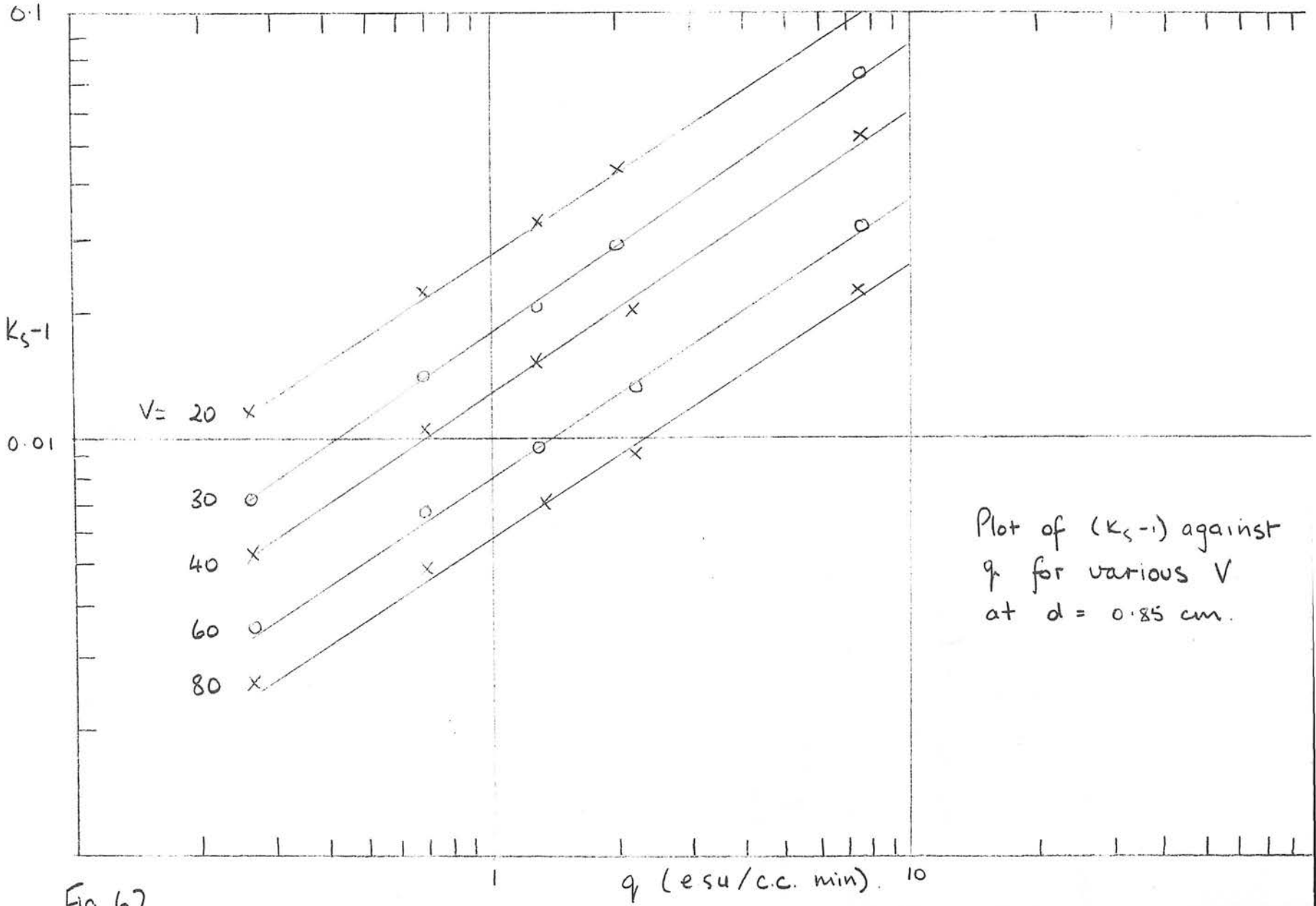

Plot of (K_s-1) against q for various V at d = 0·85 cm.

Fig 67

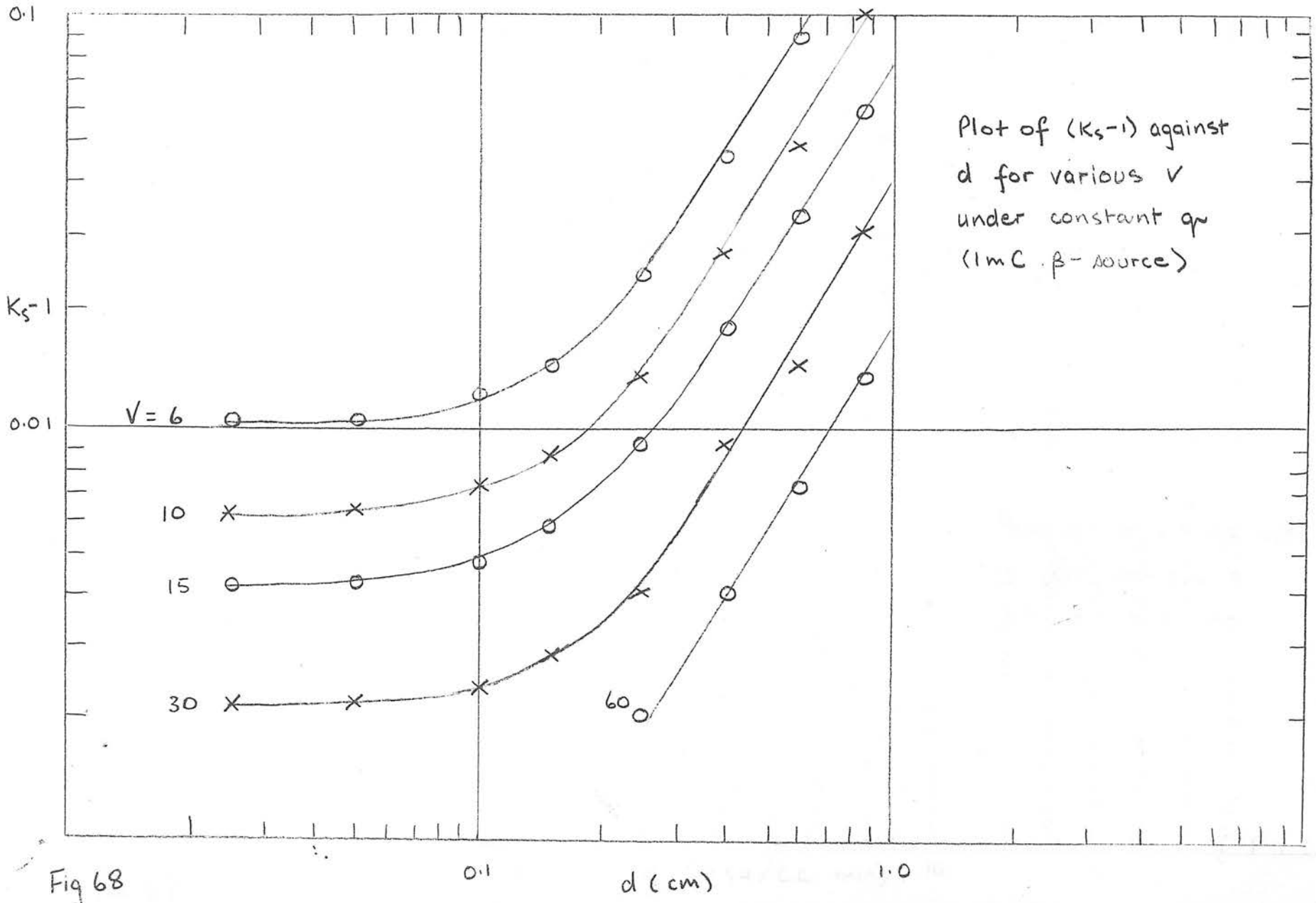
0·1
$K_s - 1$
0·01
V = 6
10
15
30
60
0·1
1·0
d (cm)
Plot of $(K_s - 1)$ against d for various V under constant qv (1mC. β- source)

Fig 68

1. $(K_S - 1) \propto V^{-1}$ (diffusion theory)

2. $(K_S - 1) \propto d\ V^{-1}$ (initial theory)

3. $(K_S - 1) \propto d^4\ q\ V^{-2}$ (volume theory).

Figs. (50, 52) showed that the average slope of log $(K_s - 1)$ against log V i.e. z was unity although, particularly in the case of the 5 m C source, z tended to increase with d, e.g. z = 1.35 for d = 0.85 cm. Ion losses would thus appear to be mainly due to diffusion and initial recombination with volume recombination occurring to a greater extent with increasing ion intensity and plate separation.

A previous discussion (Chapter 8.3) on the dependence of $(K_s - 1)$ on doserate indicated there was none for $d < 0.25$ cm. For $0.25 < d < 0.85$ cm. there is definite evidence that a rise in ionization intensity results in higher values of $(K_s - 1)$. Plots of log $(K_s - 1)$ against log q for various V and constant plate separation (Fig.67) exhibit an average slope of 2/3. This also seems to indicate that both initial and volume recombination are present.

The relationship between log $(K_s - 1)$ and log d for various V and constant q is a complex one (Fig.68). As expected for $d < 0.05$ cm. the slope is zero i.e. $(K_s - 1)$ is independent of d as predicted by the diffusion theory. For $0.25 < d < 0.85$ cm. we find the slope is approximately 2 which is intermediate between the value of 1 predicted by initial recombination theory and that of 4

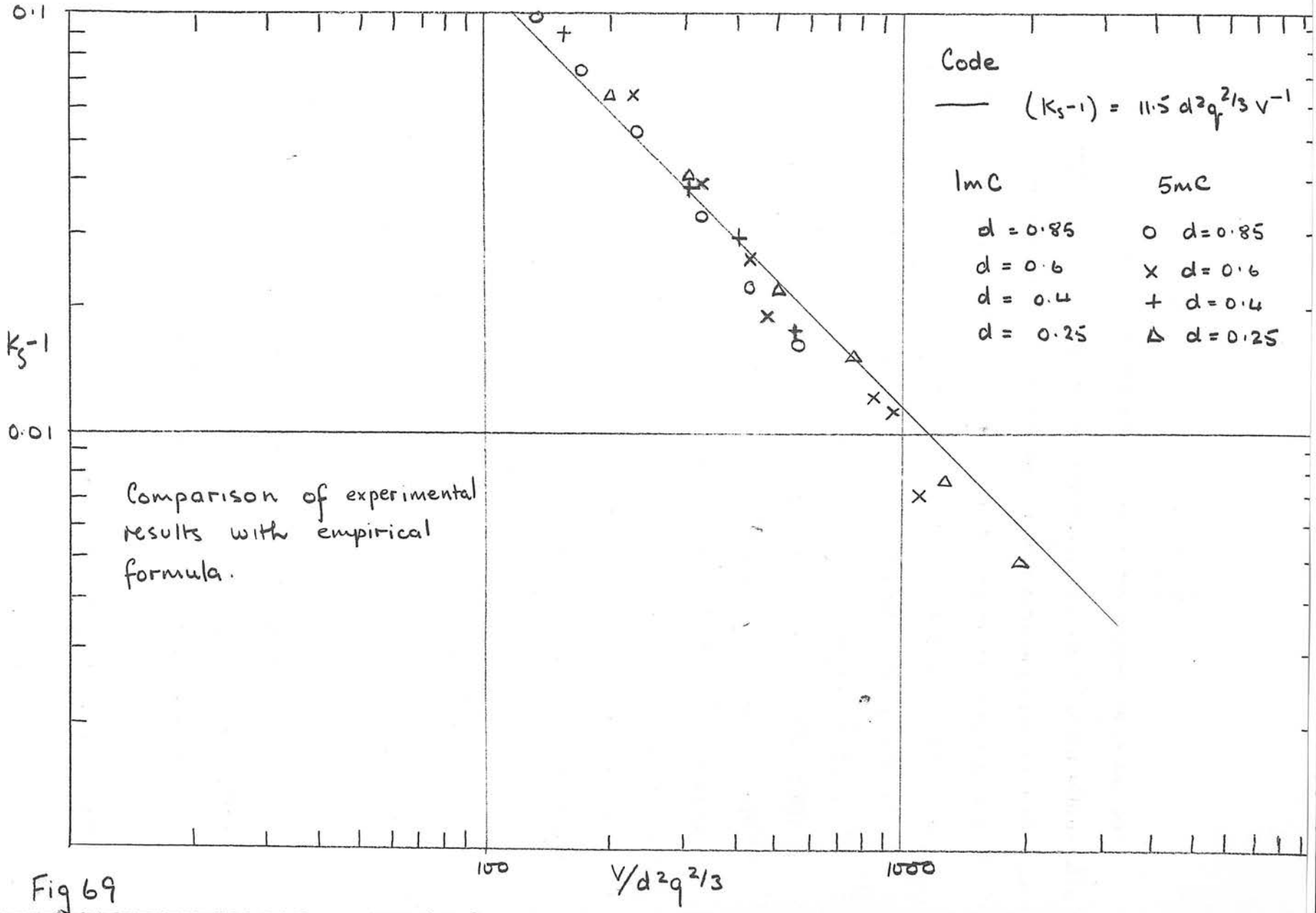
0·1
0·01
$K_s - 1$
Code
$(K_s-1) = 11.5\, d^2 q^{2/3} V^{-1}$
1mC
5mC
d = 0·85
d = 0·6
d = 0·4
d = 0·25
o d=0·85
× d=0·6
+ d=0·4
Δ d=0·25
Comparison of experimental results with empirical formula.
100
1000
$V/d^2q^{2/3}$

Fig 69

for volume recombination. Between $d = 0.05$ and 0.25 cm. the slope is changing and no average value can be given.

We cannot therefore make any quantitative estimation of the saturation losses for $0.05 < d < 0.25$ cm. In the range $0.25 < d < 0.85$ cm., however, we have shown graphically that

$$K_s - 1 \propto d^2 \, q^{2/3} \, V - 1$$

If we now plot our experimental $(K_s - 1)$ against $V/d^2 . q^{2/3}$ (Fig.69) we find the points grouped round a straight line given by

$$K_s - 1 = 11.5 \, d^2 \, q^{2/3} \, V - 1$$

We must point out that in this section we have attributed some ion losses to initial recombination at ionization intensities greater tha l e.s.u./c.c.min. This is of course at variance with results obtained using the free-air chamber (Chapter 5.7) which showed no trace of initial recombination at doserates greater than l r/min.

Several factors make us doubtful about placing much weight on the extrapolation chamber results. Kara-Michailova and Lea declared that their initial recombination theory could only be applied accurately to chambers without "wall effect", i.e. ionization arising from the walls, and suggested that in order to minimise this effect the source of radiation should be a considerable distance from the chamber and that the atomic number of the walls should approximate to that of air. Since our extrapolation chamber does not satisfy

these conditions it seems likely that even if initial recombination were present, losses would not necessarily obey the previous rules. Also we did not find any corroboration of Loevinger's empirical formula postulating $(K_s - 1) \propto d^{-1/2} \cdot V^{-1/2}$ for $0.01 < d < 0.2$ cm. These powers of d and V are quite inexplicable on the basis of any of the current theories and their very existence serves to prove the futility of attempting a theoretical analysis when results are so strongly dependent on the experimental arrangement. Lastly we have already noted (Chapter 9.3) that at the small plate separations used in the operation of an extrapolation chamber, there is evidence of a lack of electron attachment. The degree to which this occurs must also affect experimental results.

Under these circumstances we can hardly claim that our extrapolation chamber measurements offer any conclusive evidence of initial recombination at doserates greater than 1 r/min. We therefore continue to support our free-air chamber findings.

In conclusion we have been unable to find a satisfactory theoretical explanation for measurements made in this operational range of our extrapolation chamber. We believe that the empirical approach provides the most profitable solution to the problem of estimating saturation losses in this type of ionization chamber.

CHAPTER 10.

COMMENTS AND CONCLUSIONS

ON

CHAPTERS 7 - 9.

We have designed and constructed an extrapolation chamber using three micrometer heads as the dual means of supporting the upper electrode and measuring the plate separation. The surface of the upper electrode consisted of a sheet of tautened Melinex which was made conducting by the evaporation on to it of a thin layer of gold. The use of gold instead of aluminium eliminated the so-called "contact potential" effect but led to increased photo-electric absorption, when the chamber was exposed to X-radiation.

Investigations into the saturation characteristics of this extrapolation chamber have failed to produce a comprehensive theoretical expression for the dependence of ionization current on the various factors which determine losses. We have, however, shown that at small plate separations, e.g. $d = 0.05$ cm, the main cause of ion loss is diffusion and may be estimated from Rossi and Staub's formula (1949). Although it proved impossible to determine the exact distribution of ionization intensity for X-radiation due to the presence of the gold-coated electrode, support for the volume recombination theory of Boag and Wilson (1952) has been advocated. Discrepancies between experimental results and these formulae at the lowest plate separations and highest field strengths were attributed to a lack of electron attachment.

Graphical analysis of saturation losses under β -radiation ($q < 0.2$ e.s.u./c.c.sec.) led to an empirical formula for results in

the range of $0.25 < d < 0.85$ cm. which gave

$$K_s - 1 = 11.5 \quad d^2 \quad q^{2/3} \quad V^{-1}$$

It was tempting to say that this formula represented a mixture of initial and volume recombination but this conflicted with previous work using a free-air chamber (Chapter 5) proving that initial recombination has a negligible effect at doserates greater than 1 r/min. Because of the warning by Kara-Michailova and Lea that ionization arising from electrons ejected from the walls might affect the amount of recombination occurring and the fact that we failed to verify Loevinger's empirical formula, we concluded that experimental data was greatly influenced by the design and constructional materials of the chamber. Finally in view of our uncertainty as to the amount and effect of free electrons present it was felt that saturation loss measurements were not amenable to theoretical treatment.

We therefore put forward our empirical formula as being solely applicable to our own chamber and strongly recommend that the saturation characteristics of any extrapolation chamber be determined individually by graphical analysis.

Appendix 1.

Equation (5) was derived on the assumption that $n = \frac{Na}{k} V/d$

This is an obvious approximation since V/d is only the average voltage gradient between the plates. A more correct approach would be to consider

$$n_x = \frac{Na}{kE_x} = \text{number of ions/cc. at } x$$

$$\therefore \quad \frac{dEx_1}{dx_1} = - \frac{4\pi Na}{k_1 Ex_1}$$

$$\int_{E_b}^{E_x} Ex_1 . dEx_1 = - \int_{b}^{x_1} \frac{4\pi Na}{k_1} dx_1$$

$$\therefore \quad Ex_1 = \sqrt{\frac{8\pi Na}{k_1} (b - x_1) + E_b^2} \qquad \ldots\ldots\ldots(26)$$

As before $V = a E_b + \int_o^b Ex_1 . dx_1 + \int_o^b Ex_2 . dx_2$

Substituting for E_{x_1} and E_{x_2} from (26) and putting $\frac{8\pi Na}{k} = B$

$$V = \int_0^b \sqrt{\beta_1 b + E_b^2 - \beta_1 x_1 dx_1} + \int_0^b \sqrt{\beta_2 b + E_b^2 - \beta_2 x_2 . dx_2} + a . E_b$$

$$= \frac{2}{3\beta_1} \left[(\beta_1 b + E_b^2)^{3/2} - E_b^3 \right] + \frac{2}{3\beta_2} \left[(\beta_2 b + E_b^2)^{3/2} - E_b^3 \right] + a . E_b$$

$\ldots\ldots\ldots(27)$

Since equation (27) is extremely tedious to solve for E_b, the easiest way to compare equations (5) and (27) is to calculate E_b for a given V/da from equation (5) and then substitute this value in equation (27), i.e. we compare values for V/da rather than E_b. For example, results for 150 r/minute using 1/16 in. and 5/16 in. diaphrams

	Experimental V/da	V/da calculated from Equation (27)
1/16 in.	180	206
	350	351
5/16 in.	80	82.5
	300	302

This comparison implies that the space charge correction as given by equation (27) is greater than that for equation (5). The difference in values obtained, however, does not seem sufficient to warrant the use of equation (27) which is so much more cumbersome.

REFERENCES.

ATTIX, F.H. and DE LA VERGNE, L. Radiology, 63, 853, (1954).

BAILEY, V.A. Phil. Mag. 50, 825 (1925).

BOAG, J.W. Brit. J. Radiol. 23, 601 (1950).

BOAG, J.W., PILLING, F.D. and WILSON, T. Brit. J. Radiol. 24, 341 (1951).

BOAG, J.W. and WILSON, T. Brit. J. Appl. Phys. 3, 222, (1952).

BORTNER, T.E. Nucleonics 9, No. 3, 40 (1951).

BOWEN, J.S. Phys. Rev. 41, 24 (1932).

BRADBURY, N.E. Phys. Rev. 40, 508 (1932).

BRADBURY, N.E. Phys. Rev. 44, 883 (1933).

DOEHRING, A. Zeits. f. Naturforshung 7a, 253 (1952).

FAILLA, G. Radiology, 29, 202 (1937).

GREENING, J.R. Brit. J. Radiol. 20, 71 (1947).

GREENING, J.R. Brit. J. Radiol. 26, 53 (1953).

GREENING, J.R. Radiography 25, 199 (1959).

GREENING, J.R. Brit. J. Radiol. 33, 178 (1960).

HEALEY, R.H. and REED, J.W. "Behaviour of Slow Electrons in Gases" (Sydney, 1941).

HÜBNER, W. Fortschr. Rontgenstr. 89, 764 (1958).

INTERNATIONAL COMMISSION ON RADIOLOGICAL UNITS AND MEASUREMENTS - REPORT. Handbook 62 (National Bureau of Standards, Washington 1956).

JAFFÉ, G. Ann der Physik 42, 303 (1913).

KARA-MICHAILOVA, E. and LEA, D.E. Proc. Cam. Phil. Soc. 36, 101 (1940)

KEMP, L.A.W. Brit. J. Radiol. 18, 107 (1945).

KEMP, L.A.W. Brit. J. Radiol. 19, 233 (1946).

KEMP, L.A.W. and HALL, S.M. Brit. J. Radiol. 27, 853 (1954)

KEMP, L.A.W. Nature 178, 1250 (1956).

KEMP, L.A.W. and BARBER, B. Nature, 180, 1116 (1957).

KEMP, L.A.W. and BARBER, B. Phys. Med. & Biol. 3, 123, (1958).

KUFFEL, E. Proc. Phys. Soc. 71, 516 (1958).

LEA, D.E. Proc. Cam. Phil. Soc. 30, 80 (1934).

LEA, D.E. "Action of Radiations on Living Cells" (Cambridge 1946)

LOEB, L.B. "Basic Processes of Gaseous Electronics" (California, 1955)

LOEVINGER, R. Rev. Sci. Instr. 24, 907 (1953)

LOEVINGER, R. Selected Topics in Radiation Dosimetry (I.A.E.A. Vienna 1960) p. 173.

MIE, G. Ann. Phys. Lpz. 13, 857 (1904)

RADIOCHEMICAL MANUAL PART I. (Radiochemical Centre, Amersham 1962).

ROSSI, B.B. and STAUB, H.H. "Ionization Chambers and Counters - Experimental Techniques" (New York, 1949).

SAYERS, J. Proc. Roy. Soc. A.169, 83 (1938).

SCARBORO, C.T. and SILVERMAN, L.B. Health Physics, 2, 387 (1960)

SEELIGER, R. Ann. Phys. Lpz. 33, 319 (1910).

SEELIGER, R. "Physik der Gasentladungen" (Barth, Leipzig, 1934).

SEEMAN, H. Ann. Phys. Lpz. 38, 781 (1912).

SHEVYREV, V.S. Pribory i Tekhnika Eksperimenta, 6, 35 (1960).

TOWNSEND, J.S. and TIZARD, H.T. Proc. Roy. Soc. A.88, 336 (1913).

THOMSON, J.J. and THOMSON, G.P. "Conduction of Electricity in Gases". Vol. 1. (Cambridge 1928).

VICTOREEN, J.A., J. App. Phys. 20, 1141 (1949).

VON ENGEL, A. and STEENBECK, M. "Elektrische Gasentladungen ihre Physik und Tecknik" (Berlin, 1932).

WORTHLEY, B., THOMPSON, A.M. and TOOZE, M.J. Austr. J. App. Sci. 8, 261 (1957).

WYCKOFF, H.O. and ATTIX, F.H. Handbook 64 (National Bureau of Standards, Washington, 1957).

ZANSTRA, H. Physica 2, 817 (1935).

PUBLICATIONS

Reprinted from

The
BRITISH JOURNAL
OF RADIOLOGY

RECOMBINATION IN PARALLEL PLATE FREE-AIR IONIZATION CHAMBERS

By PATRICIA B. SCOTT, B.Sc., and J. R. GREENING, Ph.D., F.Inst.P.

Medical Physics Unit, Edinburgh University, Scotland

(Received May, 1961)

RECOMBINATION in parallel plate free-air ionization chambers, although of great importance in standardising laboratories, appears to have received little theoretical consideration. Hübner (1958) gives the only theoretical treatment of which we are aware. He adopts a formula derived by Von Engel and Steenbeck (1932) for the case of uniform ionization between two infinite parallel plates and applies it to a free air chamber by supposing all the ionization to be confined within the geometrical edge of the X-ray beam and virtual collecting electrodes to exist at the beam edge (Fig. 1).

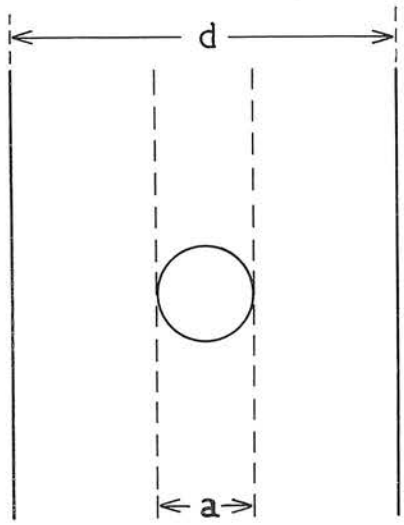

FIG. 1.
Virtual electrodes at beam edge.

Hübner derives a factor K_s by which an observed ionization current must be multiplied in order to correct for recombination. This factor is given by

$$K_s = \frac{j_s}{j} = \frac{n\left(\frac{a}{E}\right)^2 L}{\sqrt{1 + 2n\left(\frac{a}{E}\right)^2 L} - 1} \quad . \quad . \quad . \quad . \quad (1)$$

where j_s = saturation current per cm² of plate.
j = observed current per cm² of plate.
n = $69{\cdot}4\ \alpha \times 10^6/(k_1 + k_2)^2$.
a = beam diameter (cm).
E = field strength (V/cm).
L = dose rate (r/minute).
α = recombination coefficient (cm³/second).
k_1 = positive ion mobility (cm²/second V).
k_2 = negative ion mobility (cm²/second V).
e = electronic charge (esu).

Equation (1) may be rewritten as

$$K_s = \frac{\sqrt{1 + 2n\left(\frac{a}{E}\right)^2 L} + 1}{2} \quad . \quad . \quad . \quad . \quad . \quad (2)$$

Hübner claims that, when certain values are adopted for α, k_1 and k_2, the correction factors computed from his formula agree within 0·3 per cent with factors determined experimentally at the National Bureau of Standards. We find that these experimental factors covered only a limited range of conditions and as they concerned corrections usually less than 1 per cent, hardly constituted an accurate check of the theoretical formula.

We have sought to improve the theory by a more detailed consideration of several features and to check our results by experiments over a wide range of operating conditions.

Improved basic recombination formula

Previous to Hübner, Boag and Wilson (1952) had discussed the saturation curve in a plane parallel ionization chamber at high ionization intensity. Boag's treatment of this is an improvement on that of Von Engel and Steenbeck, used by Hübner, since Boag took into account the varying distributions of the positive and negative charges across the space between the plates (Fig. 2). (His approach is described here in some detail as further use will be made of his formulae in the discussion on non-uniformity of ionization.)

Suppose the ionization produced is q esu/c.c. second at all points in the gas between the plates. Then, for negligible space charge and negligible recombination, the positive charge density $\rho_1(x)$ will rise linearly from zero at the positive plate to a maximum of qd/k_1E at the negative plate while the negative charge density $\rho_2(x)$ will have a similar distribution in the opposite direction. For a collection efficiency $f = j/j_s$ less than unity, the current reaching each plate is only fqd esu/cm² second, but Boag assumed that the charge distributions remained nearly triangular for recombination up to 10 per cent.

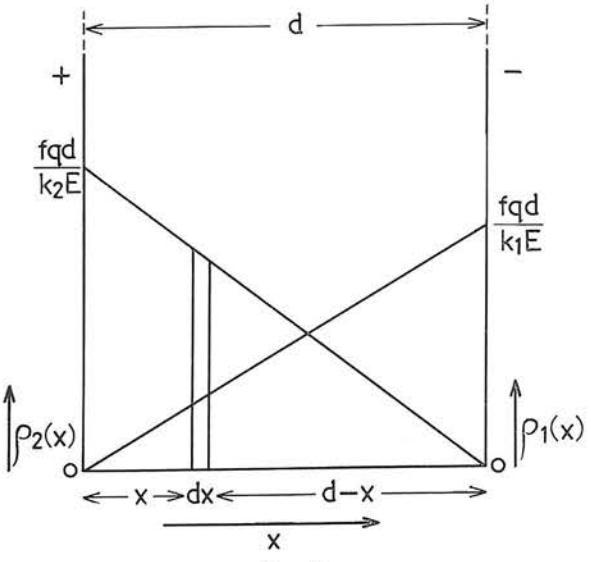

FIG. 2.

Distribution of charge density between the electrodes under near saturation conditions.

The rate of recombination of charge per unit volume at the plane x is then

$$\frac{\alpha}{e}\,\rho_1(x)\,\rho_2(x) = \frac{\alpha}{e}\left(\frac{x}{d}\cdot\frac{fqd}{k_1E}\right)\left(1-\frac{x}{d}\right)\frac{fqd}{k_2E}$$

thus total recombination throughout the space per unit area of plate per second is

$$R = \int_o^d \frac{\alpha}{e}\rho_1(x)\,\rho_2(x)\,dx = \frac{\alpha}{e}\cdot\frac{f^2q^2d^2}{E^2}\cdot\frac{d}{6\,k_1\,k_2}.$$

$$\text{Now } f = 1-\frac{R}{qd}.$$

$$\therefore f = \frac{2}{1+\sqrt{1+\zeta^2}}$$

$$\text{where } \zeta = \sqrt{\frac{2}{3}\,\frac{\alpha}{e}\,\frac{1}{k_1\,k_2}}\left(\frac{d^2\sqrt{q}}{V}\right)$$

$$\therefore \frac{1}{f} = \frac{\sqrt{1+m\left(\frac{d}{E}\right)^2L}+1}{2} \quad \text{where } m = \frac{1}{90}\,\frac{\alpha}{e\,k_1\,k_2}.$$

Hübner's method of applying this result to a free air chamber necessitates replacing d by a.

Theoretically Hübner's $K_s = j_s/j$ should equal $1/f$ and the difference in the constants n and m is due to Boag taking into account the distribution of charge. Adopting Boag's constant m, Hübner's formula becomes

$$K_s = \frac{1}{2}+\frac{1}{2}\sqrt{1+m\left(\frac{a}{E}\right)^2L} \qquad . \quad . \quad (3)$$

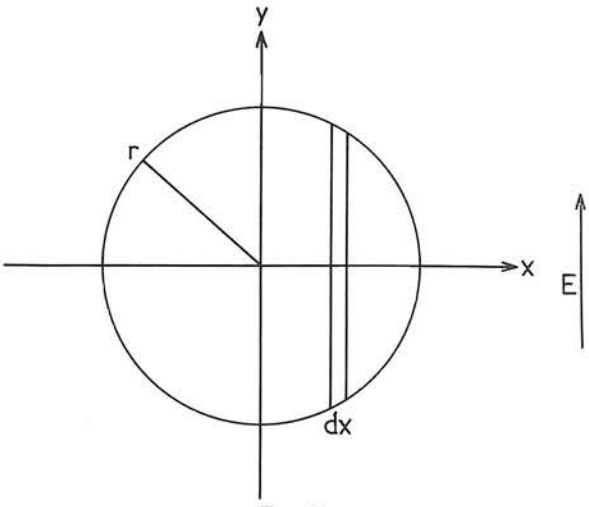

FIG. 3.

Effective cross-section of circular X-ray beam.

N.B.—Equation (3) gives rise to smaller values of K_s than does equation (2) because of the difference in constants. In his paper Hübner refers to Boag's treatment and says that Boag obtains larger values for K_s. This mistake arose because in the example Hübner took (private communication), he did not replace the d in Boag's formula by a.

Allowance for circular cross-section of X-ray beam

The theory used by Hübner considers an infinite plane sheet of ionization of thickness a. In practice it is normal to use X-ray beams of circular cross section. The theory must be modified to allow for this. Consider a strip of ionized gas parallel to the electric field and of width dx (Fig. 3). Ionization in the strip is proportional to the area, *i.e.* $2y$ dx.

From equation (3) it can easily be shown that recombination, when small, is proportional to $\left(\frac{a}{E}\right)^2L$ or, in particular to a^2.

Therefore the fractional recombination in the strip is proportional to $(2y)^2$.

$\therefore$ Total recombination in the strip $\propto 8y^3\,dx$

$$\text{Total recombination in the beam} \propto \int_{-r}^{+r} 8y^3\,dx = 3\pi r^4.$$

$$\text{Total ionization in the beam} \propto \int_{-r}^{+r} 2y\,dx = \pi r^2.$$

$$\therefore \text{Fractional recombination in whole beam} \propto 3\pi r^4/\pi r^2 \propto 3r^2 \propto \frac{3}{4}(2r)^2.$$

Hübner's theory indicates that fractional recombination is proportional to a^2 where $a = 2r$. Therefore effective diameter of circular beam of diameter a is $\sqrt{\frac{3a^2}{4}} = a\frac{\sqrt{3}}{2}$.

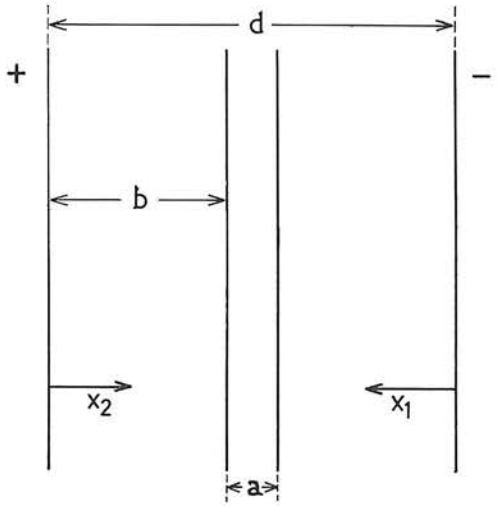

FIG. 4.
Free-air ionization chamber.

Space charge effects

Hübner did not consider space charge effects. Boag (1950) gave a very useful treatment of space charge effects in ionization chambers exposed to pulsed radiation beams. He came to the conclusion that in a chamber of plane geometry the screening effect of the space charge is negligible. This is not true, however, in the case of a free-air chamber where the beam does not completely fill the space between the plates, and there is continuous exposure to radiation.

Boag's treatment can be modified to suit these conditions (Fig. 4).

Let Ex_1 be the field at a distance x_1 from the negative plate

n_1 = Number of positive ions/c.c.
n_2 = Number of negative ions/c.c.

$$\frac{dEx_1}{dx_1} = -4\pi n_1 e$$

$$\therefore Ex_1 = E_b + 4\pi n_1 e\,(b - x_1).$$

Similarly $Ex_2 = E_b + 4\pi n_2 e\,(b - x_2)$.

Assuming a constant voltage gradient E_b in the irradiated volume of width a

$$V = E_b a + \int_o^b Ex_1\,dx_1 + \int_o^b Ex_2\,dx_2$$

$$= E_b a + 2\pi^2 b^2 e\,(n_1 + n_2).$$

Now if N is the number of ion pairs formed per c.c. per second then $n = \int N dt$ between the limits t = o and $t = \frac{a}{k\,V/d}$ (since $\frac{a}{k\,V/d}$ is the time taken for an ion of mobility k to traverse the irradiated volume under the influence of the average field across the plates, *i.e.* V/d or E).

Substituting $n = \frac{Na}{kV/d}$

we find

$$E_b = \frac{V}{d} - \frac{2\pi N e a}{V}\left(\frac{d-a}{2}\right)^2\left[\frac{1}{k_1} + \frac{1}{k_2}\right].$$

This can be expressed in a more useful form in terms of the parameter (E/a)

$$i.e.\ \frac{E_b}{a} = \frac{E}{a} - \frac{7{\cdot}75\,L}{V}(d-a)^2\left[\frac{1}{k_1} + \frac{1}{k_2}\right]$$

$$= \frac{E}{a} - 7{\cdot}75\,L\left(\frac{a}{E}\right)\frac{(d-a)^2}{da}\left[\frac{1}{k_1} + \frac{1}{k_2}\right] \quad . \quad (4)$$

A more rigorous treatment of this topic is given in the appendix.

Effect of ion spread

Hübner's theory considered uniform ionization between the two virtual plates.

In reality, however, the ranges of the secondary electrons are often greater than the beam diameter, and so the region of ionization is not restricted to the geometrical shape of the beam. This means that the ionization intensity is at a maximum along the axis of the cylinder and falls off to zero at a radius equal to the maximum range of the secondary electrons.

As mentioned before, equation (2) indicates that for small losses, $(K_s - 1)$ is proportional to $(a/E)^2\,L$. This means that Hübner's formula remains unaffected by an increase in the beam diameter if the corresponding reduction in dose-rate is uniform,

since $L \propto 1/a^2$. This may not necessarily be true, however, when one considers a central region of high density ionization surrounded by a fringe of low density ionization.

In order to investigate any change in the amount of recombination taking place due to this, let us consider a square beam of high density ionization surrounded by a larger square of lower density. Two square beams are chosen for mathematical simplicity since circular cross sections would involve more complicated integrations over width and ion density (Fig. 5).

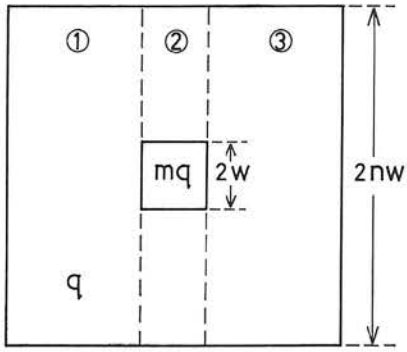

FIG. 5.

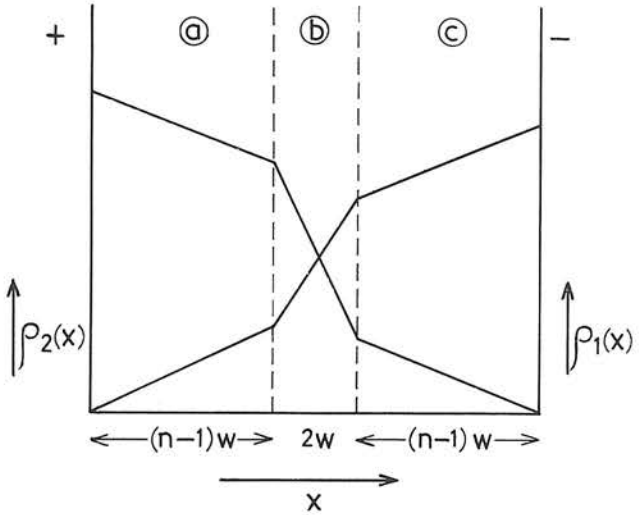

FIG. 6.

FIG. 5. Non-uniform distribution of ionization in a square X-ray beam.

FIG. 6. Distribution of charge density between the electrodes for region 2 of Fig. 5.

The diagram shows the cross section of a beam comprising a central square of side 2 w where the ion production is mq esu/c.c. second surrounded by a larger square of side 2 nw where the ion production is q esu/c.c. second.

Let $\dfrac{fqw}{k_1 k_2 E} = C.$

Boag's theory gives $R_1 = R_3 = \dfrac{a}{e}\ C^2\,(2n)^2\ \dfrac{2nw}{6}$

where R_1 represents the total recombination throughout region 1 per unit area of plate.

$$\therefore R_1 = R_3 = \frac{a}{e} C^2 \frac{4n^3 w}{3}.$$

Fig. 6 shows the charge density distributions across the plates for region 2, which can be divided into three parts (*a*), (*b*) and (*c*). In part (*a*) the positive ion density $\rho_1(x)$ rises from zero at the positive plate to a value of $C(n-1)$ at $x = (n-1)w$. In part (*b*) $\rho_1(x)$ increases more rapidly to a value of $C(n-1+2m)$ at $x = (n+1)\ w$. Finally in (*c*) $\rho_1(x)$ reaches $C(2n+2m-2)$ at the negative plate with the same slope as in (*a*).

The same argument can be applied to the negative ion density which rises in the opposite direction.

(*a*) Rate of recombination $= \dfrac{a}{e}\,\rho_1(x)\,\rho_2(x)$

$$= \frac{a}{e}\left[\frac{x}{(n-1)w} C\,(n-1)\right]\left[C\,(n-1) + 2mC + \left(1 - \frac{x}{w(n-1)}\right) \cdot C\,(n-1)\right]$$

$$R_a = \int_0^{(n-1)w} \frac{a}{e}\,\rho_1(x)\,\rho_2(x)\,dx = \frac{a}{e} C^2 (n-1)^2 w \left[\frac{2}{3} n + m - \frac{2}{3}\right]$$

(*c*) Similarly

$$R_c = R_a.$$

(*b*)

$$R_b = \int_{(n-1)a}^{(n+1)a} \frac{a}{e}\left[(n-1)C + \frac{[x-(n-1)w]}{w} mC\right]\left[(n-1)\,C + \frac{(1-[x-(n-1)w])}{2w} 2mC\right] dx$$

$$= \frac{a}{e} C^2\, 2w\left[(n-1)^2 + 2m\left(n - 1 + \frac{m}{3}\right)\right].$$

Total recombination per unit area of plate for region 2

$$R_2 = R_a + R_b + R_c$$

$$\therefore R_2 = \frac{a}{e} C^2\, 2w\,[(n-1)^2\,(\tfrac{1}{3} + \tfrac{2}{3} n + m) + 2m\,(-1 + n + m/3)].$$

Since R represents recombination throughout each region per unit area of plate, total recombination taking place between the plates is

$$r = R_1\,(n-1)w + R_2\,2w + R_3\,(n-1)w$$

$$= \frac{a}{e} C^2 \frac{4w^2}{3}\,[(n-1)^2\,(1 + 2n + 3m)$$

$$+ 2m\,(-3 + 3n + m) + 2n^3\,(n-1)].$$

Now the total number of ions formed between the plates per second.

$$= mq\,4w^2 + q\,(4n^2\,w^2 - 4w^2)$$
$$= 4w^2\,q\,(m + n^2 - 1).$$

This figure would also be obtained from a uniform intensity of ionization q esu/c.c. second over a square of side $2w\sqrt{m + n^2 - 1}$.

In this case $R = \frac{a}{e} C^2\,4\,(m + n^2 - 1)\,\frac{2w}{6}\sqrt{m + n^2 - 1}$

and $r = \frac{a}{e} C^2\,(m + n^2 - 1)\,\frac{8w^2}{6}$

$$\therefore \frac{r_{\text{unif}}}{r_{\text{non unif}}} =$$

$$\frac{2\,(m + n^2 - 1)^2}{[(n-1)^2\,(1 + 2n + 3m) + 2m\,(3n - 3 + m) + 2n^3\,(n-1)]}$$
$$= y \text{ (say)}.$$

Keeping m constant and differentiating y with respect to n, the condition for a stationary value for y is $\frac{dy}{dn} = 0$.

This occurs when $n^2 = 1 \pm m$

i.e. $n = \sqrt{1 + m}$ is the condition for a maximum

$$\therefore y \text{ max} = \frac{8m^2}{m + 7m^2} = \frac{8m}{1 + 7m}$$

$$\text{as } m \to \infty,\ y_{\max} \to \frac{8}{7} = 1{\cdot}143.$$

Similarly by keeping n constant and differentiating y with respect to m we find the condition for $\frac{dy}{dm} = 0$ is $m = 1 \pm n^2$

Substituting $m = 1 + n^2$

$$y_{\max} = \frac{8n^4}{n^2 + 7n^4} = \frac{8n^2}{1 + 7n^2}$$

$$\therefore \text{as } n \to \infty\ y_{\max} \to \frac{8}{7}.$$

This means that the maximum possible effect of non-uniformity of ionization on the amount of recombination is about 14 per cent. We have considered here a purely hypothetical situation in which there is a sharp boundary between the areas of high and low intensity ionization. In practice the distribution is not known accurately but will be approximately as in Fig. 7, and it seems reasonable to assume that $y_{\max}$ will be somewhat smaller in this case. It was decided, therefore, to ignore ion spread as far as the original Hübner formula was concerned.

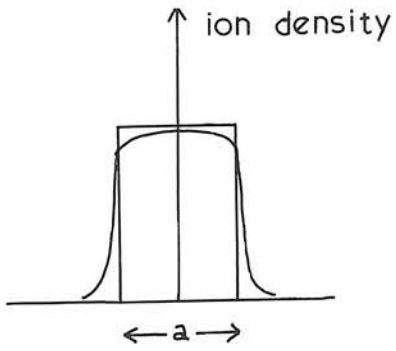

FIG. 7.

Schematic plot of ion density against distance from beam axis.

On considering the space charge correction, however, we see that a reduction in ion density, whether uniform or not, will automatically reduce the screening effect of the space charge since it will be spread out over a larger volume. To take into account the ion spread we must replace the parameter $\frac{a\sqrt{3}}{2}$ in the space charge correction formula by $(a + c)\frac{\sqrt{3}}{2}$ where c represents the increase in diameter of the beam, and also reduce the dose-rate correspondingly. As an approximation c can be taken to be twice the average range of secondary electrons.

Now at low tube voltages, *e.g.* 10 to 50 kV, over 90 per cent of the secondary electrons are photoelectrons and these cause almost all the ionization, whereas at higher voltages, *e.g.* 250 kV, most of the ionization is caused by the Compton recoil electrons. This means that for low voltages the average range of the photoelectrons should be chosen while at high voltages it is the average range of the Compton electrons which is required. At intermediate voltages, however, when neither the photo nor the recoil electron contribution can be neglected, it is extremely difficult to determine the appropriate range of the secondary electrons to be used in the theoretical formula.

The ranges adopted were determined as follows: The effective energy of the secondary electrons was obtained from a measurement of the H.V.L. of the X-ray beam. The average range of electrons (photo or recoil depending on the kilovoltage) for this energy was found from data given by Lea (1946).

Final form of theory

Although the modifications outlined here are only approximate solutions to the problems involved, their inclusion in Hübner's formula does provide an improvement.

The final form of the theoretical relation is thus:

$$K_s = \frac{1}{2} + \frac{1}{2}\left\{1 + \frac{\frac{1}{90}\frac{a}{e}\frac{1}{k_1 k_2}L}{\left[E/a\sqrt{\tfrac{3}{2}} - 7{\cdot}75\,L\left(\frac{a\sqrt{\frac{3}{2}}}{E}\right)\frac{\left[d-(a+c)\sqrt{\frac{3}{2}}\right]^2}{d\,(a+c)\sqrt{\frac{3}{2}}}\left(\frac{1}{k_1}+\frac{1}{k_2}\right)\right]^2}\right\}^{\frac{1}{2}} \quad . \; . \; (5)$$

In order to verify this formula a series of experiments was undertaken to investigate the dependence of ionization current on the various parameters involved, *e.g.* field strength, dose-rate, beam quality and aperture size and shape.

Apparatus and experimental procedure

The experimental arrangement is shown in Fig. 8. The source of X rays was a Müller superficial therapy set and the tube head was clamped to a stand at the end of the bench. A free-air chamber (Greening, 1960) was lined up as accurately as possible on the beam axis and a coin-shaped monitor chamber was placed close behind it. The two chambers were fed with voltages of opposite polarity *via* coaxial screened cables. The ionization currents were balanced on a modified version (Greening, 1953) of the Kemp Comparator which was used with the fixed condenser shorted out so that the collector plate and the guard plate of the free-air chamber were maintained at the same potential during the charge comparison. The monitor chamber was supplied with 300 volts throughout the experiments. Its plate separation, and hence its ionization current, was varied so that balance points were obtained in the most accurate region of the comparator dial.

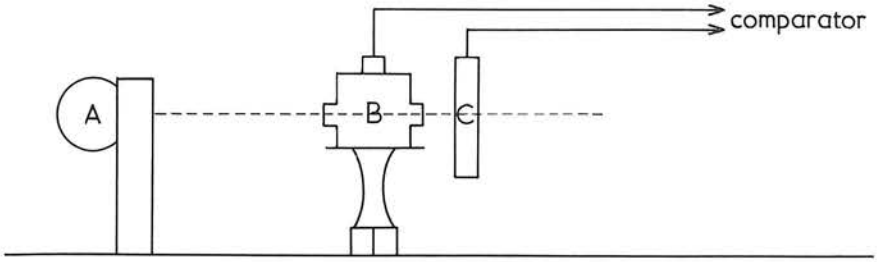

FIG. 8.
Experimental arrangement: A=X-ray tube head; B=free-air chamber; C=monitor chamber.

Measurements for up to 15 per cent ion loss were made by reducing the voltage across the free-air chamber. For the majority of the experiments the operating voltage chosen was 45 kV and the dose-rate was varied between 10 and 1,000 r/minute, simply by changing the distance of the free-air chamber from the source of X rays. Measurements made on an E.I.L. Model 37A portable electrometer connected to the free-air chamber gave the values for the dose-rates at the chamber diaphragm.

Over as wide a range of dose-rate as possible, three circular apertures were used—$\frac{1}{16}$, $\frac{1}{8}$ and $\frac{5}{16}$ in. diameters. Different aperture sizes were necessary since small apertures could not be used at low dose-rates because of lack of sensitivity while large apertures presented saturation problems at high dose-rates. In order to investigate the effect of aperture shape several square and rectangular apertures were tried at different orientations. Some experiments were also carried out at 20 and 85 kV to observe the effect of change of beam quality.

Room temperatures and pressures were recorded during each experimental run. The theoretical variation of K_s with temperature and pressure will be discussed in the next section. Since the temperature varied only slightly during the experimental series, no experimental confirmation was attempted. The effect of pressure was, however, investigated. This was done by enclosing the two chambers in an airtight tin and making experimental runs at 670 and 850 mm Hg pressure.

Experimental results

The simplest way to present the experimental results is graphically. (K_s-1) can be plotted on a double log scale against E/a with L as parameter, or against L with E/a as parameter.

Firstly, however, K_s must be corrected to standard temperature and pressure conditions, *i.e.* 22°C and 760 mm Hg. Boag (1952) defined a quantity

$$\eta = \frac{a}{3\,e\,k_1\,k_2} \cdot j \cdot \frac{d^3}{V^2}$$

and proves that $f = 1/(1+\eta)$

$$i.e.\ K_s - 1 = \eta = \frac{a}{3\,e\,k_1\,k_2} \cdot j \cdot \frac{d^3}{V^2}.$$

Thus for given V and d $K_s - 1 \propto \frac{a}{e} \cdot \frac{1}{k_1\,k_2} \cdot j$.

Now for a given L, j is proportional to density, *i.e.* $\frac{P}{T}$.

$\therefore$ for given V, d and L $K_s - 1 \propto \frac{a}{k_1\,k_2} \cdot \frac{P}{T}$.

Examples of the graphs obtained are shown in (Fig. 9). When $K_s - 1$ is plotted against E/a for various dose-rates a family of approximately straight parallel lines is obtained with an average slope of about $-2{\cdot}6$ (Fig. 9A). Curves for the $\frac{1}{16}$ in. and $\frac{1}{8}$ in. diaphragms are almost coincident, while those for the $\frac{5}{16}$ in. are displaced slightly in the direction of decreasing dose-rate. Taking E/a as parameter and plotting $K_s - 1$ against L produces another series of approximately straight parallel lines with an average slope of about 1·3 (Fig. 9B). Hübner's original formula predicts slopes of $-2{\cdot}0$ and 1·0 for these families of curves.

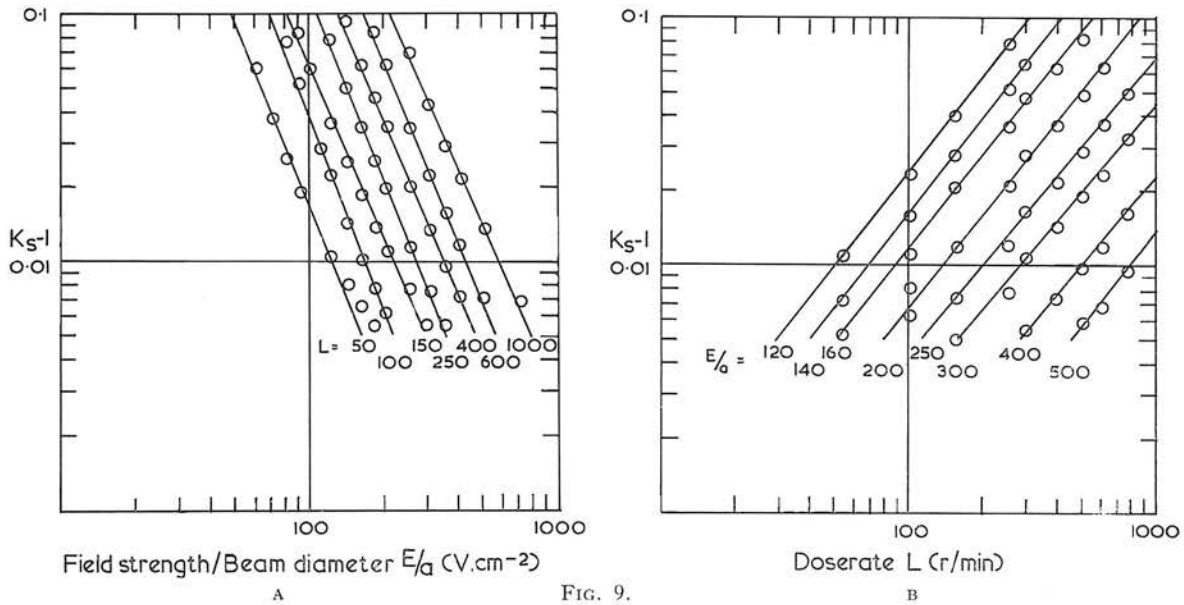

FIG. 9.

(A) Plot of $(K_s - 1)$ against E/a for various dose-rates for the $\frac{1}{16}$ in. diaphragm. (Dose-rates and beam diameter are measured at the diaphragm.)

(B) Plot of $(K_s - 1)$ against L for various E/a values for the $\frac{1}{16}$ in. diaphragm.

Von Engel (1955) discusses the variation of mobilities and recombination coefficient with temperature and pressure. He gives $k \propto 1/\text{density}$, *i.e.* $k \propto T/P$ and for air at pressures below 1,000 mm of Hg.

$$a \propto P.T^{-5/2}.$$

Thus $K_s - 1 \propto P.T^{-5/2} \cdot \frac{P^2}{T^2} \cdot \frac{P}{T} \propto P^4\,T^{-11/2}$.

The pressure dependence of K_s was verified experimentally by comparing the ratios of K_s values for the same L and E/a at the two pressures already mentioned, with the theoretical ratios. Agreement was found within 1 per cent.

Values for mobilities and recombination coefficient

Before theoretical values for K_s could be calculated, some thought had to be given to the choice of k_1, k_2 and a. The values for these constants reported in the literature proved somewhat conflicting. Our two main sources of reference were Thomson and Thomson (1928) and Loeb (1955).

(*a*) *Mobilities.* Thomson and Thomson survey the data up to 1927. They point out that there is considerable divergence between the values for mobilities obtained by different observers suggesting that the results were affected by several per cent by the experimental conditions.

They give as the probable mean value

$k_1 = 1{\cdot}36$ cm²/second V
$k_2 = 2{\cdot}1$ cm²/second V
} Room temperature and pressure.

Loeb, however, says that mobilities measured under the older standard conditions only have significance when applied to the particular experimental arrangement used, due to the ageing of the ions, impurities, method of ionization, etc. He therefore dismisses the earlier published tables as of no value except for indicating the order of magnitude. He recommends the work of Bradbury (1932) who used an X-ray ionization method of high resolving power in an all-glass, baked-out chamber.
He found

$k_1 = 1{\cdot}59$
$k_2 = 2{\cdot}21$
} filtered air at room temperature and pressure.

Since Loeb points out that Bradbury's experimental errors with his more modern techniques are only 2 per cent compared with the pre-1927 errors of at least 20 per cent, we decided to adopt Bradbury's results although no attempt had been made to filter the air in our free air chamber.

(*b*) *Recombination coefficient.* Again Thomson and Thomson list values obtained by different observers. They recommend the work of Thirkell who used X-ray ionization and Langevin's method of measurement, resulting in $\alpha = 1{\cdot}6 \times 10^{-6}$ cm³/second. Loeb has an excellent chapter on the recombination of ions. Again he criticises older methods of measurement which were carried out with outdated equipment and techniques, usually with impure gases and ions of indefinite and time-varying character. Owing to this, and to the lack of correction for losses and errors caused by diffusion, the results of earlier studies are again of little value. Loeb recommends the value obtained by Sayers (1938) using a commutator method with X-ray ionization and measurement of ion losses due to recombination. Before choosing a value for α, however, one must decide what type of recombination is taking place. Using Loeb's terminology there are two kinds which are applicable to our free-air chamber.

1. *Initial recombination*

Negative and positive ions are initially distributed in clusters along the electron tracks and recombination will be greater for this non-random distribution of ions than for a completely random distribution.

2. *Volume recombination*

This sets in when the ions have diffused to random and isotropic distributions.

Thus the recombination coefficient will decrease from its initial value as the ions begin diffusing apart until a constant value is reached. In our experiments, immediately the ions were formed they were subjected to an external field which dragged them apart. We therefore assumed that initial recombination plays a negligible part.

Sayers's value for the volume recombination in air adopted by us is $\alpha = 2{\cdot}3 \times 10^{-6}$ cm³/second.

Perhaps a comment on Sayers' paper could be made at this point. He found that the value of α changed with X-ray intensity to a remarkable extent. For example, by trebling the exposure time of the X rays, *i.e.* increasing the ion density by a factor of three, he obtained a decrease in the value for α of about 14 per cent. Also by replacing the glass wall of his ionization chamber with a piece of cardboard he found α to decrease by approximately 60 per cent. He explained the lowering of α with exposure time by postulating the formation of complex molecules which decrease the ionic mobility. These findings cast some doubt on Sayers' work, especially since in our own experiments the single value for α chosen seems to satisfy all dose-rates which differ by as much as a factor of 100.

It seems surprising that some 60 years after ionic recombination was first investigated more satisfactory information on α is not available.

Theory and experiment

These values for α, k_1 and k_2 were substituted in our formula. The value for c was taken to be 10 mm which is twice the average range in air of photoelectrons for a 45 kV beam with a H.V.L. of 0·45 mm of Al.

In calculating K_s it must be noted that a and L are the values at the centre of the measuring electrode and so are dependent on the distance of the diaphragm from the X-ray source. Thus, for a given dose-rate, the values for K_s will depend on the experimental conditions, since to vary the dose-rate one must either change the distance and hence a, or the filtration and hence c. In Fig. 10 the theoretical results for $(K_s - 1)$ are drawn in as continuous curves, while the experimental results are represented as points. Extremely good agreement is obtained between theory and experiment.

Experimental results on aperture shape and beam quality also bear out the theory. Values for the square apertures, $\frac{1}{4}$ in. and $\frac{1}{8}$ in. side, verify the choice of $a\frac{\sqrt{3}}{2}$ as parameter for circular ones, as this

step brings the graphs of K_s-1 against E/a at the same dose-rate into coincidence (Fig. 11). Rotating the square aperture through 45 deg. makes no difference to the results. This is probably to be expected since the ion spread is greater than the aperture width, and so the orientation of the square will cease to matter. Measurements made with a rectangular aperture, $\frac{1}{16}\times\frac{1}{4}$ in., show only a small change in K_s when the diaphragm is rotated through 90 deg. This also indicates that the total amount of ionization taking place is more important than the beam shape.

DISCUSSION

Our formula seems to give an adequate representation of the experimental findings although there is still room for improvement. No account has been taken of the effect of non-uniformity of ionization on recombination. We have estimated that the reduction in recombination due to this is less than 14 per cent but we did not calculate this accurately. The space charge correction chosen is only an approximation and again no allowance is made for the non-uniform distribution of ionization.

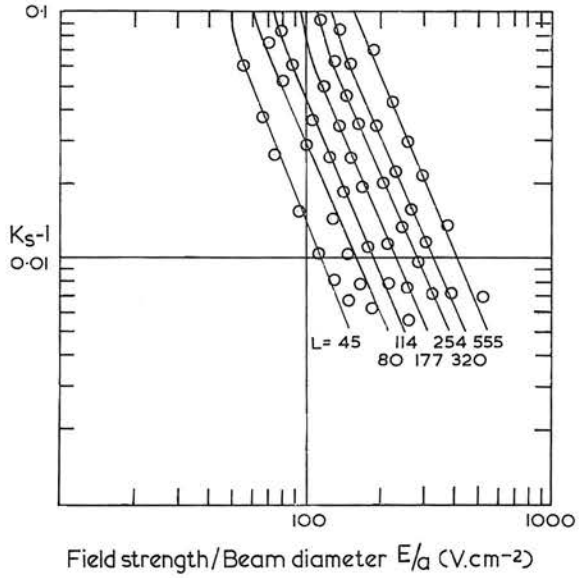

FIG. 10.

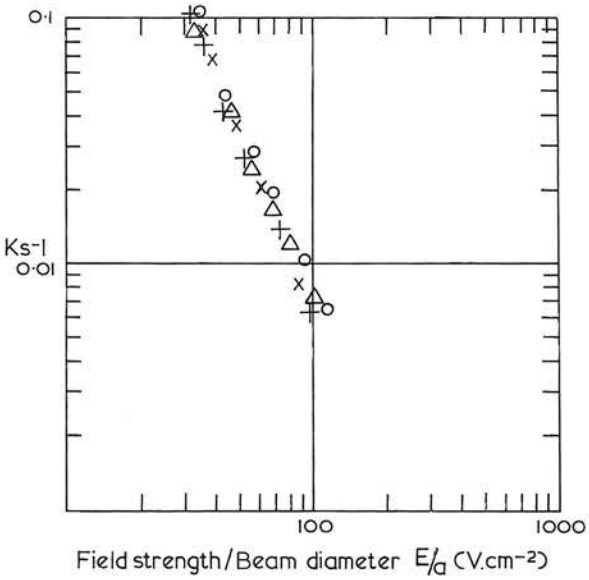

FIG. 11.

FIG. 10. Comparison for $\frac{1}{16}''$ diaphragm of theoretical values of (K_s-1) drawn as continuous curves with experimental results represented by circles. (Dose-rate and beam diameter values are measured at the centre of the collecting electrode.)

FIG. 11. Plot of (K_s-1) against E/a for various diaphragms. Dose-rate approximately 20 r/minute at the diaphragm.

Points × $\frac{1}{8}$ in. square diaphragm.
\+ $\frac{1}{4}$ in. square diaphragm.
○ $\frac{1}{8}$ in. circle diaphragm using $a\sqrt{3}/2$ as parameter.
△ $\frac{5}{16}$ in. circle diaphragm using $a\sqrt{3}/2$ as parameter.

Experiments on beam quality show that for an 85 kV beam with a H.V.L. of 4·46 mm Al there is a decrease in the slope of K_s-1 against dose-rate while with a H.V.L. of 0·762 mm Al little difference is found. This is anticipated by our theory. For a H.V.L. of 4·46 mm Al the range of the photo electrons (80 per cent of the total) is 25 mm in air. This implies that the space charge effect is negligible, since the ion spread is sufficient to fill the space between the plates. For a H.V.L. of 0·762 mm Al, however, the average range of the photoelectrons is approximately 7 mm which is only slightly greater than for the 45 kV beam.

Another point to be considered is the dose-rate "waveform" provided by the X-ray machine. The dose-rate variation with time in our experiments was investigated using a large multiplate ionization chamber (Greening, 1959) in conjunction with an oscilloscope. Traces taken showed that the output from the tube was constant to within 15 per cent. We therefore assumed that it was not necessary to modify our theory to allow for fluctuations in dose-rate. Normal unsmoothed half- or full-wave rectification would lead to pulses of ionization, and in any particular case, consideration would need to be given to the extent to which the space charge produced

by one pulse of radiation had been collected before the next pulse occurred.

Thus a completely satisfactory theory could only be evolved from a rigorous mathematical treatment of these points. It is doubtful, however, whether this is, in fact, necessary since the formula would become too cumbersome to be of any practical use. In any case the exact spatial distribution of ionization is rarely known. It is hoped that the formula derived here will be an aid both in determining the recombination losses in many experimental situations and in fundamental free-air chamber design.

SUMMARY

Consideration is given to the choice of the formula which best describes recombination between parallel plates. This formula is modified so that it may be applied to free-air ionization chambers. The modifications entail determining (i) the effective width of a circular cross-section X-ray beam, (ii) the effect of space charge and (iii) the effect of ion spread and distribution. The modified formula is checked experimentally with a small free-air chamber by varying field strength, dose-rate, beam quality and size and shape of the X-ray beam. Good confirmation is obtained.

REFERENCES

BOAG, J. W., 1950, *Brit. J. Radiol.*, *23*, 601.

BOAG, J. W., and WILSON, T., 1952, *Brit. J. Appl. Phys.*, *3*, 222.

BRADBURY, N. E., 1932, *Phys. Rev.*, *40*, 508.

GREENING, J. R., 1953, *Brit. J. Radiol.*, *26*, 53; 1959, *Radiography*, *25*, 199; 1960, *Brit. J. Radiol.*, *33*, 178.

HÜBNER, W., 1958, *Fortschr. Röntgenstr.*, *89*, 764.

LEA, D. E., 1946, *Action of Radiations on Living Cells*, (Cambridge).

LOEB, L. B., 1955, *Basic Processes of Gaseous Electronics* (California).

SAYERS, J., 1938, *Proc. Roy. Soc.*, A *169*, 83.

THOMSON, J. J., and THOMSON, G. P., 1928, *Conduction of Electricity in Gases*, Vol. I (Cambridge).

VON ENGEL, A., 1955, *Ionized Gases* (Oxford).

VON ENGEL, A., and STEENBECK, M., 1932, *Elektrische Gasentladungen ihre Physik und Tecknik* (Berlin).

APPENDIX

Equation (4) was derived on the assumption that $n = \dfrac{Na}{kV/d}$

This is an obvious approximation since V/d is only the average voltage gradient between the plates. A more correct approach would be to consider $n_x = \dfrac{Na}{k\,E_x}$

n_x = number of ions/c.c. at x.

$$\therefore \frac{d\,Ex_1}{dx_1} = -\frac{4\pi Na}{k_1\,Ex_1}$$

$$\int_{E_b}^{Ex_1} Ex_1\,d\,Ex_1 = -\int_{b}^{x_1} \frac{4\pi Na}{k_1}\,dx_1$$

$$\therefore Ex_1 = \sqrt{\frac{8\pi Na}{k_1}(b-x_1) + E_b{}^2} \quad . \; . \; (6)$$

As before $V = a.E_b + \int_0^b Ex_1\,dx_1 + \int_0^b Ex_2\,dx_2$

Substituting for Ex_1 and Ex_2 from (6), and putting $\dfrac{8\pi Na}{k} = B$

$$V = \int_0^b \sqrt{B_1 b + E_b{}^2 - B_1 x_1}\,.\,dx_1 + \int_0^b \sqrt{B_2 b + E_b{}^2 - B_2 x_2}\,.\,dx_2 + a\,.\,E_b$$

$$= \frac{2}{3B_1}\left[(B_1 b + E_b{}^2)^{3/2} - E_b{}^3\right] + \frac{2}{3B_2}\left[(B_2 b + E_b{}^2)^{3/2} - E_b{}^3\right] + a\,E_b \quad . \; . \; (7)$$

Since equation (7) is extremely tedious to solve for E_b the easiest way to compare equations (4) and (7) is to calculate E_b for a given V/da from equation (4) and then substitute this value in equation (7), *i.e.* we compare values for V/da rather than for E_b.

E.g. Results for 150 r/minute using $\frac{1}{16}$ in. and $\frac{5}{16}$ in. diaphragms:

	Experimental V/da	V/da calculated from eqn. (7)
$\frac{1}{16}$ in.	180	206
	350	351
$\frac{5}{16}$ in.	80	82·5
	300	302

This comparison implies that the space charge correction as given by equation (7) is greater than that for equation (4) especially in the case of the smallest aperture. The difference in values obtained, however, does not seem sufficient to warrant the use of equation (7) which is so much more cumbersome.